

**C¹⁰ SEMI-PEPTOID β -TURN PEPTIDOMIMETICS:
SYNTHESES, CHARACTERIZATION AND BIOLOGICAL
STUDIES**

A Thesis

by

ERNEST NNANABU

Submitted to the Office of Graduate Studies of
Texas A&M University
in partial fulfillment of the requirements for the degree of

MASTER OF SCIENCE

May 2006

Major Subject: Chemistry

**C¹⁰ SEMI-PEPTOID β -TURN PEPTIDOMIMETICS:
SYNTHESES, CHARACTERIZATION AND BIOLOGICAL
STUDIES**

A Thesis
by
ERNEST NNANABU

Submitted to the Office of Graduate Studies of
Texas A&M University
in partial fulfillment of the requirements for the degree of

MASTER OF SCIENCE

Approved by:

Chair of Committee, Kevin Burgess
Committee Members, Daniel Singleton
Michael Manson
Head of Department, Emile A. Schweikert

May 2006

Major Subject: Chemistry

ABSTRACT

C¹⁰ Semi-Peptoid β -turn Peptidomimetics: Syntheses, Characterization and Biological Studies.

(May 2006)

Ernest Nnanabu, B.S., Linfield College

Chair of Advisory Committee: Dr. Kevin Burgess

Over the years, the Burgess group has been focusing on the preparation and testing of small molecules that mimic protein secondary structures for protein-protein interactions. The most successful compounds made are C¹⁰ peptide macrocycles that effectively mimic β -turns and have given promising results from biological testing. These peptide macrocycles have also been dimerized to give even more effective ligands for protein-protein interaction.

The successes of the peptide macrocycles have enabled us to look into increasing the chemical diversity of our libraries. This we believe will not only improve our ability to obtain high affinity ligands for the receptors of interest, but will also allow us to investigate other receptors. To achieve this, peptoids were incorporated into the C¹⁰ system to replace the peptides in the $i+1$ and $i+2$ positions. With the help of Microwave irradiation, semi-peptoid macrocycles were synthesized with a total reaction time of less than 2 h. These compounds were characterized and found to mimic β -turn, and show promising biological activity towards the Insulin-like growth factor 1 receptor (IGF-IR).

DEDICATION

To my family and friends.

ACKNOWLEDGMENTS

First of all, I would like to thank my adviser, Dr. Kevin Burgess, for his enthusiasm and guidance in my research work throughout my years at Texas A&M University. I would like to express my gratitude to Drs. Daniel Singleton, Mike Manson, and Gary Sulikowski for serving on my graduate advisory committee and helping me through the difficulties.

I also would like to thank all of my colleagues especially Sang Lam, Aurora Loudet, Guan Castro, Yu li, Jing Liu, Chihyo Park and Samuel Reyes for their friendship and helpful discussions. I would like to acknowledge Aurora Loudet for proofreading this thesis and for helping me with the style and format. Finally, I would like to pay special thanks to my family for their love and support.

TABLE OF CONTENTS

	Page
ABSTRACT	iii
DEDICATION.....	iv
ACKNOWLEDGMENTS	v
TABLE OF CONTENTS	vi
LIST OF FIGURES	viii
LIST OF SCHEMES	x
LIST OF TABLES.....	xi
CHAPTER	
I INTRODUCTION.....	1
1.1 Peptidomimetics and Protein-Protein Interactions	1
1.2 Tumor Necrosis Factor- α (TNF α) and Receptors.....	2
1.3 Neurotrophins and Their Receptors.....	9
1.4 Insulin-like Growth Factor and Receptors.....	19
1.5 β -Turn Mimetics	22
1.6 Multivalent Ligands.....	25
1.7 Summary.....	28
II CYCLIC SEMI-PEPTOID TURN MIMICS	29
2.1 Introduction.....	29
2.2 Methods in Peptoids Synthesis.....	29
2.3 Preparation of Primary Amines for Cyclic Peptoid Libraries	33
2.4 Preparation of Templates for Cyclization.....	36
2.5 Optimization of Linear Peptoid Synthesis.....	36
2.6 Synthesis of Linear Peptoids	39
2.7 Formation of Peptidomimetics 1	41
2.8 Formation of Peptidomimetics 2.....	45
2.9 Conformational Analysis	47
2.10 Summary.....	50

CHAPTER	Page
III BIOLOGICAL STUDIES	51
3.1 Introduction.....	51
3.2 Cell Survival Assays with the Semi-Peptoids	51
3.3 Dimeric First Generation Peptidomimetics	59
3.4 FACS Assays of Dimeric First Generation Peptidomimetics	64
3.5 Competitive Binding Assays	65
3.6 Summary.....	66
IV CONCLUSIONS	67
REFERENCES	68
APPENDIX	79
VITA.....	133

LIST OF FIGURES

FIGURE	Page
1.1. TNF superfamily ligand-receptor interactions.....	3
1.2. Human Tumor Necrosis Factor- α (TNF α)	4
1.3. Representation of the Cysteine Rich Domains (CRDs) of TNFR1 that are involved in binding to TNF α	6
1.4. (a) Crystal structure of TNF β /TNFR1 complex. TNF β in green, TNFR1 in blue, and the two interaction surfaces in red and orange. (b) Structural view of TNF α and receptor interactions (an interaction surface in yellow). (c) Loop 1 of domain 3 of the TNFR (the critical binding site)......	7
1.5. Local conformations of the TNF α β -turn regions 1 – 4.....	8
1.6. Relationships of neurotrophins and their receptors.	10
1.7. Structure of neurotrophins (a) NGF, (b) NT-3, (c) BDNF, (d) NT-4/5.....	11
1.8. Schematic representation of neurotrophin receptors; Trk and p75.....	12
1.9. NGF/TrkA-d5 complex. (a) The binding epitopes of NGF to TrkA-d5, (b) the specific patch, (c) the conserved patch. NGF monomers are in blue and red; TrkA-d5 is in green.....	14
1.10. Binding epitopes of NT-3 to TrkC (red) and p75 receptor (green).	16
1.11. Structures of compounds A-F	17
1.12. Ribbon structure of IGF-I. The B-region (residues 3-28) shown in blue, the C-region (residues 29-41) in light yellow, A region (residues 42-62) in pink, and the D-regions (residues 63 and 64) in white. The disulfide bonds in yellow.....	20
1.13. Ribbon plot of NBP-4 (blue) and IGF-I (green) complex. Residues shown in violet constitute the binding site for interaction with NBP-4 and those shown in red are determinants for binding to IGF-IR.....	22
1.14. β -turn structure and the selected examples of β -turn mimetics.....	24
1.15. Comparison of cyclic hexapeptide with ring-fused C ¹⁰ motif.	24
1.16. (a) Production of homodimeric libraries from monomeric libraries, and (b) production of heterodimeric libraries from monomeric libraries.	26
1.17. Bivalent peptidomimetic with $K_d = 20 \pm 20$ nM.	27
2.1. Amine building blocks labeled with the amino acid residue they are used to mimic (red).	33

FIGURE	Page
2.2. CD spectra in 35% methanol, 1.0% NaHCO ₃ in water.	49
2.3. A. Simulated favored conformation of 1NK ; B. Simulated favored conformation of 2FF	50
3.1. Relative survival of cells, induced by semi-peptoids dissolved in a high concentration of DMSO (5% Serum as 100% survival).....	53
3.2. Relative survival of cells, induced by semi-peptoids dissolved in a low concentration of DMSO (5% Serum as 100% survival).....	55
3.3. Relative survival of cells, induced by semi-peptoids dissolved in HBSS (5% Serum as 100% survival)	56
3.4. Selected cell survival data of semi-peptoids dissolved in high concentration of DMSO or HBSS.	58
3.5. Selected cell survival data of semi-peptoids dissolved in low concentration of DMSO.....	59
3.6. Monomers for KB536	59
3.7. Binding Affinity of KB535 and KB536 for TrkA. Shift of the data to the left is indicative of higher affinity.....	66

LIST OF SCHEMES

SCHEME	Page
1.1. Triazole-scaffold dimerization.....	27
2.1. (a) Reductive amination with aldehydes as diversity elements, (b) reductive amination with primary amines as diversity elements.	30
2.2. Alkylation approach to solution-phase peptoid synthesis.	31
2.3. Monomer vs. submonomer solid phase synthesis according to Simon <i>et al.</i> and Zuckermann <i>et al.</i>	32
2.4. Protection of alcohol amine building blocks; (a) serine building block and (b) threonine building block.....	34
2.5. Preparations of building blocks; (A) arginine building block, (B) lysine building block, and (C) tyrosine building block.	35
2.6. Synthesis of templates for S _N 2 cyclization.	36
2.7. Synthesis of linear peptoids.	40
2.8. Synthesis of peptoids with Nosyl amides.	41
2.9. S _N 2 cyclization reaction.	43
2.10. S _N Ar cyclization reaction.	46
3.1. (i) Synthesis of monomer a , (ii) linker and fluorene triazine attachments.	60
3.2. (i) Synthesis of monomer b , (ii) linker attachment.....	62
3.3. Dimerization to form KB536	64

LIST OF TABLES

TABLE	Page
1.1. Sequences of turn regions in TNF α postulated for binding to TNFR1.....	8
1.2. Sequences of turn regions in NGF.....	18
1.3. Sequences of turn regions in human NT-3	19
1.4. Classification of β -turns	23
2.1. Acylation conditions for peptoid synthesis.....	38
2.2. Optimization of microwave-assisted peptoid synthesis.....	39
2.3. Conditions for S _N 2 cyclization.....	42
2.5. Purity and yield data for the cyclic semi-peptoids 1	44
2.6. Microwave conditions for S _N Ar cyclization	45
2.7. Purity and yield data for the cyclic semi-peptoids 2	46
3.1a. Cell survival data of semi-peptoids dissolved in high concentration of DMSO.....	52
3.1b. Cell survival data of semi-peptoids dissolved in low concentration of DMSO.....	54
3.1c. Cell survival data of semi-peptoids dissolved in HBSS.	56
3.2a. Selected cell survival data of semi-peptoids dissolved in high concentration of DMSO or HBSS.	57
3.2b. Selected cell survival data of semi-peptoids dissolved in low concentration of DMSO.....	58
3.3. Summary of FITC-peptidomimetic binding to TrkA-NIH cells or TrkC-NIH cells, by FACScan assays. Mean channel fluorescence (MCF) of FITC-labeled ligands binding to TrkA or TrkC. n= 3 \pm sd. Where no sd is shown, only 2 assays were carried out.....	64

CHAPTER I

INTRODUCTION

1.1 Peptidomimetics and Protein-Protein Interactions

At the core of life are protein-protein interactions. Many physiological processes require protein associations or dissociations to take place. Cellular activities such as cell division, information transfer (signal transduction), cell growth and death, cell-cell recognition, and cellular defense require very precise and careful scripting of protein associations.^{1,2} A lot of successful work has been done in elucidating the binding sites (hot spots) via X-ray crystallography and genetic mutations.²⁻⁴ Although protein-protein interactions have been identified as a key area of study in medicinal chemistry, the identification of small molecules that bind favorably to protein hot spots compared to natural ligands has been difficult.⁵ Interest in generating small molecules that can bind to proteins and affect their functions is enormous because developing these compounds will help in finding cures to a lot of diseases that affect humans today.

Unlike natural proteins and peptides, which are usually large molecules, expensive, and very difficult to get into the cell, small molecules can be cheaper and easy to work with. Most of the early work done on mimicry of ligands that bind to receptor proteins focused mainly on the side chains similarities of the binding sites to the small molecules.⁶ The major issue why small molecules do not compete favorably with natural ligands is surface area.⁷ The binding sites for protein-protein interactions have large surface area of about 600 Å².⁸ This allows the proteins to reduce problems caused by solvation, which most of the early work on small molecule peptidomimetics neglected.⁸

This thesis follows the style of the *Journal of Organic Chemistry*.

Now the question is how can chemists overcome solvation problems without resorting to large molecules that will be very difficult to get into the cell? Goodsell and co-workers⁸ found out that most of the protein-protein/peptide interactions involve a hydrophobic core surrounded by a hydrophilic periphery. The hydrophobic center helps the interactions by eliminating the water that solvates the protein and, therefore bringing interacting molecules close together. Based on these observations, molecules with a hydrophobic core and hydrophilic sides were designed. To increase the surface area of the system, many hydrophilic small molecule mimics of peptide side chains were built on a hydrophobic scaffold.

1.2 Tumor Necrosis Factor- α (TNF α) and Receptors

The TNF ligand family are pleiotropic cytokines produced mostly by activated macrophages and lymphocytes.^{9,10} They are made up of 18 genes encoding 19 type II transmembrane proteins, with a conserved trimeric C-terminal domain called the TNF homology domain (THD), which is responsible for receptor binding and has a sequence identity between family members of 20-30 %.^{9,11,12} Type II transmembrane proteins are proteins with an intracellular N-terminus and extracellular C-terminus. Although the ligands are formed as membrane proteins, for cell-cell contact transfer of signaling information between neighboring cells, they have to be cleaved and solubilized to become active cytokines (Figure 1.1).¹¹ Proteases involved in these cleaves are ligand specific. Metalloproteases of the ADAM (a disintegrin and metalloproteinase domain) family act on TNF ligands.^{9,11} Other members of this superfamily include 4-1BB ligand, APRIL, CD 27, CD 30, CD 40, FAS ligand, LT- α (TNF B), LT- β (TNF C) etc.

TNF, in addition to causing necrotic cell death, may also cause apoptotic cell death, cellular proliferation, differentiation, inflammation, tumorigenesis and viral replication.¹¹ Though the primary role of the ligand is immune regulation, they are also known to be heavily involved in pathological disorders like rheumatoid arthritis, asthma, septic shock, irritable bowel disorder, hemorrhagic fever, and cachexia.^{11,13} Most of the works on TNF have focused on disrupting steps in the TNF pathway.^{11,14} Inhibitors of the

actions or production of $\text{TNF}\alpha$ includes some monoclonal antibodies, pentoxifylline, p65 antisense, oligonucleotides, and metalloproteinase inhibitors. Some protein therapies based on soluble recombinant TNF receptor and anti-TNF, humanized monoclonal antibodies, have been approved by the FDA. The recombinant TNF receptor (Etanercept or Enbrel) and the monoclonal antibody (Infliximab or Remicade) are now being used to treat rheumatoid arthritis and Crohn's disease respectively. These therapies are very expensive because of the fact that large proteins are used, hence the need for development of small molecule-based drugs. Figure 1.1 shows an overview of the activation (trimerization) and binding of both the ligands and receptors of the TNF superfamily. These will be discussed in detail in later sections.

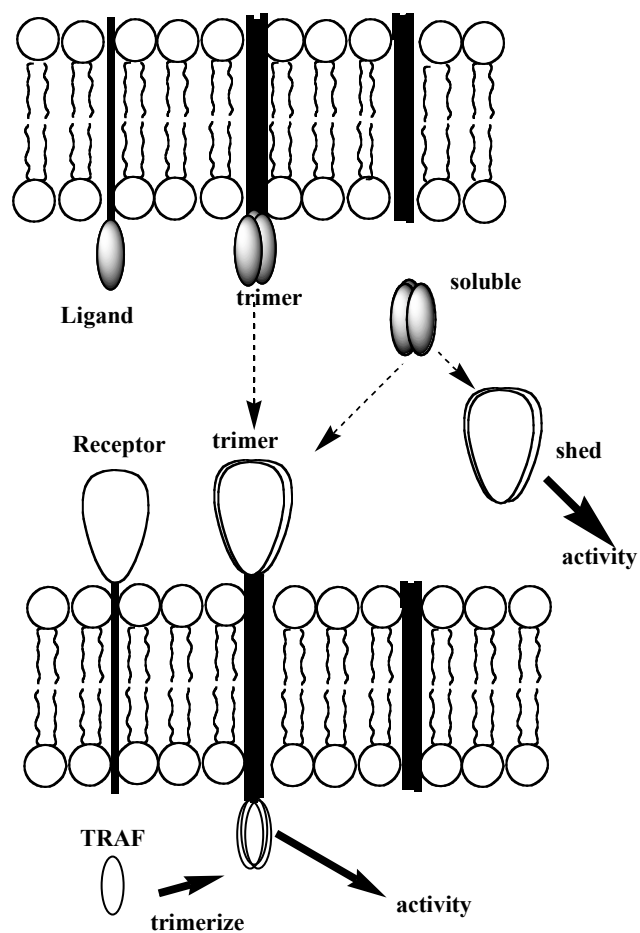


Figure 1.1. TNF superfamily ligand-receptor interactions.

1.2.1 Structure of TNF α

TNF ligand (also called TNF- α , cachectin, differentiation inducing factor DIF, and TNFSF2) is a 26 kDa transmembrane protein.¹⁴ It is cleaved by the metalloprotease TNF α -converting enzyme (TACE) into a 17 kDa soluble TNF form.¹¹ The THD is a 150 amino acid sequence with a conserved framework of aromatic and hydrophobic residues.

The THDs of the superfamily share a virtually identical tertiary fold and associate to form trimeric proteins.¹⁵ They are β -sandwiched structures with two stacked β -pleated sheets which are formed by 5 anti-parallel β -strands that adopt a classical ‘jelly-roll’ topology.^{16,17} The THD trimers (Figure 1.2) are bell shaped truncated pyramids about 60 Å high, with variable loops coming out of the conserved anti-parallel β -strands.⁹ The arrangement of the inner sheets allow for a maximum Vander Waals interaction between the monomers.⁹ TNF contains a single disulfide bridge that links the CD and EF loops (Figure 1.2).^{11,13}

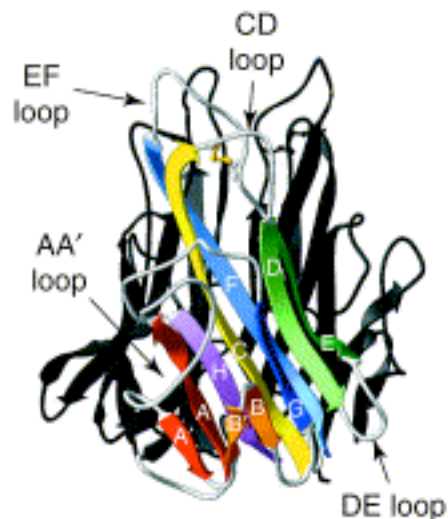


Figure 1.2. Human Tumor Necrosis Factor- α (TNF α)*

*Reprinted with permission from “The molecular architecture of the TNF superfamily” Bodmer, J. L.; Schneider, P.; Tschopp, J. *TRENDS in Biochem. Sci.* **2002**, 27, 19-26. © 2002 Elsevier Science Ltd.

1.2.2 TNF Receptors

The TNF receptors are members of a superfamily of about 29 proteins that are activated by one or more ligands.⁹ They are characterized by extracellular domains of repeated cysteine- rich domains (CRDs) (Figure 1.3) which are involved in binding to the ligands. Most of the TNF receptors are type I (extracellular N-terminus and intracellular C -terminus) transmembrane proteins. Soluble receptors can also be generated by proteolytic activity⁹ or the alternative splitting of the exon encoding the transmembrane domain.^{9,11,18} The soluble receptor are important in modulating the activities of their cognate ligands such as interaction of with TNF that interfere with the inflammatory responses.^{11,19,20}

Some TNF receptor family binds to non-TNF ligands. For instance both NGFR and P75 bind with low affinity to neurotrophins.^{9,21,22} TNF α binds to two receptors (in the receptor family); the TNF Receptor 1 (TNFR1), and the TNF Receptor 2 (TNFR2).^{*} Both TNFR1 and TNFR2 contain an extracellular pre-ligand binding assembly domain (PLAD) which is distinct from the ligand binding region. The PLAD pre-complexes the receptors and helps trimerization particularly upon activation by TNF.¹¹ TNFR1 contains a death domain (DD) motif of about 80 amino acids that induces cell death.¹¹ The DD interacts with a number of proteins that primarily signal cell death. These proteins are prevented from binding to the death domain by the silencer of the death domain protein (SODD).¹¹ The binding of the TNF- α causes a dissociation of the SODD-DD complex and allows other proteins to access the DD module.¹¹ TNFR2 does not have the death domain motif, it signals for cell death through its cytoplasmic domain by inducing mTNF expression which then signals apoptosis via TNFR1.¹¹ TNF- α has a 20-30 times higher affinity to TNFR1 than TNFR2.¹¹ The binding of TNF to TNFR1 also activates various cell activities like inflammation and proliferation via NF κ B, *c-Jun* kinase (JNK), and other proteins.^{9,11,19-21,23}

*TNFR1 is also called p55, p55TNFR, TNFRSF1A, CD120a, TNF-R55, p60, TNF -R-I, TNFAR, and TNFR-b, while TNFR2 is also known as TNFRSF1B, CD 120b, p75, p75TNFR, TNFR-75, p80, TNF-R-II, TNFBR, and TNFR-a.

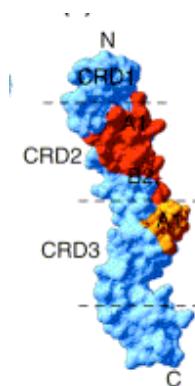


Figure 1.3. Representation of the Cysteine Rich Domains (CRDs) of TNFR1 that are involved in binding to TNF α .*

1.2.3 Hot spots and Interaction of TNF- α with TNFR1

TNF α and LT α (TNF β) are highly homologous proteins which binds to both TNFR1 and TNFR2 to induce biological activities. There is no known crystal structure of the TNF α /TNFR1 complex. The structure of the TNF β and TNFR1 complex which is available (Figure 1.4a), was used to study the binding of TNF α and TNFR1 since TNF α and TNF β are homologous.²⁴ With some adjustments the interaction of TNF α and TNFR1 was proposed to involve turn regions of the ligand as shown in Table 1.1 and Figure 1.5. This is consistency with results of from site directed mutagenesis studies.^{16,25,26} Figure 1.4b shows the TNF and TNFR1 interaction and the critical binding site on the receptor.²⁴

*Reprinted with permission from “The molecular architecture of the TNF superfamily” Bodmer, J.-L.; Schneider, P.; Tschopp, J. *TRENDS in Biochem. Sci.* **2002**, 27, 19-26. © 2002 Elsevier Science Ltd.

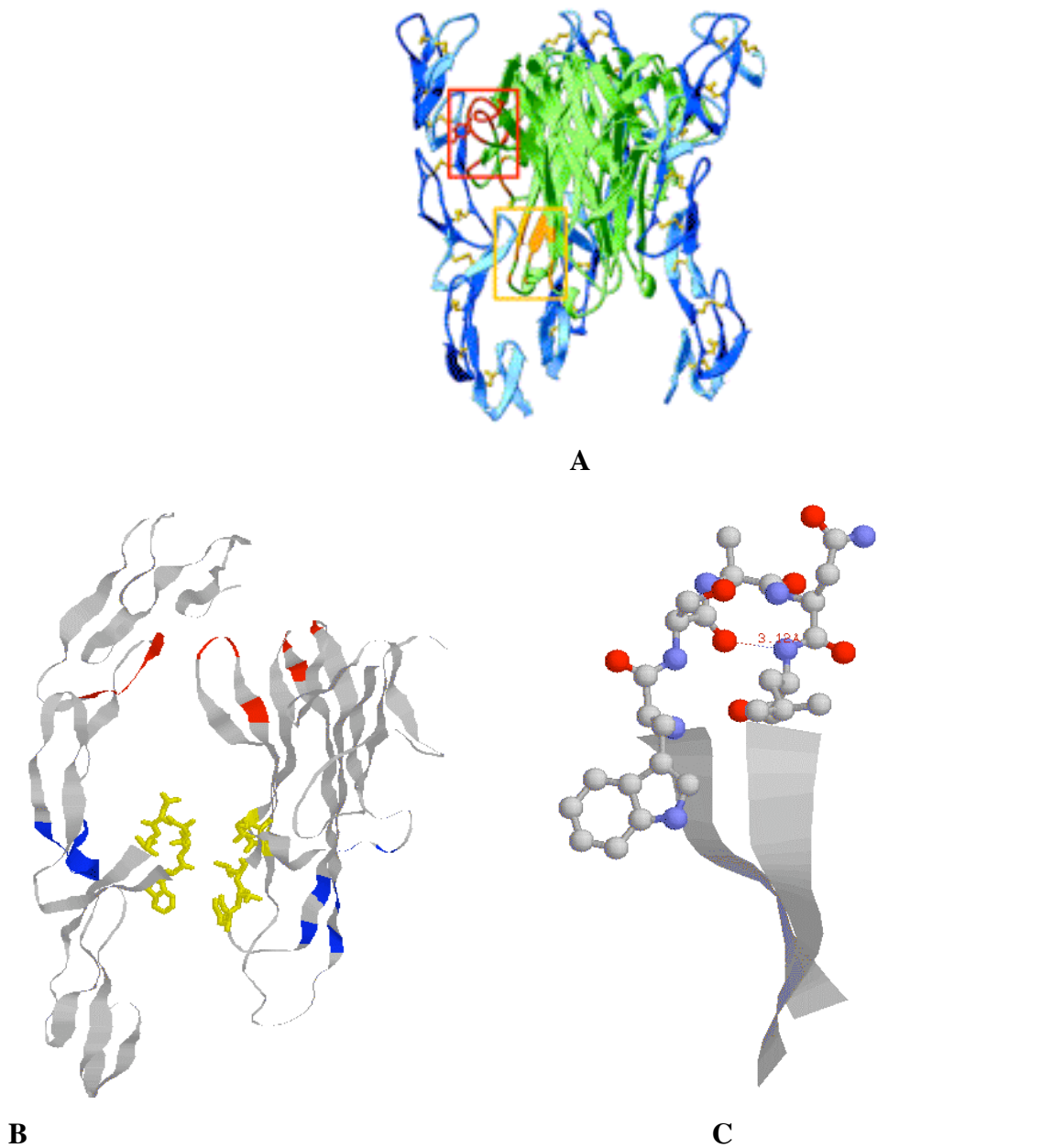
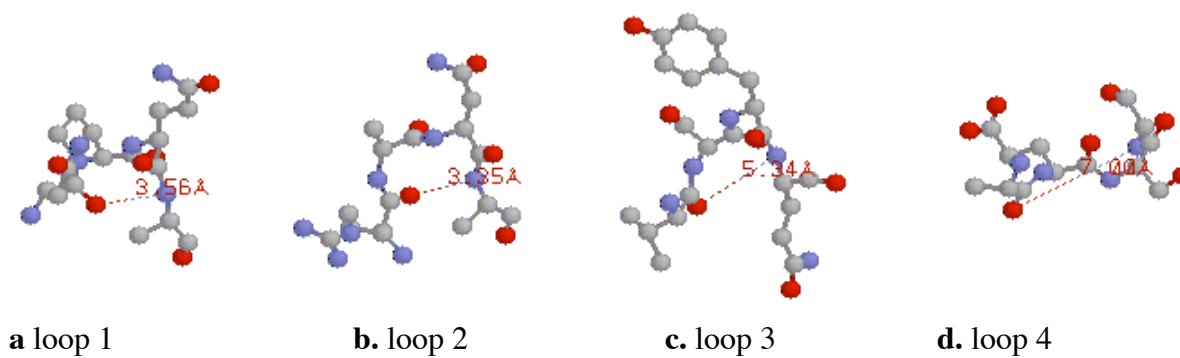


Figure 1.4. (a) Crystal structure of TNF β /TNFR1 complex. TNF β in green, TNFR1 in blue, and the two interaction surfaces in red and orange.* (b) Structural view of TNF α and receptor interactions (an interaction surface in yellow). (c) Loop 1 of domain 3 of the TNFR (the critical binding site).

*Reprinted with permission from “The molecular architecture of the TNF superfamily” Bodmer, J.-L.; Schneider, P.; Tschopp, J. *TRENDS in Biochem. Sci.* **2002**, 27, 19-26. © 2002 Elsevier Science Ltd.

Table 1.1. Sequences of turn regions in TNF α postulated for binding to TNFR1.

Loop: residues	i	i + 1	i + 2	i + 3
1: 19 – 22	Asn	Pro	Gln	Ala
2: 32 – 35	Arg	Ala	Asn	Ala
3: 85 – 88	Val	Ser	Tyr	Gln
4: 145 – 148	Ala	Glu	Ser	Gly

**Figure 1.5.** Local conformations of the TNF α β -turn regions 1 – 4.

1.2 Neurotrophins and Their Receptors

Neurotrophins are a family of dimeric proteins that regulate differentiation and survival of neurons of the central and peripheral nervous systems.²⁷⁻²⁹ There are four members of this protein family; nerve growth factor (NGF), neurotrophin-3 (NT-3), brain-derived neurotrophic factor (BDNF), and neurotrophin-4/5 (NT-4/5), each controlling distinct neuronal populations.²⁷⁻³⁰ These and other biological activities of the neurotrophins depend on their interactions with their transmembrane receptors, namely tyrosine kinases (Trk) and TNFR2 (p75). Abnormalities of NGF and other neurotrophins are thought to be directly implicated in neurodegenerative diseases such as Alzheimer and Parkinson's diseases, and certain types of cancer.^{28,31,32} This has led to efforts to understand their structures and function to develop therapeutic agents to treat these important diseases.

Docking of the neurotrophins to their respective receptors induces dimerization of these receptors which causes activation of cell signaling processes.^{27,33} Neurotrophins bind to Trk selectively with high affinity ($K_d \sim 10^{-11} \text{M}$).³⁴ Figure 1.6 shows that NGF binds specifically to TrkA,³⁵ while BDNF and NT-4/5 are specific to TrkB.^{36,37} NT-3 interacts with all the Trk receptors but it is more selective for TrkC,^{33,36} All neurotrophins bind to the p75 receptor with lower affinities ($K_d \sim 10^{-9} \text{M}$) than their interactions with Trk receptors.³⁸⁻⁴⁰

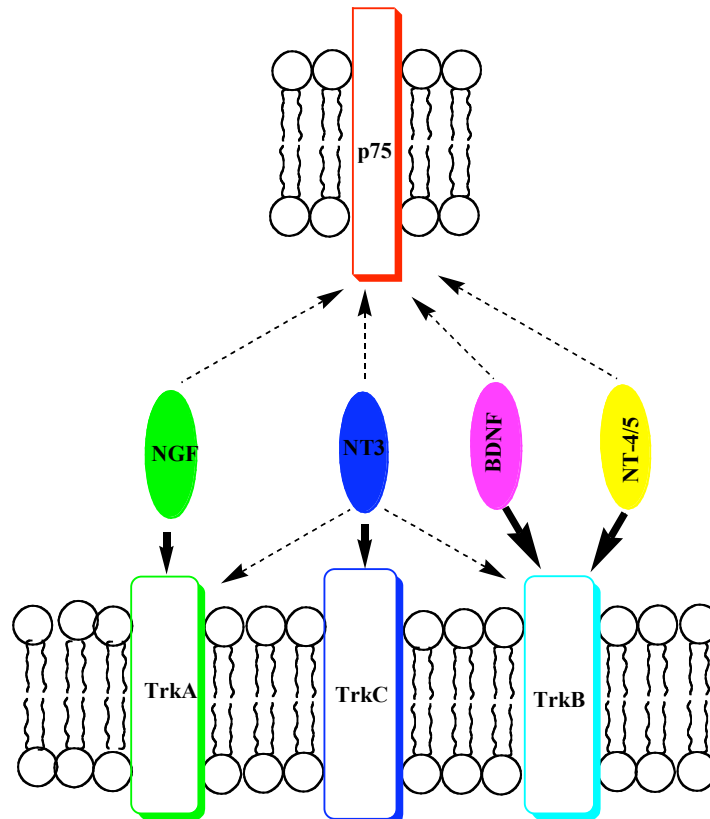


Figure 1.6. Relationships of neurotrophins and their receptors.

1.3.1 Structure of Neurotrophins

Neurotrophins are members of the cystine knot superfamily, a group of proteins that share a common structural feature of three disulfide bridges. They are approximately 25 kDa proteins that exhibit high sequence homology (more than 50 % identical) and exist exclusively as dimers.^{27,28} Each monomer (Figure 1.7) consists of three antiparallel pairs of β -strands connected with four β -hairpin loops, with three disulfide bonds forming the core of the structure (cystine knot). Hydrophobic residues along the β -strands stabilize the dimer form of the proteins. The residues along the β -strands help in maintaining the proteins fold structure. While highly variable residues in the *N*-termini, *C*-termini, and turn regions are thought to be involved in receptor binding and activation.^{27,41,42}

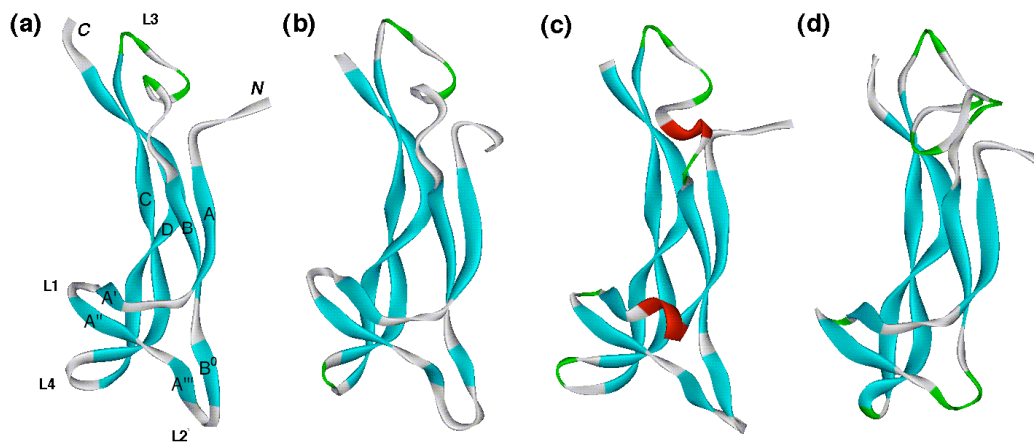


Figure 1.7. Structure of neurotrophins (a) NGF, (b) NT-3, (c) BDNF, (d) NT-4/5.*

1.3.2 Structure of Neurotrophin Receptors

The sequences of the Trk family receptors are highly homologous.³³ Although the complete three-dimensional structure of any Trk receptors is unknown, their extracellular domains have been classified into five sub-domains based on sequence similarities to other known receptors (Figure 1.8).⁴³ These sub-domains made up of two cysteine rich clusters (sub-domain 1 and 3), with leucine-rich motif (sub-domain 2) between them, and two immunoglobulin (Ig)-like domains (4 and 5), located close to the membrane.^{33,37,44} The intracellular domain contains a phosphorylation site, which upon activation, triggers downstream signaling pathways that mediate neurite outgrowth, neuronal differentiation, or survival.⁴⁵⁻⁴⁷

The p75 receptor (TNFR2) is a member of the tumor necrosis factor (TNF) receptor superfamily, which has been discussed in the TNF receptor section. The exact roles of the p75 receptor are not known, but it was shown that this receptor could induce various responses depending on the cellular context in which it is expressed.

*Reprinted with permission from “Molecular Basis of Neurotrophin – Receptor Interactions” Mookda Pattarawarapan and Kevin Burgess; *Journal of Medicinal Chemistry* **2003**, 46, 5278. © 2003 American Chemical Society.

Binding of neurotrophin to p75 can cause apoptosis in cells that over expressed the receptor,⁴⁸⁻⁵⁴ It can also work in cooperation with Trk to mediate Trk activities at low neurotrophin concentration in cells that co-express both the receptors.^{34,38,45,55,56}

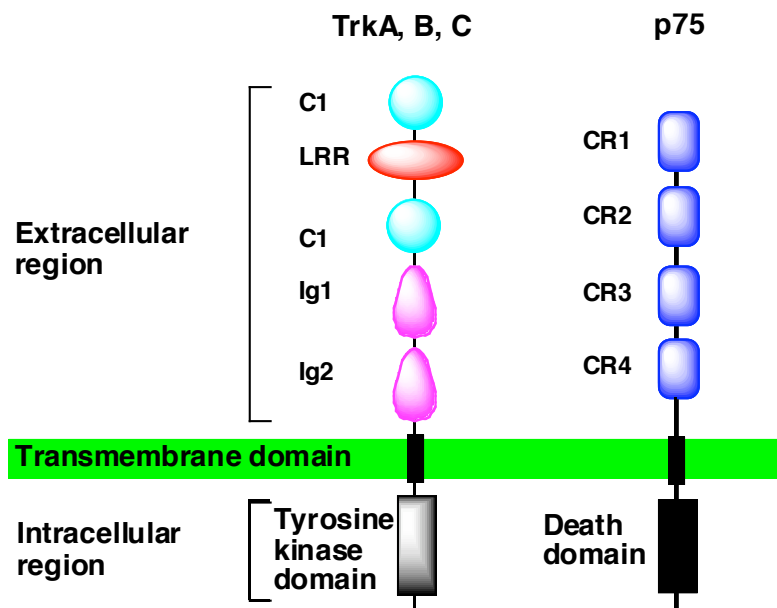


Figure 1.8. Schematic representation of neurotrophin receptors; Trk and p75*

1.3.3 Hot Spots and Interaction of NGF and Receptors

NGF is the most studied neurotrophin. These studies involve extensive site-directed mutagenesis experiments,⁵⁷⁻⁶⁹ and crystal structures for NGF,^{70,71} its receptor (TrkA-d5)⁴ and NGF/TrkA-d5 complex.⁷² The mutagenesis experiments have revealed *N*-terminus to be the most important region for NGF specificity to TrkA.^{57,61,63,63,60} The *C*-terminal residues (112-118) are also shown to be essential for receptor activation.^{57,64} Mutations of the β -hairpin loops have been shown to affect binding of NGF to TrkA.⁶⁰

*Reprinted with permission from "Molecular Basis of Neurotrophin – Receptor Interactions" Mookda Pattarawarapan and Kevin Burgess; *Journal of Medicinal Chemistry* **2003**, 46, 5278. © 2003 American Chemical Society.

Point mutations studies show that residues 48-49 in loop 2 and 96-98 in loop 4 also induce NGF-like activity when substituted into NT-3 skeleton.^{68,69} Scattered points in the β -strand bundles are important for binding to TrkA.^{59,66} The charged residues located on two discontinuous regions of the ligand are important in binding to p75 as shown by alanine mutation of three lysine residues (K32, K34 in loop 1 and K95 in loop 4), loop 3 (D72, K74, H75) and the C-terminus (111-115).^{58,64,65,73,74}

Crystallographic analysis of NGF/TrkA-d5 complex supports the results from mutagenesis studies that residues in the *N*-terminus and along the β -sheet regions can contribute significantly to the binding of NGF to TrkA.⁷² The crystal structure reveals two ligand-receptor binding interfaces (Figure 1.9a). The region involving the *N*-terminus (residues 2-13) of NGF, adopts a single helix structure upon complexation with the hydrophobic pocket on the 'ABED' sheet of TrkA. This interface was called the "specific patch" (Figure 1.9b), which implies that the *N*-terminus of NGF governs specificity for binding to TrkA.³⁹ The other region involving NGF residues along the β -strand bundle and in loop 1 (30-35) packs against the loops at the C-terminal end of TrkA-d5. This interface was called the "conserved patch" (Figure 1.9c) because residues in this region are highly conserved in all the neurotrophins.⁴³

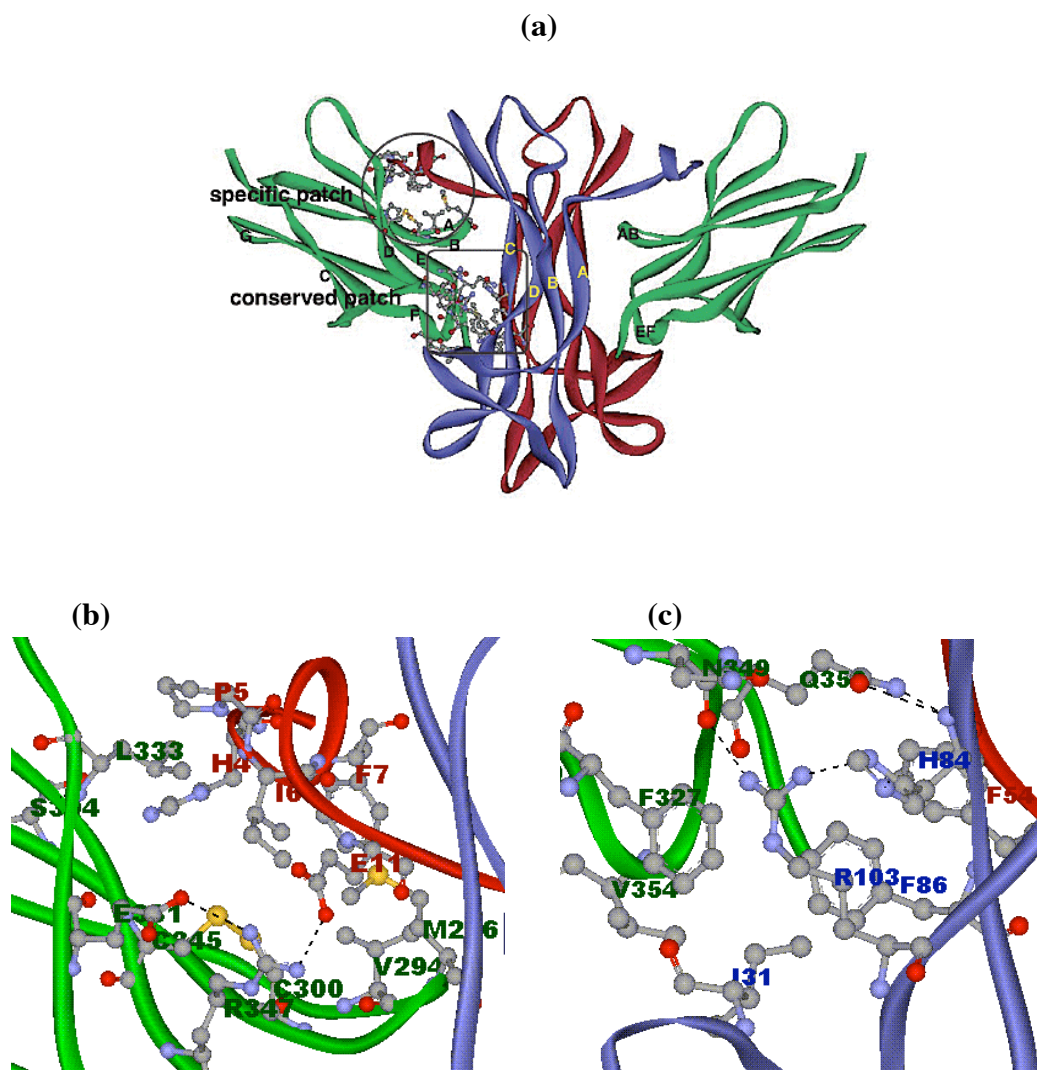


Figure 1.9. NGF/TrkA-d5 complex. (a) The binding epitopes of NGF to TrkA-d5, (b) the specific patch, (c) the conserved patch. NGF monomers are in blue and red; TrkA-d5 is in green.*

*Reprinted with permission from “Molecular Basis of Neurotrophin – Receptor Interactions” Mookda Pattarawarapan and Kevin Burgess; *Journal of Medicinal Chemistry* **2003**, 46, 5278. © 2003 American Chemical Society.

1.3.4 Interactions of NT-3 with TrkC and p75

The crystallographic structure of the complexation of NT-3 and TrkC has not been reported, but the crystal structures of NT-3 and the fifth domain of TrkC is known. Mutagenesis studies have revealed key structural information concerning the hot spots that seem to determine NT-3 affinity to TrkC and p75.^{62,68,73,75}

Interaction of NT-3 with TrkC seems to be different from the NGF/TrkA binding. It was found from replacement experiment, that the *N*-terminus of NT-3 is not essential for binding of NT-3 to TrkC.⁶⁰ Residues on the central β -strand bundles are shown to cause maximum effect on TrkC binding after mutation.^{73,75} Alanine mutation of R103 of NT-3 indicates that R103 is the most important binding determinant for association with TrkC.⁷³ Hydrophilic residues along the β -strands (T22, Y51, E54, R56, K80 and Q83) were also identified from alanine scanning mutagenesis to be critical for TrkC binding affinity and activity.⁷³ Replacing residues in the loop regions of NT-3 with corresponding residues from NGF does not sufficiently affect NT-3 activities.⁷⁵ But, replacing loop of NGF with corresponding loop of NT-3 induces TrkC activities.⁶⁸ This means that the loop region plays somewhat a role in NT-3 binding to TrkC.

Just like in NGF, the key recognition elements of NT-3 for binding to the p75 receptor have also been found via mutagenesis, to be the positively charged residues.^{74,76} These residues included R31, H33, Q34 in loop 1 and K73 in loop 4.^{73,74} Figure 1.10 shows the critical residues for NT-3 binding to its receptors.⁷⁶

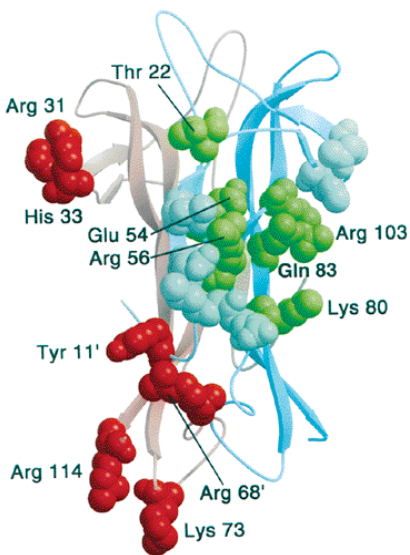


Figure 1.10. Binding epitopes of NT-3 to TrkC (red) and p75 receptor (green).*

1.3.5 Structure Based Design of Functional Mimics of Neurotrophins

Neurotrophins, large polypeptides that play important role in regenerating the central and peripheral neurons during and after neuronal damages, are very valuable in the treatment of neurodegenerative diseases.^{28,31,32} These hormones are not efficient therapeutic agents due to poor bioavailability (ie proteolytic instability and low blood brain barrier permeability) .⁷⁷ Furthermore, they are expensive and can partially bind to multiple receptors thereby causing pleiotrophic effects. Hence the need for stable bioavailable small molecules that can selectively activate or inhibit the activities of the Trk receptors.

Small molecule ligands that can mediate NGF responses (Figure 1.11) have been identified via high throughput screening, but none have been reported for the other members of neurotrophin family. These small molecules do not interact directly with

*Reprinted with permission from “Crystal Structure of Neurotrophin-3 Homodimer shows distinct regions are used to bind to its Receptors” Butte, M. J.; Hwang, P. K.; Mobley, W. C.; Fletterick, R. J. *Biochemistry* **1998**, 37, 16846-52.

TrkA receptor, they function through indirect mechanisms.⁷⁸⁻⁸⁴ Small molecules related to cyclosporins such as GPI-1018 (**A**) mimic NGF responses, but do not act on either of the receptors (p75 and TrkA) and do require expression of them. They bind and affect immunophilins.^{80,81} SR57746A (**B**) induces NGF activities by increasing production and release of NGF.⁷⁹ NG-061 (**C**) was shown to enhance and mimic trophic effects of NGF, with no evidence that it binds to TrkA.⁷⁸ Kyanurenic acid derivatives such as **D** have been shown to inhibit the NGF/p75 interaction by binding to NGF.⁸² The K-252a (**E**) binds to an unknown target downstreaming the signal transduction pathway.⁸³ ALE-0540 (**F**) was found to acts as competitive inhibitor of NGF for binding to p75 and TrkA.⁸⁴ It is believed that this compound does not bind to NGF but no direct binding to TrkA is evident. Although these compounds are active antagonists of NGF, they are none specific to neurotrophin receptor. Hence they can cause severe side effects if used as therapeutic agents.

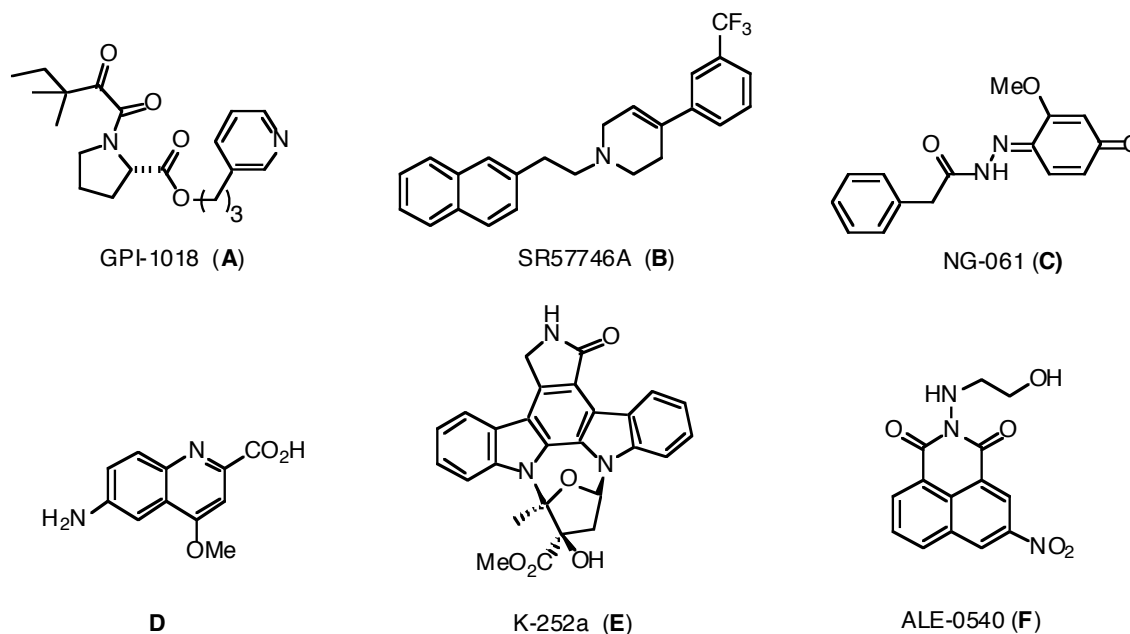


Figure 1.11. Structures of compounds **A-F**.

Alternatively, structure based designing of neurotrophin analogs can be used to develop compounds that are receptor specific. The sequence diversity observed on the loop regions of the neurotrophins suggests that these turns are important in defining the specificities of the hormone to the Trk receptors. Many cyclic peptides derived from

these loop regions have been shown to function via the neurotrophin receptors. Disulfide-linked cyclic hexapeptides based on NGF loops 2 (43-48) and 4 (92-97) have been shown to antagonize NGF by associating with TrkA and possibly p75.⁸⁵⁻⁸⁷ Other cyclic peptides derived from NGF have been reported to bind to p75, while those from the loop regions on BDNF were found to be BDNF antagonists.⁸⁸⁻⁹¹ Only the cyclic compounds with β -turn conformations are active, the respective linear analogs exhibited no response.^{92,93} This means that β -turn conformations are important in biological activities of these mimics. Therefore, it is important to investigate the possibility of using β -turn mimetics as a tool to mediate neurotrophin responses. Such molecules can be useful in therapeutic applications and can also provide means to understand molecular basis of neurotrophin/receptor interaction. Tables 1.2 and 1.3 show the amino acid sequences of the turn regions of the neurotrophins that we are interested in.

Table 1.2. Sequences of turn regions in NGF.

Source	Loop: residues	i	i +1	i + 2	i + 3
Human					
	1:30-33	Asp	Ile	Lys	Gly
	2: 44-47	Ile	Asn	Asn	Ser
	3: 93-96	Asp	Gly	Lys	Gln
Murine					
	1:30-33	Asp	Ile	Lys	Gly
	2: 44-47	Ile	Asn	Asn	Ser
	3: 93-96	Asp	Glu	Lys	Gln
Bovine					
	1:30-33	Asp	Ile	Lys	Gly
	2: 44-47	Ile	Asn	Asn	Ser
	3: 93-96	Asp	Asn	Lys	Gln
Guinea pig					
	1:30-33	Asp	Ile	Lys	Gly
	2: 44-47	Val	Asn	Asn	Asn
	3: 93-96	Asp	Gly	Lys	Gln

Table 1.3. Sequences of turn regions in NT-3.

Source	Loop: residues	i	i + 1	i + 2	i + 3
Human					
	1:29-32	Asp	Ile	Arg	Gly
	2: 42-45	Lys	Thr	Gly	Asn
	3: 92-95	Glu	Asn	Asn	Lys
Mouse					
	1:29-32	Asp	Ile	Arg	Gly
	2: 42-45	Lys	Thr	Gly	Asn
	3: 92-95	Glu	Asn	Asn	Lys

1.4 Insulin-like Growth Factor and Receptors

The insulin-like growth factor (IGF) system comprises of two ligands (IGF-I and IGF-II), two receptors (IGF-IR and IGF-IIR) and at least six distinct binding proteins.^{94,95} The IGF-I and IGF-II promote growth and differentiation of neurons and glial cells in the central nervous system.⁹⁴ Both IGF-I and IGF-II bind to IGF-IR with high affinity ($K_d = 1.5$ and 3.0 nM respectively).⁹⁴ The IGF-I receptor is a heterotetrameric glycoprotein composed of four subunits (2 α and 2 β) linked together by disulfide bridges.^{94,95} The IGF-II receptor is a monomeric receptor with extracellular domain made of 15 repeating cysteines and is identical to the cation-independent mannose-6-phosphate receptor.⁹⁴ The IGF binding proteins (IGF-BPs) are multifunctional proteins that regulate the activities of the insulin-like growth factor (IGF).^{94,96} They play crucial roles in the transportation of IGFs in the blood stream, cerebrospinal fluid, and across the capillary barriers to the target cells.^{95,97-100} IGF-BP-3 and IGF-BP-5 also associate with an acid labile subunit (ALS), thereby increasing the half-life of IGFs.⁹⁴ IGF-BPs are present in the extracellular matrix or cell surface where they can enhance or inhibit IGF activities.⁹⁸ They are also involved in a host of other IGF independent cellular activities.^{94,98,101}

1.4.1 Interactions of IGF-I with IGF-IR or IGF-BPs

The IGFs and insulin consist of a small hydrophobic core formed by three helices stabilized by three disulfide bonds. The disulfide bonds in the single-chain IGFs are intramolecular while they connect the A and B chain in insulin.^{95,96} The A and B regions of the IGFs are connected by a loop known as the C-region (IGF-I; residues 29-41, Figure 1.12). This loop is found to be largely responsible for binding specificity of the IGF-IR for IGF-I.⁹⁶ Mutation of Try 31 reduces the affinity of IGF-I for IGF-IR but has no effect on its binding to either IR or IGF-BPs.⁹⁵ The crystal structure of the IGF-I shows that C-region forms a type II β -turn. The B helix forms a type II' β -turn, which redirects the backbone of the B-helix into an extended region as shown in Figure 1.12. Residues 24-27 form a type VIII β -turn, allowing the C-region to extend away from the core of the molecule forming a type II β -turn (30–33) with Try 31 prominently exposed at the $i+1$.⁹⁶

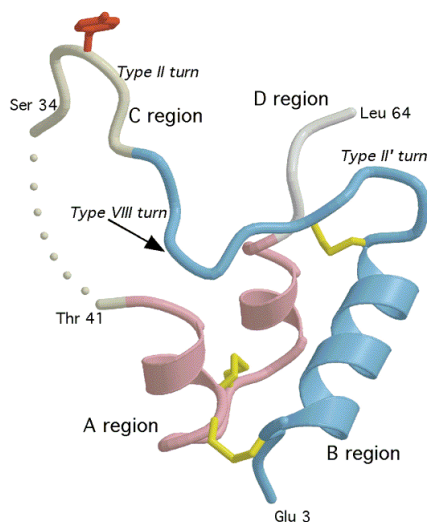


Figure 1.12. Ribbon structure of IGF-I. The B-region (residues 3-28) shown in blue, the C-region (residues 29-41) in light yellow, A-region (residues 42-62) in pink, and the D-region (residues 63 and 64) in white. The disulfide bonds in yellow.*

* Reprinted with permission from “Crystal Structure of Human Insulin-like Growth Factor-1: Detergent Binding Inhibits Binding Protein Interactions” Vajdos, F. F.; Ultsch, M.; Schaffer, M. L.; Deshayes, K. D.; Liu, J.; Skelton, N. J.; de Vos, A. M. *Biochemistry* **2001**, 40, 11022-11029. Copyright 2001 American Chemical Society.

There are no crystal structures for the IGF-I/IGF-IR complex because the IGF receptor is a large trans-membrane protein, which is difficult to isolate and crystallize. The structures of the IGF complexes with IGF-BPs are available.^{94,96,101,102} These crystal structures, in addition to mutagenesis and NMR studies have been used to elucidate the hot-spots on the IGF-I. Site directed mutagenesis studies mapping the binding sites of IGFs for IGF-IR and insulin receptor (IR) show that Tyr 60, Try 24, Phe 23, and Val 44 are the major determinants for binding in IGF-I.⁹⁵ Also Phe 25 and Arg 21 are important in the IGF-I binding.⁹⁵ Structural studies on the miniNBP-5/IGF-I* complex indicate that Phe 23, Try 24, Phe 25, Val 44 and Try 60 form a fully solvent-exposed hydrophobic binding site for IGF-IR that is located on the opposite side of the IGF that is used to bind to miniIGFBP-5.⁹⁵

The binding of NBP-4, which was found to inhibit the binding of IGF-I to its receptor was studied (Figure 1.13). The *N*-terminus of the NBP-4 was found to interact with the Phe 23, Tyr 24 Phe 25 of the IGF-I by filling the hydrophobic cleft and backbone C=O...NH H-bonding between the interacting proteins.⁹⁵

*NBP-5 refers to the N-terminal Domain of IGFBP-5 miniNBP-5 is a polypeptide from the NBP-5.

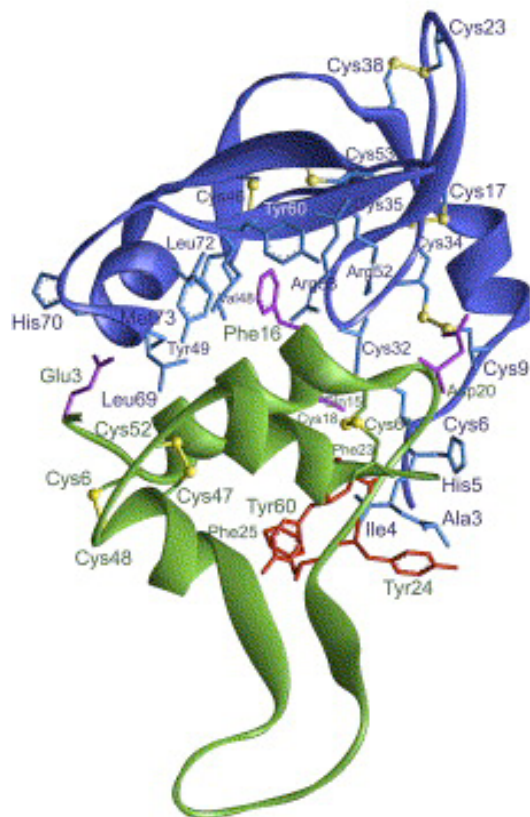


Figure 1.13. Ribbon plot of NBP-4 (blue) and IGF-I (green) complex. Residues shown in violet constitute the binding site for interaction with NBP-4 and those shown in red are determinants for binding to IGF-IR.*

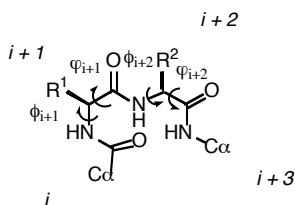
1.5 β -Turn Mimetics

β -turns are found in many of the ‘hot spots’ for molecular recognitions in proteins.^{103,104} Contacts between proteins in the immunoglobulin family, growth factors and adhesion molecules are known to often involve turn residues. Therefore, β -turns can be used as scaffolds in ligand design. β -Turns are composed of four amino acid residues i to $i+3$ where a peptide chain reverses its direction.¹⁰⁵ These turns are often stabilized by

*Reprinted with permission from “Structural Basis for the Regulation of Insulin-like Growth Factors by IGF Binding Proteins” Siwanowicz, I.; Popowicz Grzegorz, M.; Wisniewska, M.; Huber, R.; Kuenkele, K.-P.; Lang, K.; Engl Richard, A.; Holak Tad, A. *Structure* **2005**, 13, 155-67. © 2005 Elsevier Ltd

a 10-membered intramolecular hydrogen bond between the CO_{*i*} and the NH_{*i*+3} residues. β -Turns can be classified into subtypes based on torsional angles of the middle dipeptide backbones as shown in Table 1.4.¹⁰⁴ Types I and II are the most common in proteins.

Table 1.4. Classification of β -turns



β -turn type	backbone torsional angle (°)			
	ϕ_{i+1}	ψ_{i+1}	ϕ_{i+2}	ψ_{i+2}
I	-60	-30	-90	0
I'	60	30	90	0
II	-60	120	80	0
II'	60	-120	-80	0
IV	bend with two or more angles with $> \pm 40$ from above turn			
VIa	-60	120	-90	0
VIb	-120	120	-60	0
VIII	-60	-30	-120	-120

Efforts have focused on design and development of β -turn mimetic of proteins. Many turn mimics have been based on mono- and bicyclic systems, designed to replace the turn hydrogen bond with covalent bond while retaining the side chain topology of the *i*+1 and *i*+2 residues (Figure 1.14).¹⁰⁶⁻¹¹³ The critical side chains corresponding to the target turn are difficult to be incorporated into these mimetics, and the synthetic methods used to obtain these compounds makes it difficult for them to be incorporated into efficient production of libraries.^{112,114,115}

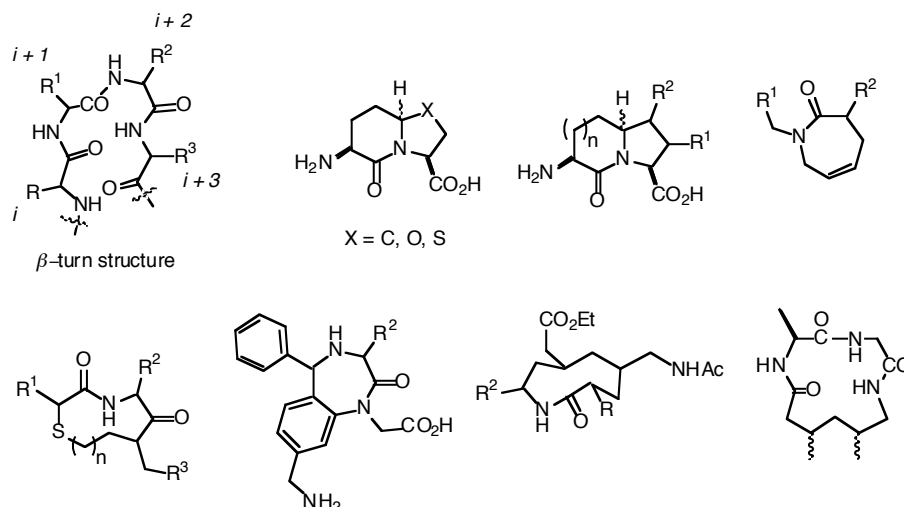


Figure 1.14. β -turn structure and the selected examples of β -turn mimetics.

In addition to synthetic ease, β -turn mimetics should be reasonably rigid to avoid entropic penalty upon binding to target proteins. They should also be able to withstand proteolytic activities in the cell. Our goal is to design and develop efficient solid-phase and solution-phase synthetic methods for β -turn peptidomimetics. Our original design concept is based on “ring-fused C^{10} ” macrocyclic systems as shown in Figure 1.15.¹⁰⁸ These molecules are inspired by cyclic hexapeptide in turn-extended-turn conformations, but designed so that the extended part would be replaced by non-peptidic turn inducer moieties. The turn inducers force turn conformation and improve bioavailability of the molecules.

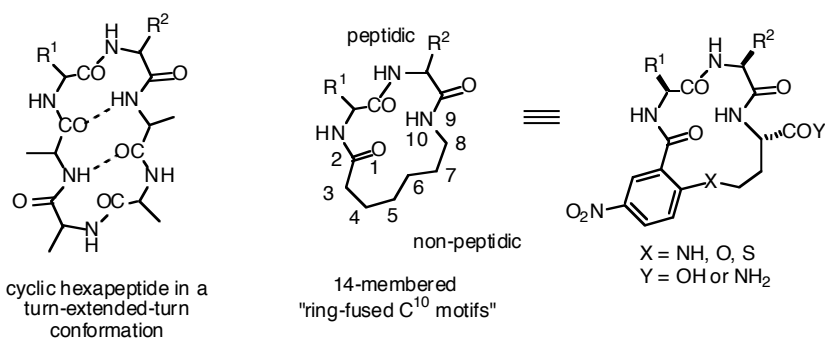


Figure 1.15. Comparison of cyclic hexapeptide with ring-fused C^{10} motif.

A more constrained peptidomimetics have been made by replacing the template amino acid with more rigid, non-peptidic turn inducing moieties. Reduction of peptidic character can improve bioavailability of the mimics and also provide more reliable model of bioactive conformation to be used to develop later generations of therapeutic candidates. Efficient solid-phase syntheses of these analogs have been developed. The synthesis, conformation studies and their biological activities have been published. In order to further improve the bioavailability of these compound, replacement of the natural peptidic parts of the C¹⁰ system with peptoids was employed. The synthesis and characterization of these peptoids is discussed in chapter II.

1.6 Multivalent Ligands

Due to their size, small molecule ligands tend to exhibit low selectivity and weak binding since ligand/receptor interaction generally involves a large surface area. Even though tight binding requires a relatively small fraction of a key region. Fesik and others have demonstrated that two small molecules that bind a protein weakly can be linked to form higher affinity bifunctional ligands.¹¹⁶⁻¹²³ This idea could be used to obtain functional mimic of NGF and NT-3. Since activation of Trk receptor requires dimeric neurotrophins, monovalent turn analogs of neurotrophins are expected to be either antagonistic or inactive. However, work in our group has shown that many monomeric β -turn mimetics can act as partial TrkA and TrkC agonists via synergizing with neurotrophins. This suggests that a more complicated molecular pathway may be involved. It is interesting to explore how bivalent turn analogs interact with receptors. It is predicted that bivalent turn analogs that bind to one Trk molecules could be more potent antagonist and those that bind on two Trk molecules could gain full agonistic activities. Indeed, dimers of cyclic peptides or large loops mimicking two turn regions of NGF have been shown to be TrkA agonists whereas those related monomeric compounds exhibited antagonistic responses.^{48,124,125} In addition to improving the activities of ligands, dimerization also increases the library pool of ligands from the existing pool (Figure 1.14).

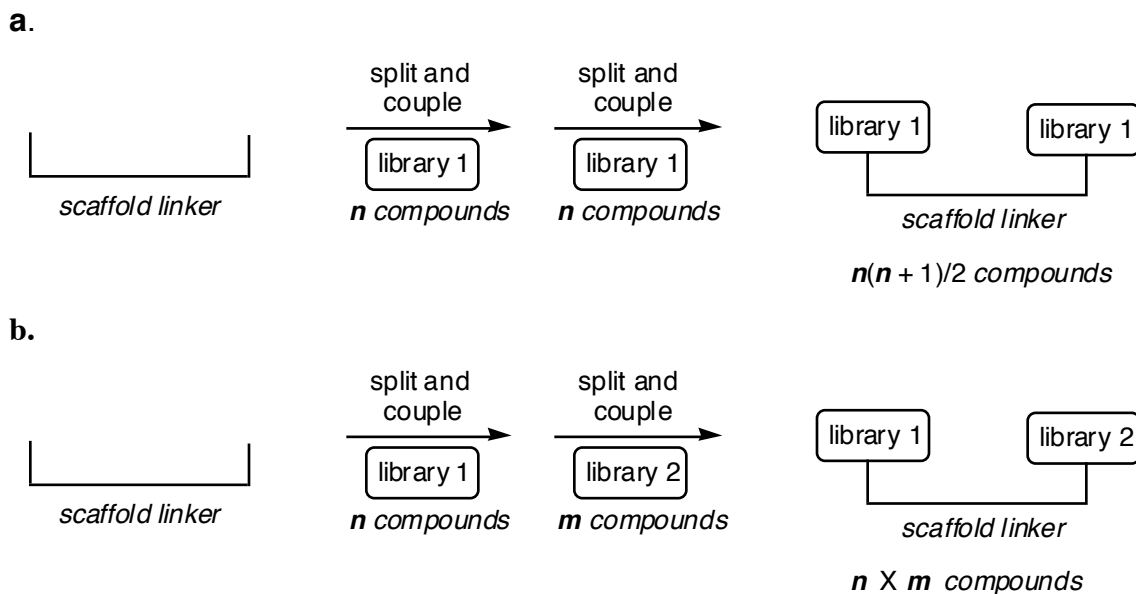
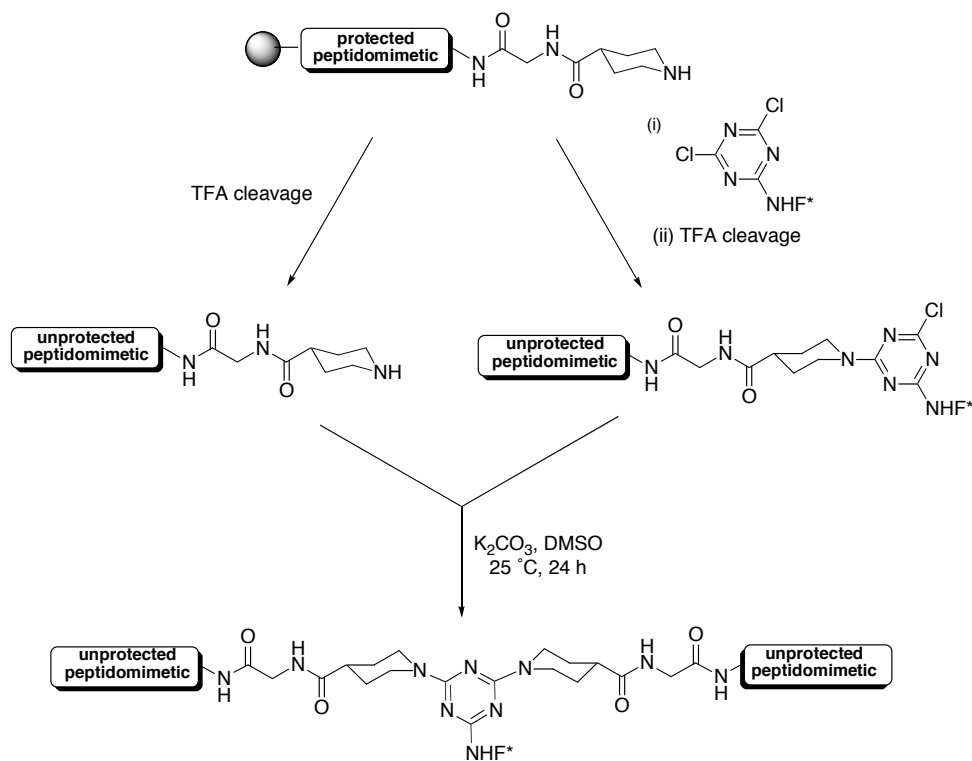


Figure 1.16. (a) Production of homodimeric libraries from monomeric libraries, and (b) production of heterodimeric libraries from monomeric libraries.

There are many approaches reported for preparation of bivalent and multivalent peptidomimetics. The approach shown in Scheme 1.2 involves solution-phase chemoselective linkage of unprotected peptidomemetics using triazine scaffold. This is the most efficient approach and is being used in our group today to develop bivalent ligands. The beauty of this technique does not only lie on the fact that the dimerization reaction is so clean that no purification is needed, it can also be applied to both solid phase and solution phase monomers.

Scheme 1.1. Triazole-scaffold dimerization.



Using this method, bivalent compound **KB536** (Figure 1.15) was synthesized and was found to bind TrkA with an impressive dissociation constant of 20 ± 20 nM in a competitive binding assay with radiolabeled NGF (see chapter III). This result indicates that dimerization can greatly improve the activities of peptidomimetics.

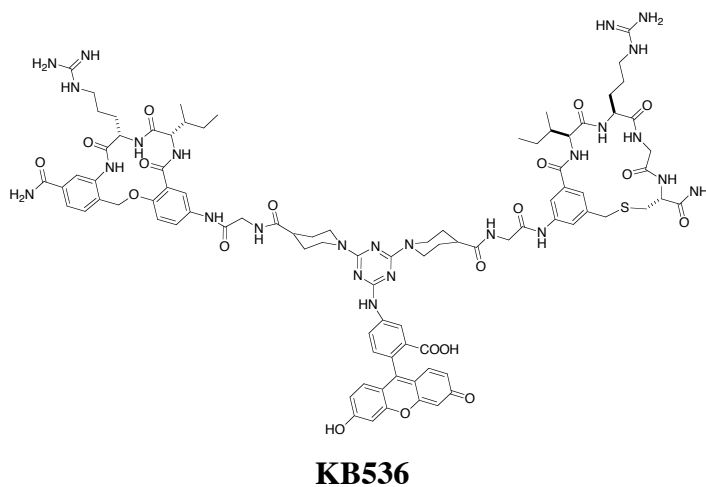


Figure 1.17. Bivalent peptidomimetic with $K_d = 20 \pm 20$ nM.

1.7. Summary

The importance of protein-protein interaction to biological systems cannot be over emphasized. Hence the great interest in this area of research. Due to the large size of most proteins and natural ligand involved, most researchers have focused on the development of small molecule ligands that can interact with receptor proteins and trigger physiological activities.

Research in our group has focused on synthesis of turn mimics of neurotrophins and TNF α . Peptidomimetics that interact favorably with Trk receptor have been made. These peptidomimetics are C¹⁰ β -turn mimics that contain a peptidic turn part and non-peptidic constrained region. Due to the fact that these peptidomimetics contain natural peptides, they are less likely to survive proteolytic activities in cell.

In order to overcome proteolytic activities, peptidomimetics that does not contain natural peptides are needed. One way to achieve this goal is development of peptoids. Peptoids are proven to resist proteolytic activities. Chapter II discusses the synthesis, characterization, and conformational analysis of peptoid libraries.

CHAPTER II

CYCLIC SEMI-PEPTOID TURN MIMICS

2.1 Introduction

Progress in genomics and proteomics has led to development of small molecules that play roles in activating or disrupting protein association, and other biological activities. Many groups have shown interests in synthesis of mimics of protein secondary structures such as α -helices and β -turns.¹²⁶⁻¹²⁸ Our group is interested in peptidomimetics that mimic β -turns of neurotrophins and TNF α . We focus on 14-membered macrocycles that involve dipeptides on the $i + 1$ and $i + 2$ region and a non-peptidic region to constrain the compound, thus reducing entropy on binding.^{108,129,130} Although compounds made in our group using the above idea have proven to be biologically potent, the need to develop compounds that are less peptidic, that could further diversify our library is crucial. An obvious step is to develop non-peptidic molecules with the same motif as the active peptides, which can increase the bioavailability without paying so much price for the activity. We decided to develop peptoid macrocycles that retain the same backbones as the tested peptides.

Peptoids have become increasingly used today in medicinal chemistry to mimic protein secondary structures, such as α -helix, and β -sheets.¹³¹⁻¹³³ They have also been employed in the mimics of nucleic acids and as affinity ligands in protein separations.¹³³⁻

136

2.2 Methods in Peptoids Synthesis

With the discovery of peptoids as a good substitute for natural peptides in drug discovery, chemists have focused over the years on development of efficient synthetic methods that could be used for large libraries of peptoid compounds. Various methods involve either solution-phase synthesis or solid-phase synthesis, although solid-phase synthesis appears to be the most prevalent approach.

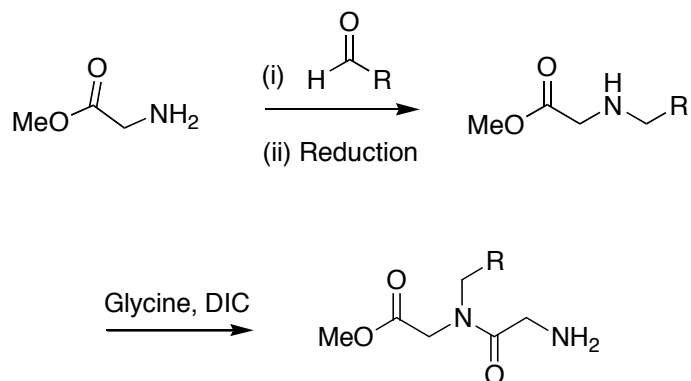
2.2.1 Solution-phase Approaches to Peptoids

Solution phase synthetic methods are the less well explained for peptoid synthesis than solid phase methods. This might be due to the purification task often required for every step in the synthesis. Unlike solid-phase synthesis, solution-phase often requires extra steps that deal with either protection and deprotections, or reductions (reductive amination). Nevertheless, solution-phase synthesis affords large-scale production of compounds at affordable price. Two methods have been reported for solution-phase synthesis of peptoids; the *N*-alkylation method¹³⁷ and the reductive amination method.¹³⁸

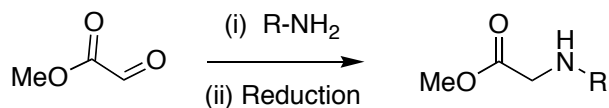
The reductive amination method requires the imination of an aldehyde followed by reduction of the imine. This can be done in two ways; the use of aldehydes as diversity elements on glycine¹³⁹ (Scheme 3a), and the use of primary amines as diversity elements on α -aldocarboxylic acids (Scheme 3b).^{140,141}

Scheme 2.1. (a) Reductive amination with aldehydes as diversity elements,
(b) Reductive amination with primary amines as diversity elements.

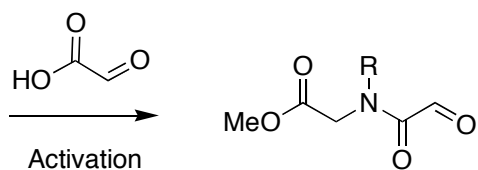
a.



b.



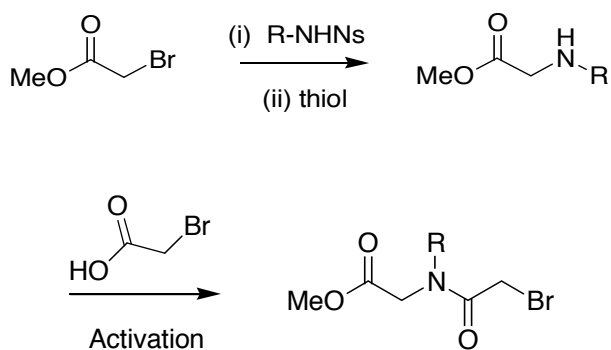
Scheme 2.1 continued



While the use of aldehyde as diversity element poses a problem to chemist because there are limited supplies of aldehydes that can mimic specific amino acid side chains, the aldehyde in the second step of Scheme 3b tend to react and form tertiary amine. This reduces the yield of the reaction.

The alkylation method is the most attractive method for synthesis of peptoids. Dialkylation is often prevented by protection of the amines. The protecting group often used is the Nosyl protecting group, because it is orthogonal to most reaction conditions, and also makes *N*-alkylation easy. This method shown in Scheme 4 often requires purification after deprotection of the Nosyl group. Efforts in development of this method have improved the deprotection techniques that do not require purification. This is achieved by using water solution thiol that will force the thioether byproduct into the aqueous phase during workup.¹³⁷

Scheme 2.2. Alkylation approach to solution-phase peptoid synthesis.

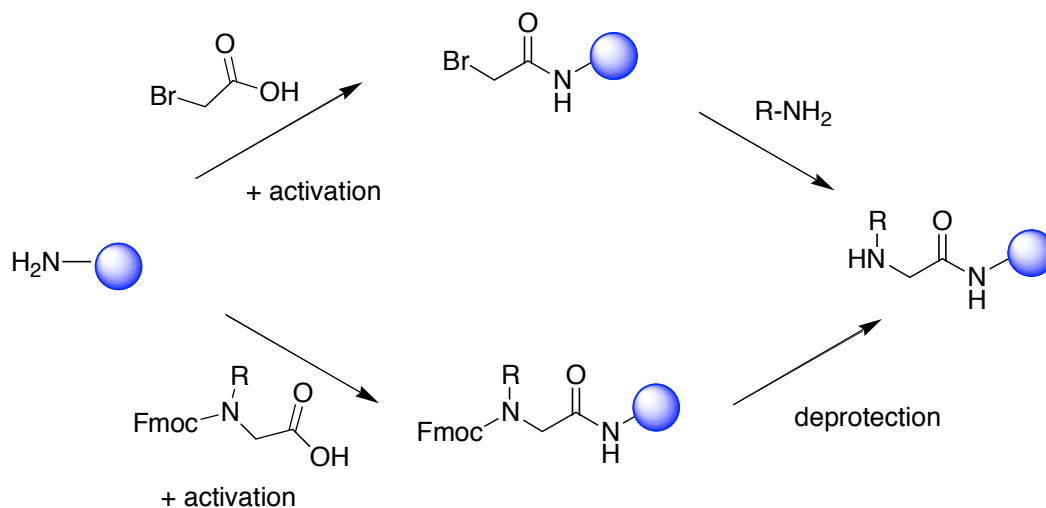


2.2.2 Solid-phase Approaches to Peptoid Synthesis

This is the most widely used approach to peptoids. With the introduction of automation and microwave synthesis, quicker and easier routes to peptoids are now available. Both alkylation and reductive amination methods can be used to construct peptoids on solid support, but the reductive amination is less effective and is similar to the solution-phase amination method. Hence this section will focus on the alkylation (submonomer) method,¹⁴² and the normal solid-phase peptide synthesis with *N*-substituted glycine (monomer) method.¹⁴¹

The monomer approach involves either Boc synthesis¹⁴¹ or the Fmoc synthesis,^{140,143,144} but the Fmoc synthesis is mostly used. Here *N*-alkylglycines are used as the building block in the construction of peptoids. The setback to this method is the limited supply of the *N*-alkylglycines and the difficulty in preparing them. The submonomer solid-phase synthesis is the most successfully used method for peptoid synthesis. The success of this method could be attributed to the fact that primary amines required for diversity are abundant and the method can easily be automated.

Scheme 2.3. Monomer vs. submonomer solid phase synthesis according to Simon *et al.*¹⁴⁴ and Zuckermann *et al.*¹⁴²



Even with success achieved in the submonomer approach, work is still being done on further improving the coupling conditions. Although the use of diisopropylcarbodiimide (DIC) as the activating agent is popular, many groups have also used acid halides. Other improvements involve the use of automated systems at 35 °C,^{145,146} and the use microwave irradiation.^{147,148} The microwave synthesis has impressively improved peptoid synthesis, each reaction step can be carried out in 1 min or less with significant improvement in yield and purity.

2.3 Preparation of Primary Amines for Cyclic Peptoid Libraries

Below is the list of primary amines building blocks for the peptoid libraries (Figure 2.1). Each used to mimic a specific side chain in the turn regions of the protein of interest.

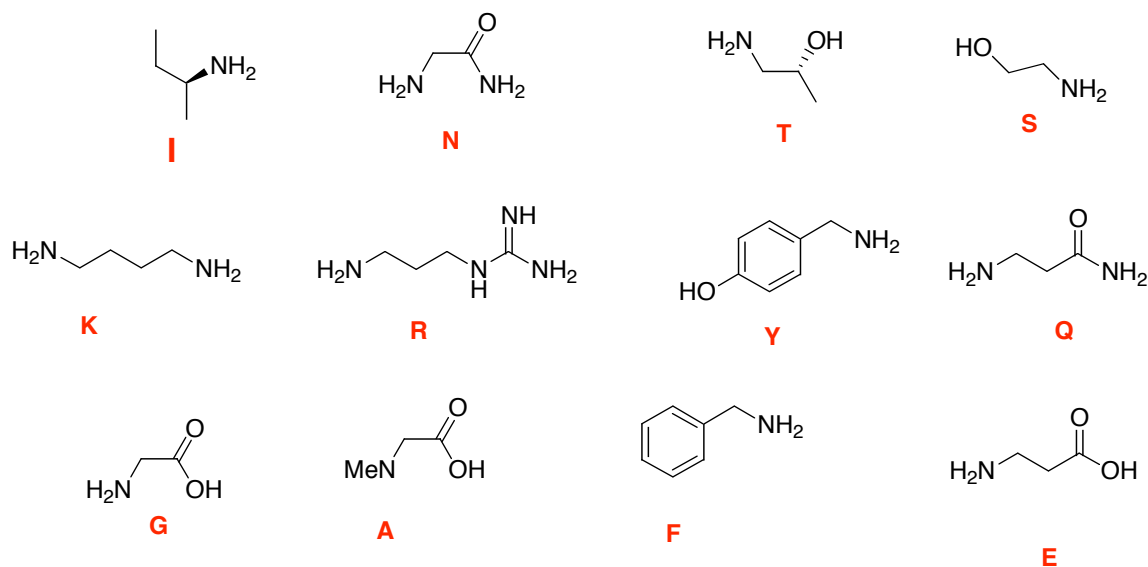


Figure 2.1. Amine building blocks labeled with the amino acid residue they are used to mimic (red).

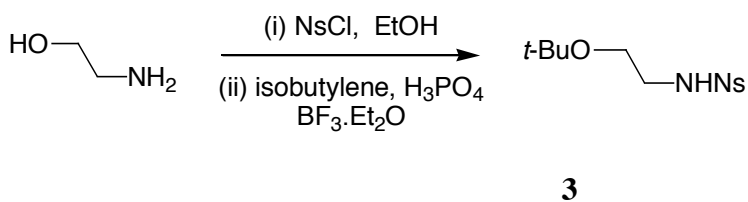
2.3.1. Protection of Alcohol Amines

The building blocks with alcohol residues needed for mimicking serine (**S**) and threonine (**T**) have to be protected to avoid *O*-alkylation during synthesis. To protect the

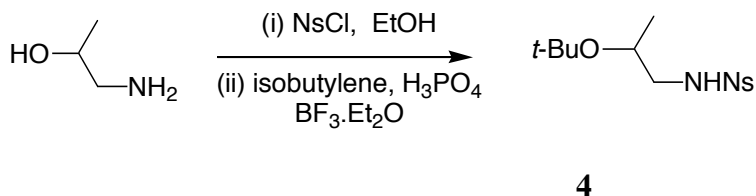
alcohol group, the more reactive primary amine has to be first orthogonally protected. This is achieved by the nosylation of the amine.¹⁴⁹ Scheme 2.4, shows how the alcohol amines were reacted with 2-nitrobenzoyl chloride in ethanol, to afford the sulfonamides, which were then reacted with isobutylene in acidic condition to generate compounds **3** and **4**.¹⁵⁰

Scheme 2.4. Protection of alcohol amine building blocks; (a) serine building block and (b) threonine building block.

a.



b.



2.3.2 Preparations of Arginine, Lysine and Tyrosine Building Blocks

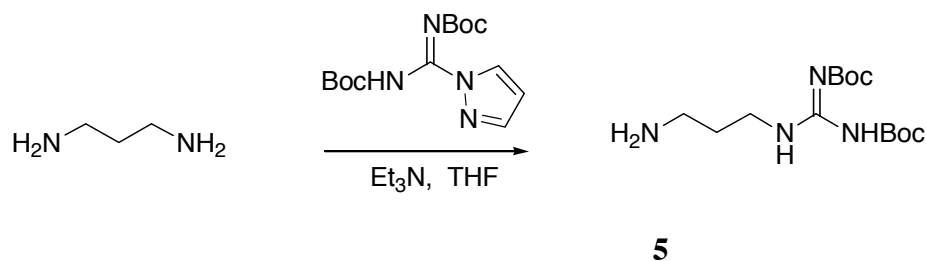
Preparation of primary amine blocks for lysine and arginine require mono coupling to diamines. Arginine block was prepared by dropwise addition of a THF solution of *N,N*-bis-Boc-1-guanylpiperazine¹⁵¹ to an excess THF solution of 1,3-aminopropane. The mixture was stirred overnight, and the product recrystallized in ethanol (Scheme 2.5a).

Lysine requires mono-Boc protection of 1,4-diaminobutane (Scheme 2.5b). This is achieved by dropwise addition of ethanol solution of Boc-anhydride to an excess solution of 1,4-diaminobutane, and stirred overnight at ambient temperature to give amine **6** after purification.¹⁵²

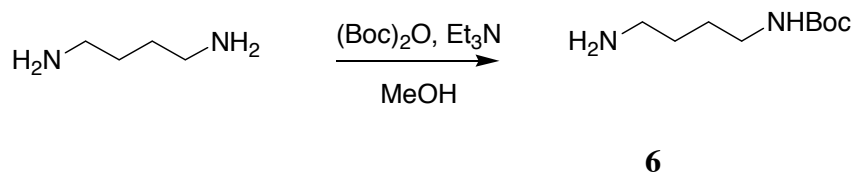
The 4-aminomethylphenol needed for tyrosine building block was prepared by azidation of the corresponding benzyl alcohol followed by *in situ* Staudinger reduction of the azide (Scheme 2.5 c).¹⁵³

Scheme 2.5. Preparations of building blocks; (A) arginine building block, (B) lysine building block, and (C) tyrosine building block.

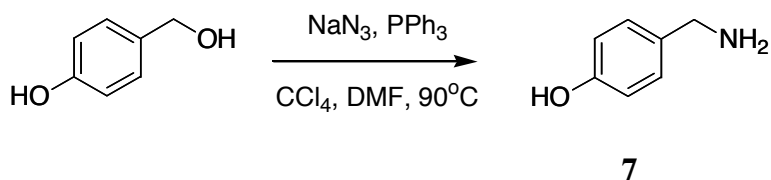
A.



B.



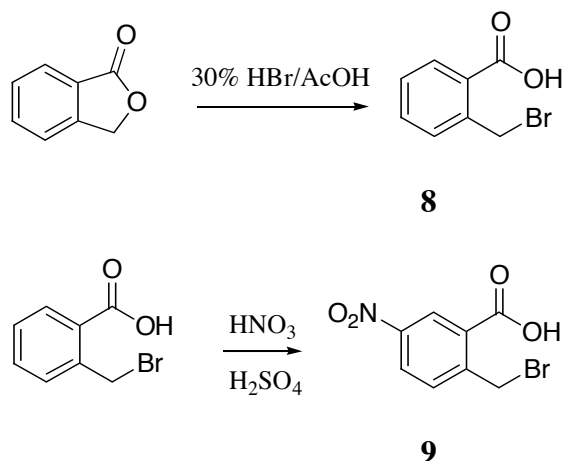
C.



2.4 Preparation of Templates for Cyclization

The templates for S_N2 cyclizations were prepared from existing methods in our lab. The template **7** was prepared by refluxing phthalide in bromic acid solution overnight as shown in Scheme 2.6. The nitration of compound **8** in nitric acid and sulfuric acid mixture yielded a nitro-template **9**, which is unstable and difficult to work with.

Scheme 2.6. Synthesis of templates for S_N2 cyclization.

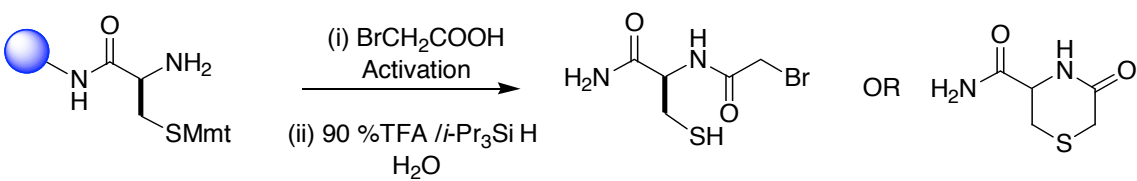


2.5 Optimization of Linear Peptoid Synthesis

The syntheses of the peptoids were first attempted at room temperature and conventional heating using various concentrations of reagents,¹⁴ but the yields and purities for the linear and cyclization reactions were low. Kodadek, *et al.* reported a microwave assisted peptoid synthesis in which they used a domestic microwave instrument to generate pure compounds in minutes.¹⁴⁷ This method could not be repeated on our (CEM: Discover) microwave instrument, which records a much higher temperature at 100 W than reported by Kodadek. To generate an efficient microwave method, development of optimal microwave technique for both the acylation (Table 2.1) and alkylation (Table 2.2) reactions were performed.

2.5.1 Optimization of the Acylation Step for Peptoid Syntheses

After the initial coupling of the cysteine to the Rink amide MBHA resin via DIC/HOBt coupling protocol and removal of Fmoc protection, the acylation with bromoacyl moiety was studied to develop the best condition for this coupling step. This is done using different reaction conditions as shown in Table 2.1 below. The analyses of these reactions are uncertain, because of the possibility of the cleaved bromoacyl moiety to cyclize via S_N2 attack by the free thiol. Attempts to clarify which of the two products were present after cleavage proved to be difficult because the amounts cleaved could only be used for mass spectrometric analysis. The mass spectrum (EI) of entry 6 (Table 2.1) was inconclusive as both molecular ions were present. Since the initial HPLC analysis shows 99 % purity, it was necessary to check the HPLC after a long period of time. The purity of the product in MeCN/H₂O was reduced to 42% after 24 h of cleavage. This means that the linear bromoacyl product was converting to the lactam

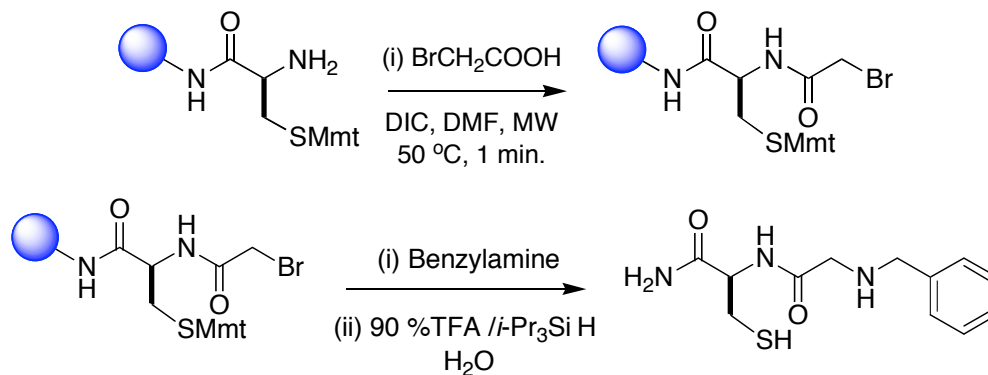
Table 2.1. Acylation conditions for peptoid synthesis.


entry	reactants	DIC (M)	DIEA (M)	solvent	temp (°C)	time (mins)	purity ^a (%)
1	bromoacetyl bromide (3 eq)	0	1	CH ₂ Cl ₂	25	60	70
2	bromoacetyl bromide (2 M)	0	2	CH ₂ Cl ₂	25	60	65
3	bromoacetic acid (2 M)	2	0	DMF	25	120	76
4	bromoacetic acid (2 M)	2	0	DMF	35	60	86
5	bromoacetic acid (2 M)	2	0	DMF	40	60	89
6	bromoacetic acid (2 M)	2	0	DMF	50 ($\mu\omega$)	1	99

^a Assessed by HPLC of crude product, monitored with ELS.

2.5.2 Optimization of the Acylation/Alkylation Procedure for Peptoid Syntheses

The resin bound bromoacetyl amide from entry 6 in Table 2.1 was used to study the alkylation reactions (Table 2.2)

Table 2.2. Optimization of microwave-assisted peptoid synthesis.

entry	solvent	temp (°C)	time (min)	purity ^a (%)
1	DMF	25	120	53
2	DMSO	25	120	55
3	DMF	35	90	79
4	DMF	40	60	85
5	DMF	50 ($\mu\omega$)	1	99
6	DMSO	50 ($\mu\omega$)	1	98

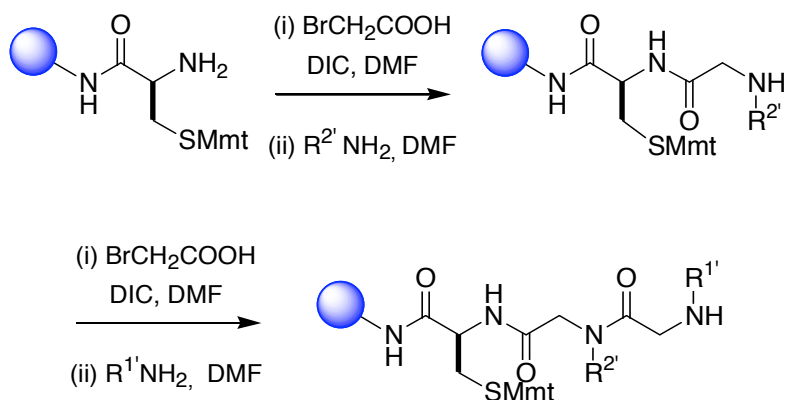
^a Assessed by HPLC of crude product, monitored at 254 nm via UV detector

2.6 Synthesis of Linear Peptoids

Microwave irradiation at 50 °C for 1 min (entry 5 on Table 2.2) was found to be the optimal procedure for the peptoid synthesis and was employed in this project. The deprotected cysteine or homocysteine bound resin is washed and treated with a solution of bromoacetic acid and DIC and irradiated with microwave. Then the resin was washed and treated with a solution of primary amine and microwaved again. This protocol is repeated again as shown in Scheme 2.7. Blackwell and coworkers recently reported that microwave irradiation is not necessary for peptoid synthesis involving unhindered primary amines. They reported being able to synthesize peptoids of high

quality within the same reaction time as in microwave, at room temperature.¹⁴⁸ This is very interesting, since reactions we carried out during the early stages of this project at room temperature did not give us pure enough substrate to be used in macrocyclization after 2 h reaction time each. This could mean that we have been leaving our reactions to run for an unnecessary amount of time with unnecessary heating.

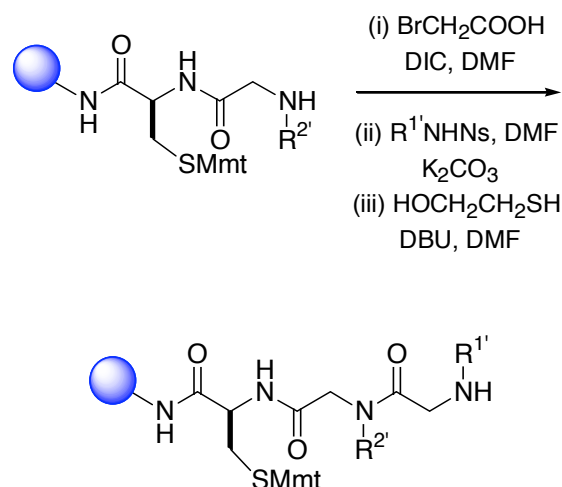
Scheme 2.7. Synthesis of linear peptoids.



2.6.1 Linear Peptoids with Alcohol Sidechains

Microwave synthesis of linear peptoids in Scheme 2.7 above was not used for the addition of the (S) and (T) monomers for the compounds **1SG**, **SY** and **TG**, because the removal of the nosyl of the precursors **3** and **4** to regenerate primary amines were not successful.¹⁴⁹ The products were difficult to isolate. To overcome this problem, the nosylated compound was alkylated to the resin bound bromoacetic amide substrate (Scheme 2.8). The thioether byproducts after deprotection were washed away to generate pure linear dipeptoids.

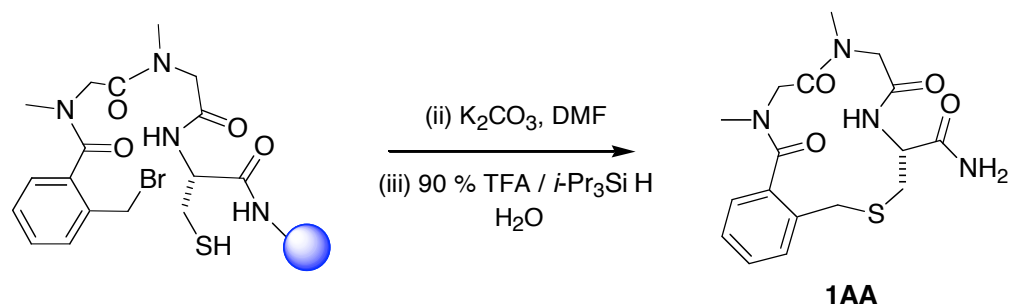
Scheme 2.8. Synthesis of peptoids with nosyl amides.



2.7 Formation of Peptidomimetics 1

The base mediated cyclization reactions were unsuccessful at room temperature as HPLC and mass spectra show mostly starting material after a 48 h reaction (table 2.3). This is surprising because it takes about 36 h of reaction time to obtain a macrocycle of normal 14-membered ring peptides via $\text{S}_{\text{N}}2$, with high purity and yield.^{108,129,154} The increased difficulty of peptoids to cyclize compared to peptides may be due to the fact that linear peptoids are more flexible (they vibrate and rotate much faster) and hence have higher entropy.¹⁵⁵ To be able to obtain good quality macrocycles, optimization of the $\text{S}_{\text{N}}2$ cyclization protocol was carried out (Table 2.3).

The $\text{S}_{\text{N}}2$ cyclization studies shown in Table 2.3 were performed using resin bound Cys-NAla-NAla (NAla = sacrosine, *ie* N-methylglycine). This starting material was prepared on Rink-functionalized polystyrene resin with a conventional Fmoc approach using DIC/HOBt couplings.

Table 2.3. Conditions for S_N2 cyclization.

entry	temp(°C)	time (h)	purity ^a (%)
1	25	48	30
2	35	48	53
3	40	48	57
4	50 (μω)	0.17	97

^a Assessed by HPLC of crude product, monitored at 254 nm via UV detector

The result from entry 4 of Table 2.3 above was employed for macrocyclization reaction. The free thiol linear system was treated with excess K₂CO₃, DMF and irradiated with microwave for 10 min (Scheme 3). The resin was washed dried *in vacuo* and cleaved to generate relatively pure compounds (Table 2.4). The crude products were purified with preparative HPLC, lyophilized to powders in relatively good yield (Table 2.4).

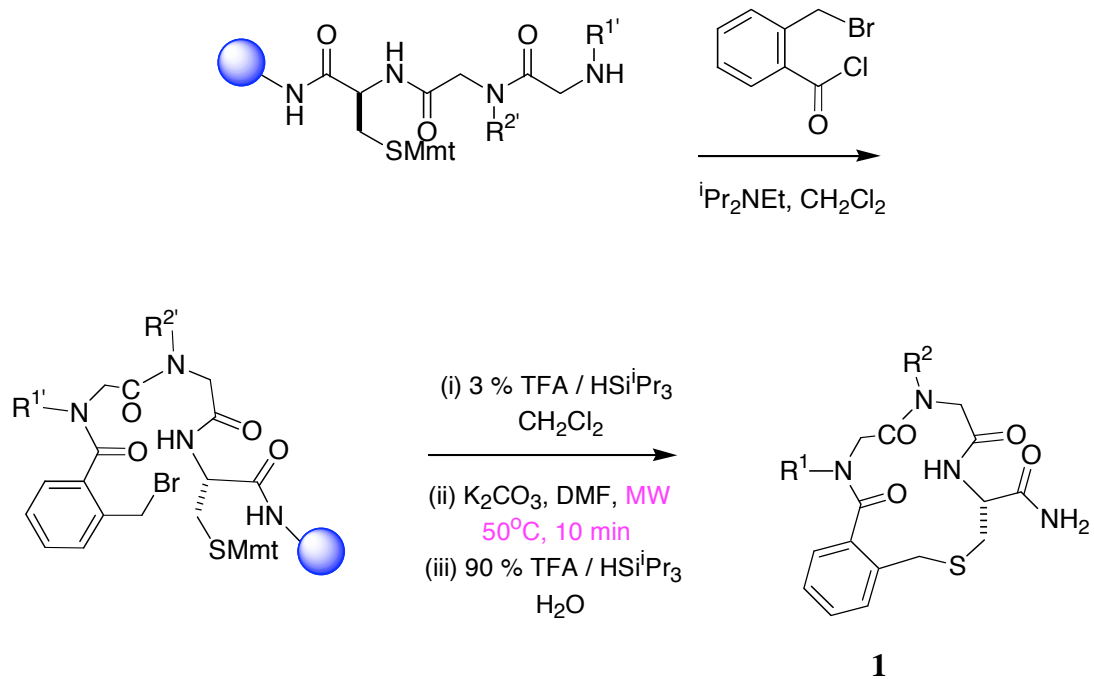
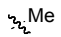
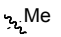
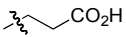
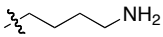
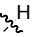
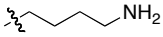
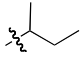
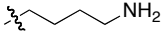
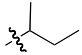

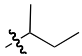
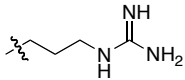

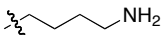


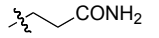
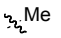
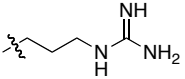
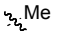
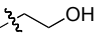
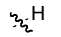
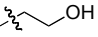
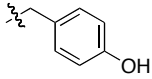
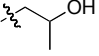
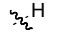
Scheme 2.9. S_N2 cyclization reaction.

Table 2.4. Purity and yield data for the cyclic semi-peptoids 1.

1	R¹	R²	purity UV/ELS (%)	yield (%)
AA			99/98	70
EK			87/89	65
GK			100/98	60
IK			85/80	45
IN			90/92	60
IR			89/80	80
NK			80/82	68
NN			80/75	35
QA			91/70	55
RA			95/93	50
SG			80/80	30
SY			86/84	45
TG			75/78	52

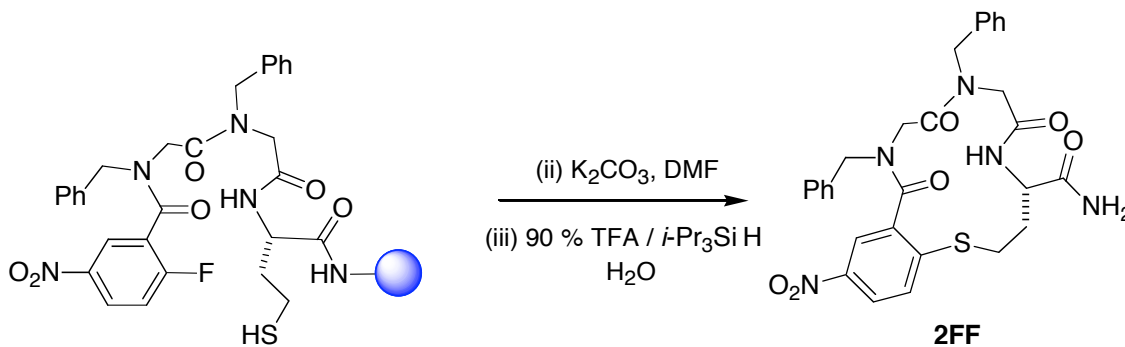
*Purity as assessed by HPLC of crude product, monitored by UV absorption at 254 nm and using an evaporative light scattering detector (ELS)

2.8 Formation of Peptidomimetics 2

Since our group is interested in bivalent peptidomimetics, compounds **1** could not be used to make either bivalent compounds or monomeric compounds with chromophore, because there is no point of linker attachment. To develop peptidomimetics with a point of linker attachment, the original compounds can be modified in two possible ways; nitration of the 2-bromomethylbenzoic acid template, or replacing the cysteine with a homocysteine and use 2-fluoro-5-nitrobenzoic acid as the template.

The first method proved to be very difficult because 2-bromomethyl-5-nitrobenzoic acid is unstable and tend to form nitro phthalide. Hence the second approach was used to generate peptidomimetics **2** via S_NAr . The macrocyclization method develop for the S_N2 systems was not efficient for the S_NAr system, hence the need for an optimal protocol (Table 2.5). The S_NAr cyclization reaction was performed on a resin bound linear semi-peptoid moiety constructed on a homocysteine scaffold (Scheme 2.1)

Table 2.5. Microwave conditions for S_NAr cyclization.



entry	temp (°C)	time (min)	purity ^a (%)
1	50	10	84
2	60	10	90
3	50	15	98

^aAssessed by HPLC of crude product, monitored at 254 nm via UV detector

Scheme 2.10 shows how peptidomimetics **2** were generated. The procedure is very much like that for peptidomimetics **1** except for longer reaction time for the S_NAr cyclization step. The yields and purities for **2** are relatively high (Table 2.6).

Scheme 2.10. S_NAr cyclization reaction.

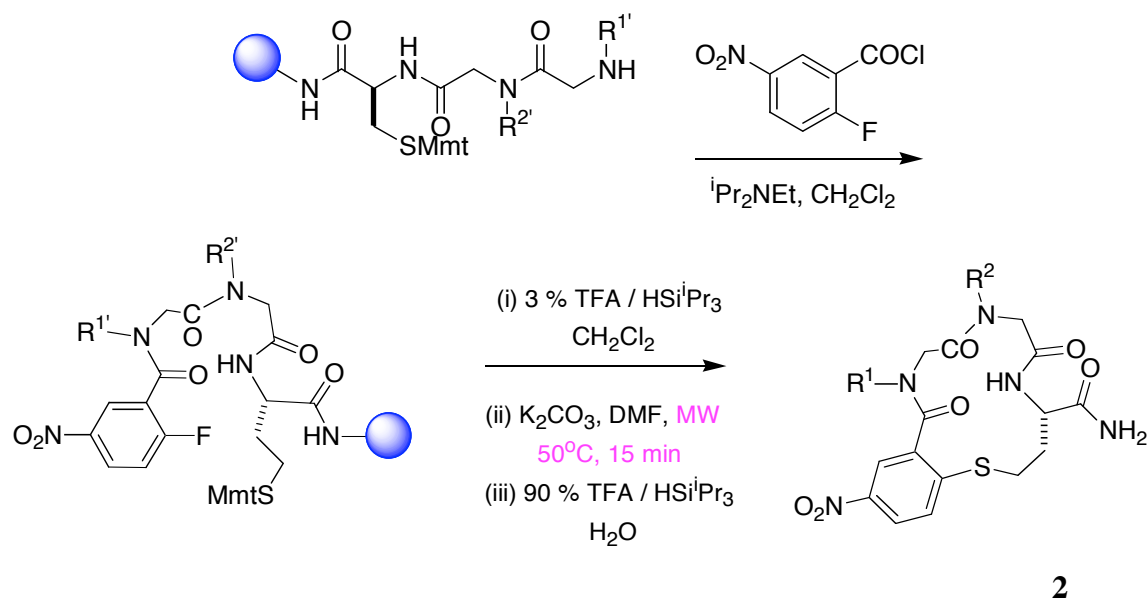


Table 2.6. Purity and yield data for the cyclic semi-peptoids **2**.

2	R ¹	R ²	purity UV ^a /ELS (%)	yield (%)
ek			91/88	62
ff			99/98	70
if			95/93	50
ik			85/83	47
ir			89/80	40
nn			86/72	44
qa			93/77	52

*Purity as assessed by HPLC of crude product, monitored UV absorption at 254 nm and using an evaporative light scattering detector (ELS).

2.9 Conformational Analysis

Conformation analysis of small molecules is very important in medicinal and biological chemistry. Although conformations of molecules in solution are not steady, it is possible to look at a prevailing population of conformers at a given time using techniques such as NMR. This could be used to predict how the molecules would interact with specific receptors. Approaches used in our conformation studies include NMR, CD, and QMD studies. Our use of NMR was limited to temperature coefficient experiments because there are no NH and tertiary $\alpha\text{-CH}$ to look at in the $i + 1$ and $i + 2$ regions for 2D NMR. This was also a problem during QMD Studies (see section 2.9.3)

2.9.1 Intramolecular Hydrogen Bonding

Intramolecular H-bonding in peptides and proteins can be identified via a variable temperature NMR experiment. Slope from plots of the amide chemical shift against temperature is referred to as the temperature coefficient (Tc), or NH temperature gradient ($\Delta\delta_{\text{NH}}/\Delta T$).¹⁵⁶ Temperature coefficient of amide protons in DMSO that are either involved in hydrogen bonding or shielded from solvent are greater than -3 ppb/K because of steric shielding. Values of -3 to -6 ppb/K indicated intermediate protection, while fully exposed amide protons have high negative Tc values (-6 to -10 ppb/K).^{157,158} This technique does not provide identification of hydrogen bond acceptor, therefore careful consideration has to be taken in the interpretation of the data. Amino acids such as Asp, Asn, Glu, and Gln contain side chains carbonyl which is a good hydrogen bond acceptor can skew the results of this experiment.^{157,159}

Amide proton exchange experiment is another approach used to detect the existence of hydrogen bonds in peptide.^{159,160} Slow amide proton-deuterium (H/D) exchange indicates solvent shielded as a result of either steric protection or the presence of a hydrogen bond, while fast H/D exchange shows solvent exposed amide proton.^{159,161} This method is not good for dictation of H-bonding in small peptides because amide hydrogens of small peptides in DMSO/D₂O are often exposed and hence tend to exchange too fast for useful information to be obtained from them.¹⁵⁶

The temperature coefficient for $i+3$ NH of peptidomimetics **1NK** was determined in DMSO-d_6 to be -4.7 ppb/K. This indicates that the NH is not strongly involved in H-bonding or shielded from solvent. On the other hand the Tc for the $i+3$ NH of peptidomimetics **2FF** measured in DMSO-d_6 shows much higher value (-1.2 ppb/K) indicating a strong H-bonding or shielding from solvent.

2.9.2 CD Studies

Circular dichroism (CD) spectroscopy has been used to study protein secondary structures.¹⁶²⁻¹⁶⁵ CD characteristics of β -turn have been theoretically determined and classified into class A, B, and C spectra.^{165,166} Experimental studies of various peptides containing turn conformation revealed that type II β -turn conformation generally show class B CD spectra.^{162,164,167} These feature weak, negative $n-\pi^*$ bands near 225 nm, strong positive $\pi-\pi^*$ bands between 200-205 nm, and strong negative bands between 180-190 nm.¹⁶⁵ Types I and II' β -turn give class C spectra with a negative $n-\pi^*$ band near 220 nm, a negative $\pi-\pi^*$ band near 210 nm, and a positive $\pi-\pi^*$ band near 190 nm.^{163,165,168}

In our CD studies the usual 20 % methanol in water used as the solvent system in turn mimics studies did not dissolve the semi-peptoid mimics. Hence a 35% methanol in water with 1.0% NaHCO_3 was used. The spectrum (Figure 2.2) shows a positive peak 200-205 nm and a negative peak near 190 nm for compound **1NK**. This is a class B spectrum indicating a possible Type II β -turn conformation for this compound. On the other hand, compound **2FF** shows a strong minimum at 210 nm and a maximum at *ca* 225 nm (class C) indicating possible type I β -turn conformation.

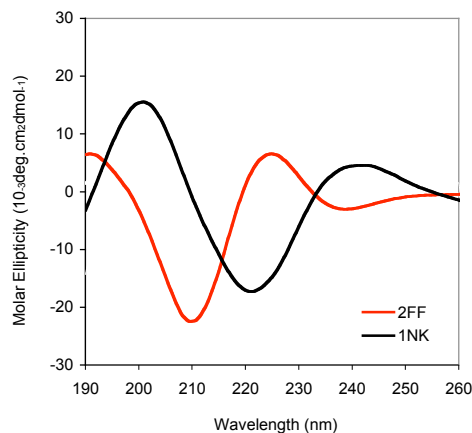


Figure 2.2. CD spectra in 35% methanol, 1.0% NaHCO₃ in water.

2.9.3 Quenched Molecular Dynamic (QMD) Studies

Molecular dynamics are used to predict conformational states available for a given compound at a given condition. They are often used to complement NMR in determining the most prevalent conformational state for a molecule.

Molecular simulation has been extensively applied to visualize preferred conformation of small molecules. The quenched molecular dynamics (QMD) technique^{169,170} is used to generate structures during a high-temperature dynamic simulation. A number of individual conformations from the molecular dynamics trajectory are periodically extracted and quenched via minimization to produce a conformational ensemble rather than a single conformation. These conformations are sorted into subsets according to their structural properties (families), which are used to represent the most probable conformations of the molecules of interest.

The QMD analysis of compounds **1NK** and **2FF** were performed. Although the Φ and Ψ could not be measured due to lack of NH and tertiary $\alpha\text{-CH}$ in the $i+1$ and $i+2$ regions, the distances between $\text{C}=\text{O}_i$ and NH_{i+1} , and between the first carbons of the side chains (β -atoms) were measured and compared to the ideal β -turn types. The $\text{C}=\text{O}_i\cdots\text{H}-\text{N}_{i+1}$ was measured to be 4.7 Å which is longer for H-bonding. The β -atoms distance was found to be 5.34 Å, which is close to that of a type 1 β -turn (5.2 Å). The Figure 2.3 shows the lowest energy structures for the peptidomimetics **1NK**, and **2FF**. Unlike **1NK**, the distance $\text{C}=\text{O}_i\cdots\text{H}-\text{N}_{i+3}$ for **2FF** (2.05 Å) is close to hydrogen bonding

distances ideal for a β -turns (2.0 Å). The simulated H-bonding distances for both compounds are consistent with the temperature coefficient data. Also the distance between the turn sidechains for **2FF** is close to type I distance (5.36 Å vs. 5.2 Å).

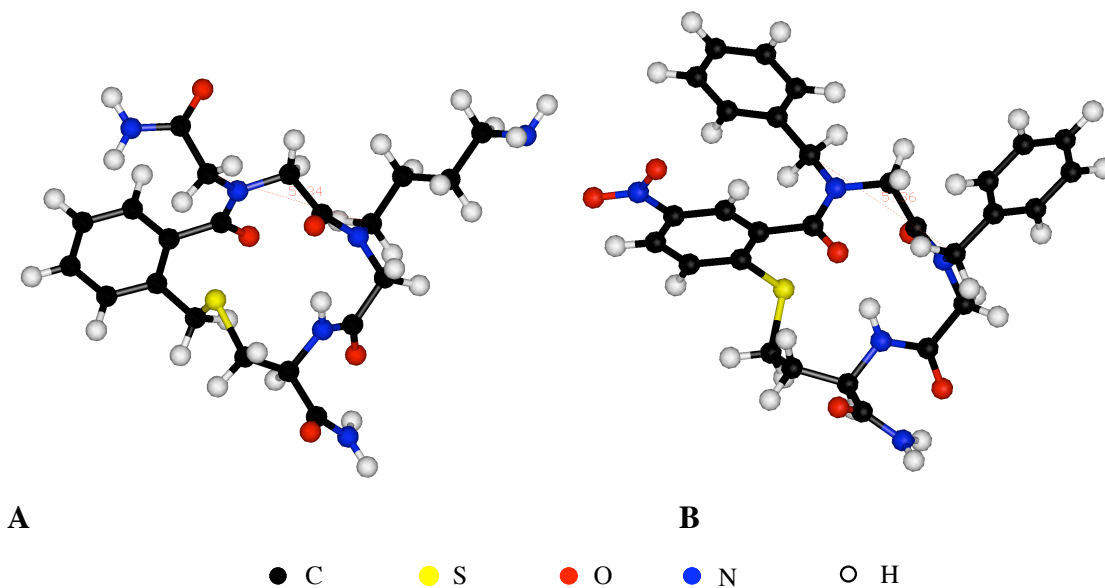


Figure 2.3. **A.** Simulated favored conformation of **1NK**; **B.** Simulated favored conformation of **2FF**.

2.10 Summary

This chapter focussed on the development of synthetic methods for the preparation of the semi-peptoid compounds. After the primary amines and templates needed for the synthesis were prepared, optimization studies were performed for certain steps of the synthesis that were not optimal. It was demonstrated that the solid phase synthesis of peptoids on polystyrene functionalized with Rink-linker proceed rapidly and efficiently if the acylation and alkylation reactions were irradiated with microwave at 50 °C for 1 min. The cyclization reactions were found to be extremely slow under thermal conditions but significantly improved with microwave irradiation at 50 °C. The semi-peptoids **1** and **2** were prepared and characterized. Limited conformational analyses were performed on selected compounds (**1NK** and **2FF**), and were found to mimic β -turns.

CHAPTER III

BIOLOGICAL STUDIES

3.1 Introduction

All the bioassays were performed by Dr. Uri Saragovi and co-workers at McGill University in Canada. Cell survival assays were the primary screening method used to access the potency of peptidomimetics. The assay uses a culture cells overexpressed with the membrane receptor of interest in deprived serum. The culture is then treated with solutions of compounds to see if cell growth is affected or not. The compounds were also injected into culture of other cells expressing receptor that are not targeted as control.¹⁷¹ After leads are found in cell survival assay, they are subjected to FACS assay, competitive binding assays, and phosphorylation assay.

3.2 Cell Survival Assays with the Semi-Peptoids

These are the first step in determining the activity of a compound. They provide information on the agonism or antagonism, selectivity, specificity and toxicity. Antagonism occurs when non-cytotoxic compounds induces cell death, while agonism occurs where high level of survival is observed. Agonism can also be tested by the ability of the compounds to rescue cells from apoptosis in a serum free media, in the absence of natural ligands. Receptor specificity occurs if activity is observed in only cells expressing one receptor and not in cells that do not express that receptor (e.g. survival in NIH-TrkA but no survival in NIH-Trk C, and NIH-IGFIR).⁵⁴

The testing of the semi-peptoids was a bit difficult due to the low water solubility of these compounds. Hence DMSO/water mixture and Hank's Balanced Salt Solution (HBSS) were used to dissolve them (see Appendix B). It is important to mention that the results reported in this section are preliminary. They need to be confirmed with at least three independent experiments. Hence the error analyses reported might not be statistically significant. They are calculated from 2 measurements of the same solution at 2 different dates. The NTF level employed in all the experiments was 5 % serum as

positive control (100 % survival). The initial screens with 3 μ M concentrations of the peptidomimetics indicated little or no activity (Tables 3.1a-c, and Figures 3.1-3.3). This might be caused by low concentration of the compounds.

Table 3.1a. Cell survival data of semi-peptoids dissolved in high concentration of DMSO.

Comp'ds	E25 cells (TrkA)		TrkC-C1 cells (TRKC)		IGF1-R cells (IGF-IR)	
	Serum free media	Low NGF	Serum free media	Low NT-3	Serum free media	Low IGF-1
None	0.00	0.00	0.00	0.00	0.00	0.00
2FF	3.69±2.11	4.17±1.44	0.95	2.55	0.73±0.15	4.46±0.47
2NN	-0.07±0.45	-0.23±0.59	0.24	-2.20	0.73±0.26	-3.63±2.49
1RA	0.55±0.66	-1.51±0.82	-0.30	-2.37	-1.04±0.47	-7.47±3.69
1GK	1.60±1.17	-1.87±1.16	-0.12	-2.20	0.73±0.47	0.73±0.05
1IR	0.75±0.91	-0.9±0.18	-0.36	-3.08	0.93±0.08	-2.28±1.66
1TG	0.48±0.70	1.10 ±0.94	-0.12	-2.73	1.87±0.78	2.49±0.99
50 %	-1.16±0.12	0.23±0.25	0.30	-1.60	-2.59±0.83	-3.11±1.87
DMSO						
40 %	-0.80±0.10	3.01±1.25	1.20	-0.77	4.80	6.33
DMSO						

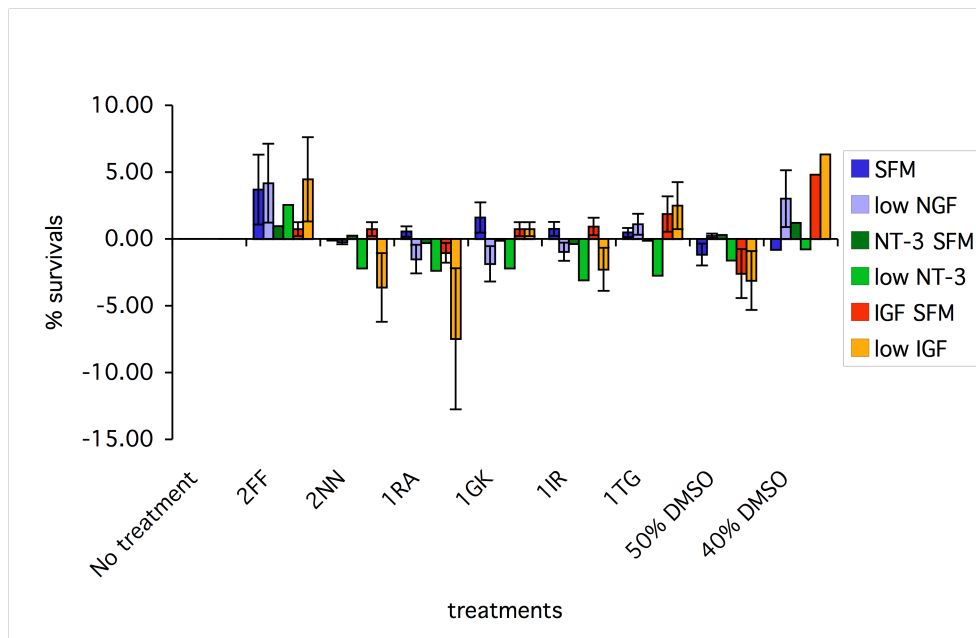


Figure 3.1. Relative survival of cells, induced by semi-peptoids dissolved in a high concentration of DMSO (5% Serum as 100% survival).

Table 3.1b. Cell survival data of semi-peptoids dissolved in low concentration of DMSO.

Comp'ds	E25 cells		TrkC-C1 cells		IGF1-R cells	
	Serum free media	Low NGF	Serum free media	Low NT-3	Serum free media	Low IGF-1
None	0.00	0.00	0.00	0.00	0.00	0.00
2IK	2.02±1.34	2.14±1.43	1.22	-1.90	-	-
					1.45±0.26	4.55±1.86
1IK	3.97±2.35	4.96±2.65	-0.07	-0.14	-	-
					2.48±1.35	5.01±0.03
1EK	3.15±1.85	1.93±1.29	-0.36	0.68	-	-
					3.72±1.91	1.29±1.90
1SG	-0.28±0.06	1.58±0.96	-0.34	-1.77	-	-
					3.62±1.81	-6.10±4.86
30 %					-	-
DMSO	0.46±0.62	0.37±0.73	-1.16	-1.70	4.75±2.03	2.76±0.56
20 %					-	-
DMSO	-0.64±0.10	-1.19±0.13	-0.07	-2.58	2.89±1.49	10.44±7.09
10 %	0.34±0.47	3.67±1.59	0.63	-3.67	-	-
DMSO					3.00±1.19	-0.21±1.35

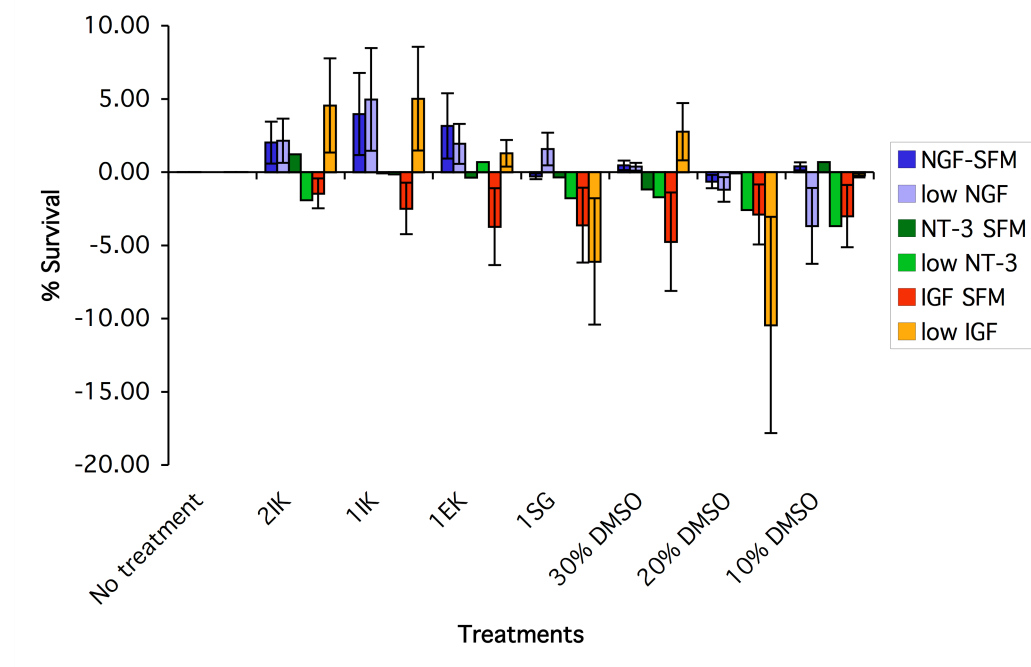
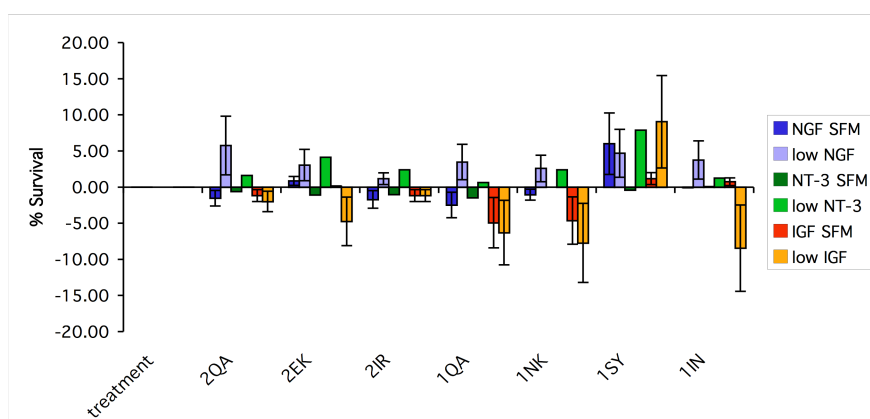


Figure 3.2. Relative survival of cells, induced by semi-peptoids dissolved in a low concentration of DMSO (5% Serum as 100% survival).

Table 3.1c. Cell survival data of semi-peptoids dissolved in HBSS.

Comp'ds	E25 cells		TrkC-C1 cells		IGF1-R cells	
	Serum free media	Low NGF	Serum free media	Low NT-3	Serum free media	Low IGF-1
None	0.00	0.00	0.00	0.00	0.00	0.00
2QA	-1.53±0.67	5.75±2.04	-0.61	1.61	1.17±0.80	-2.00±2.12
2EK	0.86±0.81	3.05±1.70	-1.08	4.12	0.09±0.10	-4.75±3.55
2IR	-1.72±0.49	1.15±0.20	-1.01	2.40	1.17±0.37	-1.17±1.50
1QA	-2.48±0.90	3.46±1.42	-1.48	0.63	4.93±2.25	-6.30±3.74
1NK	-1.05±0.43	2.58±1.29	0.00	2.40	4.63±2.28	-7.73±4.94
1SY	6.01±3.23	4.68±1.63	-0.40	7.89	1.17±0.30	9.05±1.59
1IN	-0.05±0.48	3.75±1.96	0.07	1.25	0.75±0.64	-8.45±5.24

**Figure 3.3.** Relative survival of cells, induced by semi-peptoids dissolved in HBSS (5% Serum as 100% survival).

After the initial screens with 3 μ M concentration of compounds, the compounds with promising activities were selected. The concentration of these compounds were increased to 10 μ M and screened for survival activities (Tables 3.2a & b, Figures 3.4 & 3.5). The results of these screens show some survival, but these survivals are not restricted to any of the cell lines. There are higher rates of survival in NIH- IGF1-R cells, especially with **2FF** (23%). This result could indicate a real potentiation (partial agonism) of the IGF1 receptor by **2FF**, which has phenylalanine side chains. Phenylalanine is critical to IGF1 /IGF1-R interactions.

Table 3.2a. Selected cell survival data of semi-peptoids dissolved in high concentration of DMSO or HBSS.

Comp'ds	NIH-TrkA cells		NIH-TrkC-C1 cells		NIH-IGF1-R cells	
	Serum free media	Low NGF	Serum free media	Low NT-3	Serum free media	Low IGF-1
None	0.00	0.00	0.00	0.00	0.00	0.00
2FF	2.59	6.68	0.20	7.20	7.23	23.66
1TG	-1.44	2.37	-0.65	-2.27	1.86	12.05
2QA	-3.35	-1.56	0.00	1.32	1.75	12.05
2EK	-0.96	-1.08	-1.95	10.77	1.97	14.46
SY	0.19	4.19	-0.58	5.58	2.52	8.00
50 % DMSO	-3.52	-0.93	-1.10	-1.36	-0.22	8.98

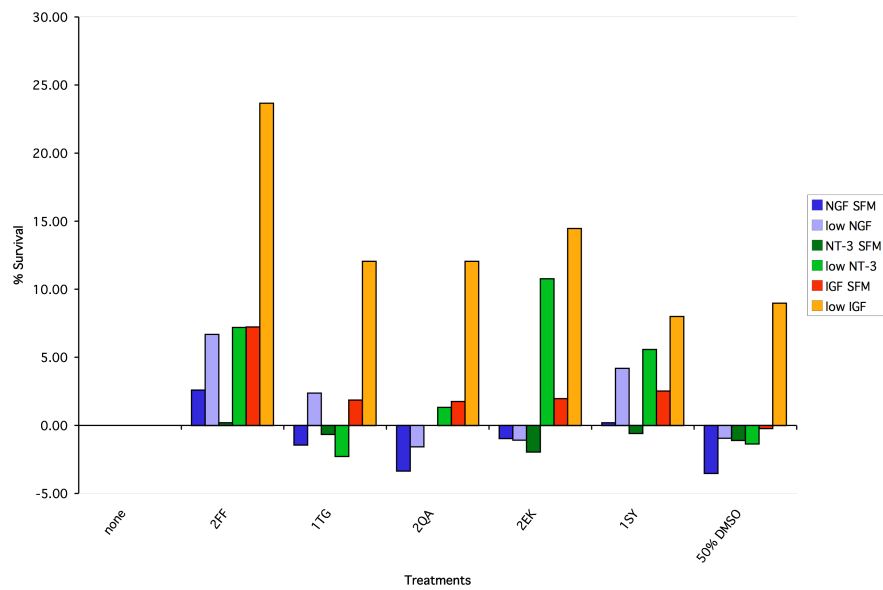


Figure 3.4. Selected cell survival data of semi-peptoids dissolved in high concentration of DMSO or HBSS.

Table 3.2b. Selected cell survival data of semi-peptoids dissolved in low concentration of DMSO.

Comp'ds	NIH-TrkA cells		NIH-TrkC-C1 cells		NIH-IGF1-R cells	
	Serum free media	Low NGF	Serum free media	Low NT-3	Serum free media	Low IGF-1
None	0.00	0.00	0.00	0.00	0.00	0.00
2IK	-4.67	-6.22	-1.61	-0.18	2.74	1.48
1IK	-2.01	-1.10	-1.01	11.57	5.91	14.98
1EK	-9.92	-10.63	-0.94	4.12	3.38	10.76
10 % DMSO	-11.67	-14.33	-0.07	0.56	1.90	3.38
20 % DMSO	-11.61	-15.24	-0.60	2.51	-1.27	6.96
30 % DMSO	-11.41	-13.10	-1.41	3.31	2.85	4.33

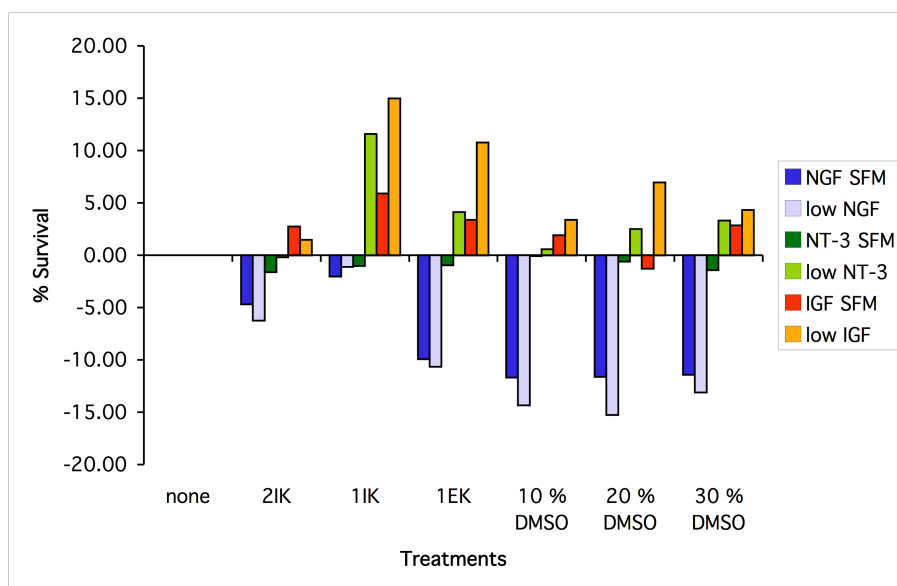


Figure 3.5. Selected cell survival data of semi-peptoids dissolved in low concentration of DMSO.

3.3 Dimeric First Generation Peptidomimetics

The dimers reported in these assays were originally prepared by Drs H. B. Li and M. Pattarawarapan in our lab, but re-prepared in collaboration with Samuel Reyes and Jing Liu. The synthetic steps for a selected compound (**KB536**) are described below to illustrate how the library of dimers was put together. The compound is made of two monomers **a** and **b** (Figure 3.6), whose synthesis is described in Schemes 3.1 and 3.2 respectively.

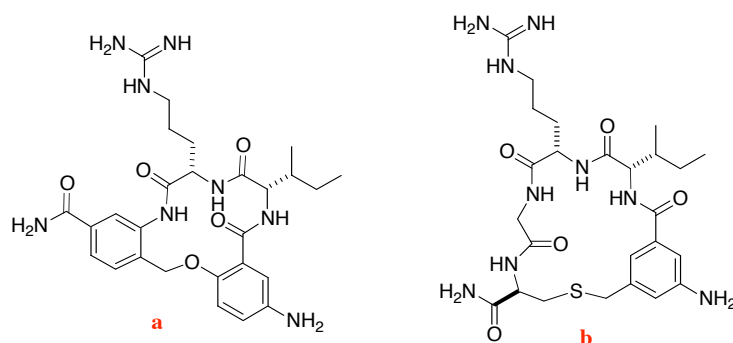
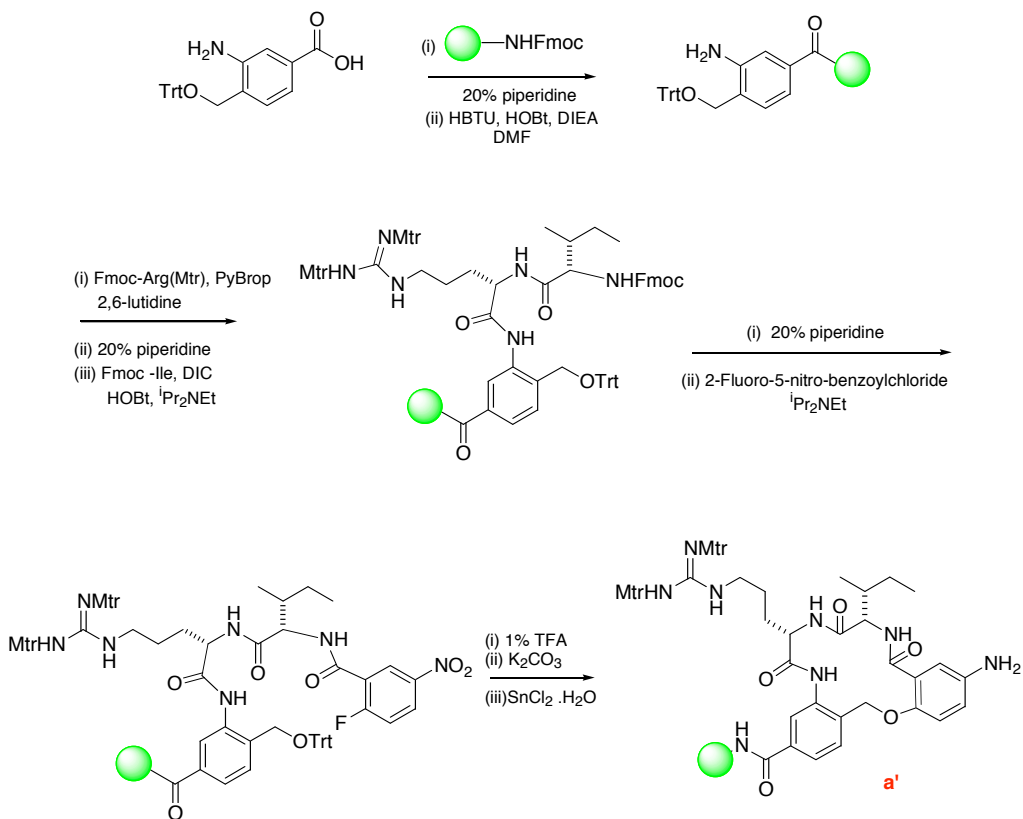


Figure 3.6. Monomers for **KB536**.

The synthesis of both monomers follows fmoc synthesis on Rink functionalized polystyrene resin. The aromatic amino acid template (compound **a**) was coupled to the resin using HBTU/HOBt coupling reagent mixture. The second amino acid coupling is a bit difficult due to the less nucleophilic aniline. Hence PyBrop™ with 2,6-lutidine a method already worked out in our group in earlier publications, was used.¹²⁹ The rest of the synthesis follows well known fmoc synthesis and S_NAr cyclization.

Scheme 3.1. (i) Synthesis of monomer **a**, (ii) Linker and flouresciene triazine attachments.

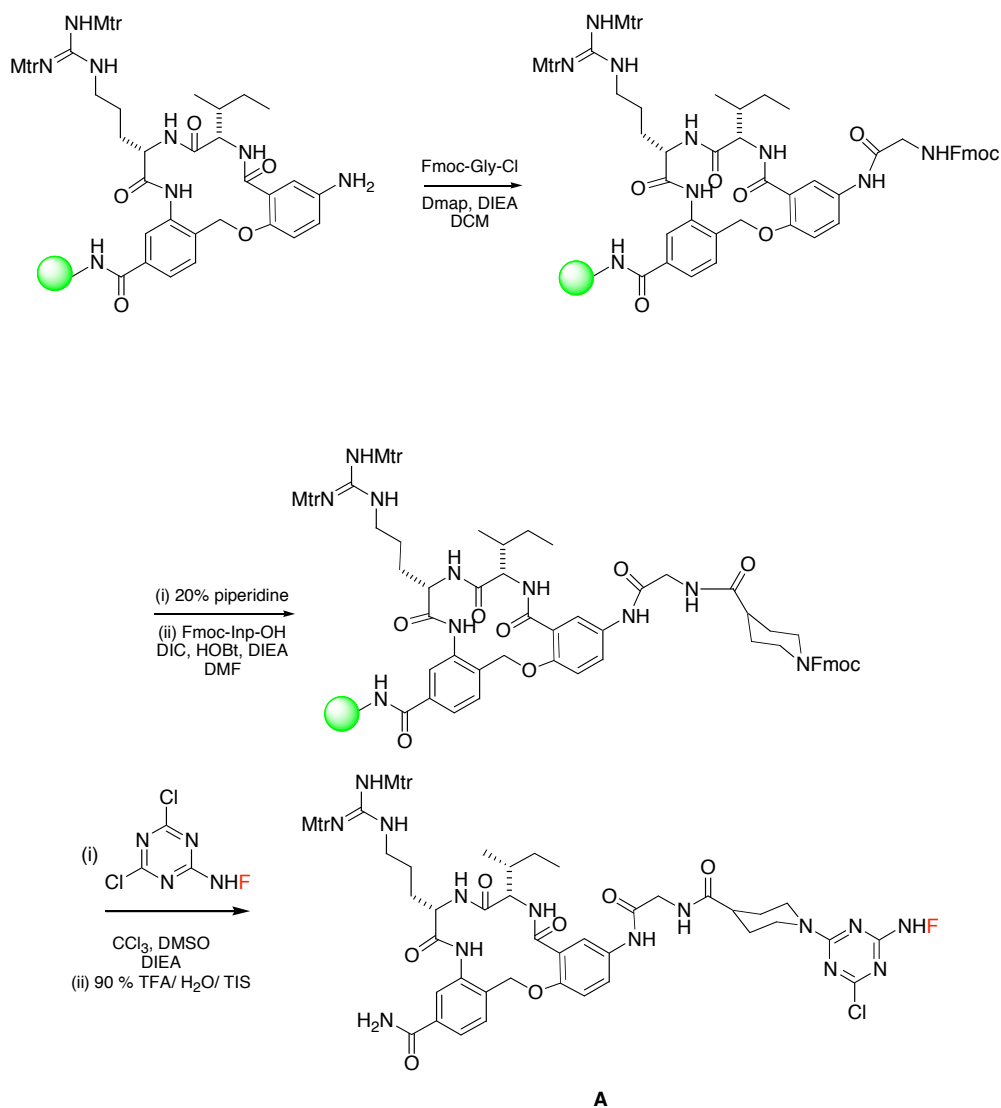
i.



F = Flourescein

Scheme 3.1 continued

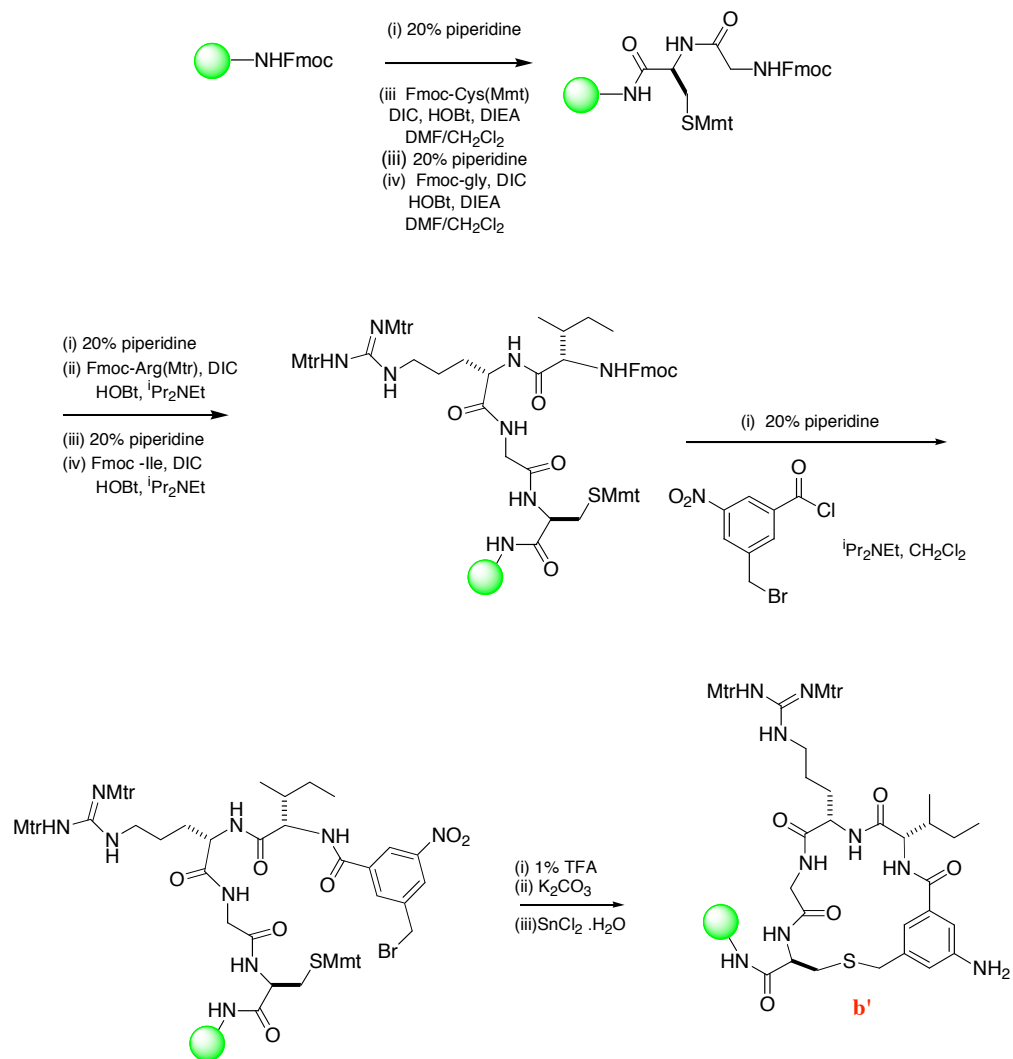
ii.



Scheme 3.2 shows the synthesis of monomer **b**, which involves an S_N2 cyclization. The assembly of the linear peptide for this compound is easier and involves DIC/HOBt coupling and the usual acid chloride addition of the cyclization template.

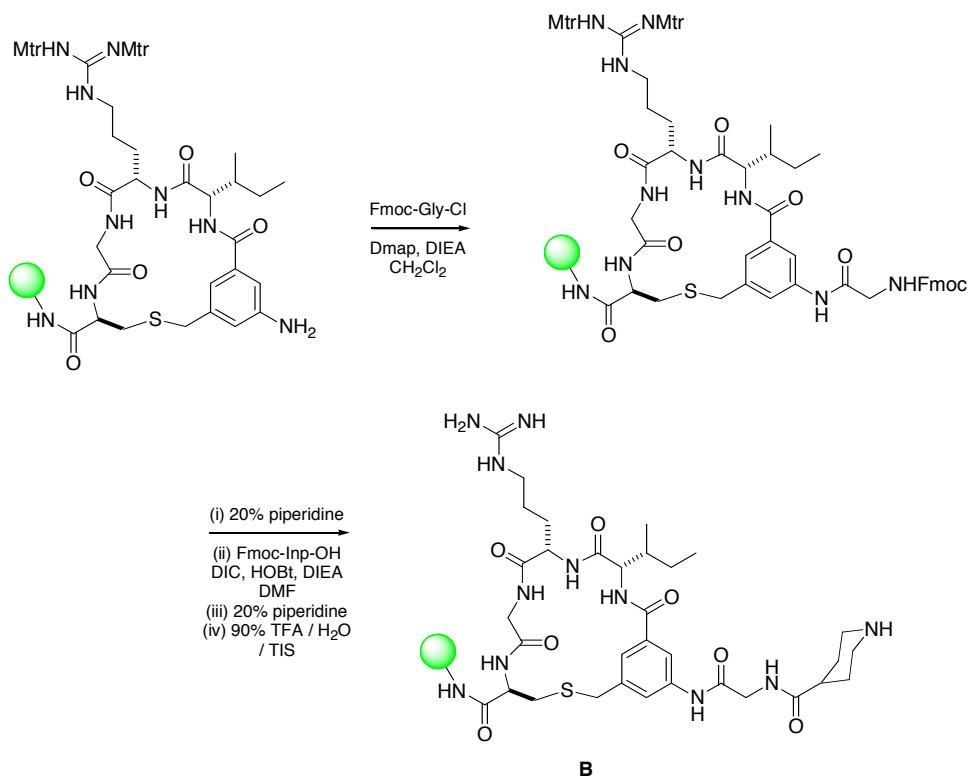
Scheme 3.2. (i) Synthesis of monomer b, (ii) Linker attachment.

(i)



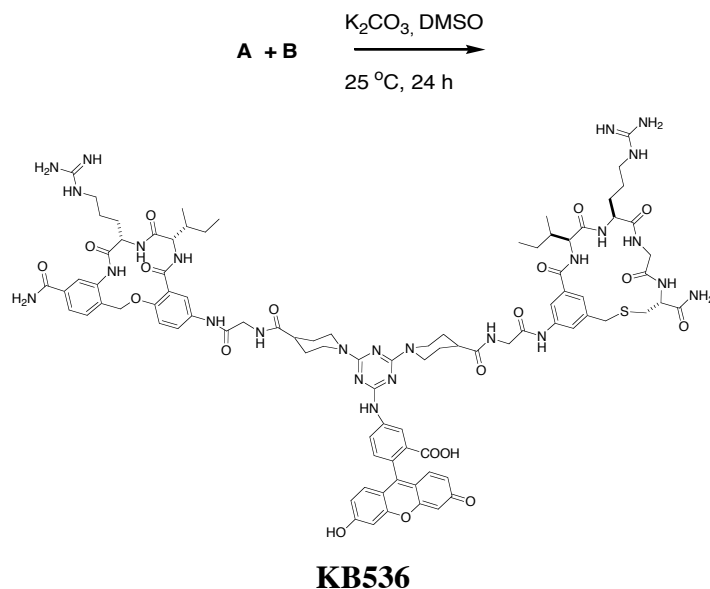
Scheme 3.2 continued

(ii)



After purification via preparative HPLC, compounds **A** and **B** were mixed in a base solution of DMSO at room temperature for overnight to generate pure **KB536** (Scheme 3.3).

Scheme 3.3. Dimerization to form KB536



3.4 FACS Assays of Dimeric First Generation Peptidomimetic

The quantitative FACScan studies on cells indicated in Table 3.3 were performed using FITC- labeled peptidomimetics or anti-receptor mAbs as positive control (5C3 for TrkA and 2B7 for TrkC). NIH-IGF1-R cells were used as negative control.¹³⁵

The results (Table 3.3) indicate that **KB536** has the highest affinities to both TrkA and TrkC expressing cells even higher than the positive control. The affinity of **KB536** is highest for TrkC.

Table 3.3. Summary of FITC-peptidomimetic binding to TrkA-NIH cells or TrkC-NIH cells, by FACScan assays. Mean channel fluorescence (MCF) of FITC-labeled ligands binding to TrkA or TrkC. $n= 3 \pm \text{sd}$. Where no sd is shown, only 2 assays were carried out.

FITC-Ligand	NIH-TrkA	NIH-TrkC
5C3 mAb	290 \pm 34	175 \pm 37
KB526	2	-2
KB527	21 \pm 9	-14 \pm 1
KB528	23 \pm 2	-19 \pm 3
KB529	6	2
KB530	85 \pm 60	-12 \pm 13
KB531	60 \pm 30	-2 \pm 6
KB532	-10	-24
KB533	-3	3
KB534	-3	-11
KB535	111 \pm 17	-20 \pm 40
KB536	335 \pm 76	349 \pm 61
KB537	47 \pm 13	9 \pm 6
KB538	70 \pm 14	50 \pm 26
KB539	9 \pm 11	2 \pm 12

3.5 Competitive Binding Assays

The assays were based on ^{125}I -NGF and mAb 5C3 binding competitions.¹⁷² The two compounds with the highest affinities in FACs assay (**KB535** and **KB536**) were selected for this assay to determine their K_d values with TrkA. The assays were carried out at constant ^{125}I -NGF concentration (5 nM), which gives a maximum binding without

competition (16,500 cpm). NGF, **KB535**, and **KB536** were the competitive inhibitors used in this assay. The IC_{50} of **KB535** is 1000-fold higher than that of NGF as shown in Figure 3.1(10,000 nM vs 10 nM) indicating a K_d value of $\sim 100 \pm 20$ nM. The IC_{50} of **KB536** is 200-fold higher than NGF's competition, hence a $K_d = \sim 20 \pm 20$ nM. This is an impressive result and confirms the hypothesis that dimerization enhances activity of peptidomimetics. Although the FACS result indicates a higher affinity of **KB536** for TrkC, the K_d value of this compound for TrkC could not be determined due to the fact that radiolabeled NT-3 need for this assay is very pricey. Also over-expressing and purification of TrkC cells in high quantity is expensive.

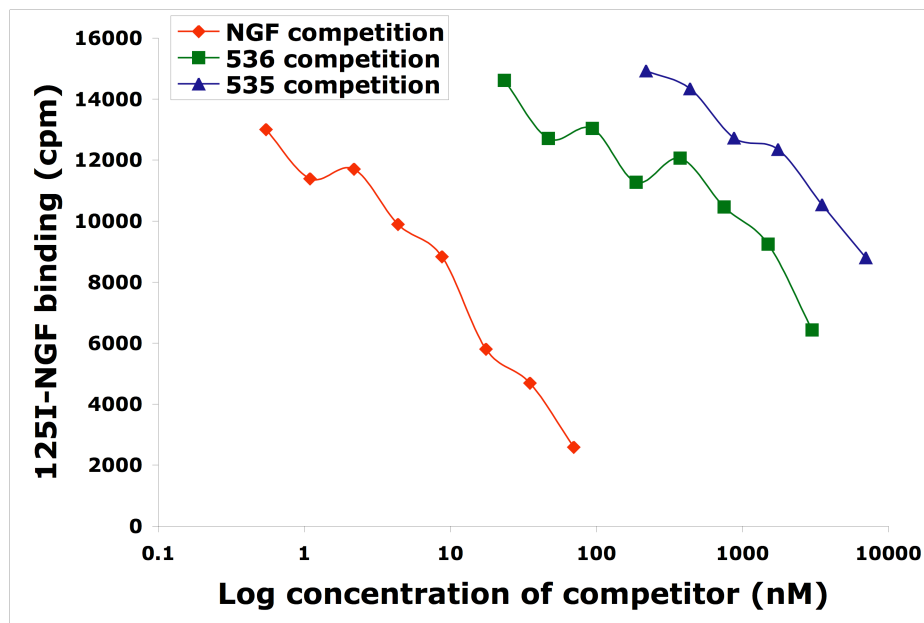


Figure 3.7. Binding Affinity of **KB535** and **KB536** for TrkA. Shift of the data to the left is indicative of higher affinity.

3.6 Summary

Biological activities of peptidomimetics were reported. The cell survival assay indicates a potentiation of IGF1-R cells by **2FF**. This indicates that **2FF** could be an agonist of IGF-R. Further experiments need to be performed to confirm this result. Also the FACS and competitive binding show promising results for bivalent compounds, **KB536** show high affinity for both TrkA and TrkC.

CHAPTER IV

CONCLUSIONS

The underlying concept in our ligand design is based on the turn regions of TNF- α and neurotrophins, which are predicted to be involved in binding to their receptors. Strategies in the design and synthesis of these ligands were discussed. Early Ligands designed in our group contain a peptidic turn region, which are predicted to have low bioavailability due to the fact that peptides are prone to proteolysis and low membrane permeability. These new approaches involve preparation of new types of β -turn analogs with peptoids in the turn region to enhance bioavailability. Two designs based on our early works on peptide microcycles were developed. They involve the use of S_N2 and S_NAr for macrocyclizations.

Chapter elaborated on the development of microwave synthetic methods, which allowed us to produce good quality compounds in less than 1 h of total reaction time. The conformational states of these semi-peptoids in solution (DMSO) were examined using a combination of NMR, CD, and molecular dynamic simulation studies (Chapter II). The NMR and QMD studies were somewhat limited due to the fact that the important markers (NH and $C^\alpha H$) needed for unambiguous identification of turn types, are not present in these compounds. There are no $NH/C^\alpha H$ couplings to look at for dihedral angles and no $NH/C^\alpha H$ or NH/NH ROESY cross peaks. Nevertheless the conformational analyses of **1NK** and **2FF** show that they indeed resemble β -turn.

The cell survival assay for the semi-peptoids did not show much result except for **2FF**, which shows agonist tendencies towards IGF-IR. This is an encouraging and needs to be confirmed with further testing. The binding assay on the bivalent compounds shows that **KB536** has an impressive K_d for TrkA and could even have higher dissociation constant with TrkC as shown by the FACS assay. These results further prove that dimerization is a great way to improve the activities of peptidomimetics.

REFERENCES

- (1) Toogood, P. L. *J. Med. Chem.* **2002**, *45*, 1543-58.
- (2) Tsai, C. J.; Lin, S. L.; Wolfson, H. J.; Nussinov, R. *Crit. Rev. Biochem. Mol. Biol.* **1996**, *31*, 127-52.
- (3) Cornish, V. W.; Mendel, D.; Schultz, P. G. *Angew. Chem. Int. Ed.* **1995**, *34*, 621-33.
- (4) Ultsch, M. H.; Wiesmann, C.; Simmons, L. C.; Henrich, J.; Yang, M.; Reilly, D.; Bass, S. H.; de Vos, A. M. *J. Mol. Biol.* **1999**, *290*, 149-59.
- (5) Guo, Z.; Zhou, D.; Schultz, P. G. *Science* **2000**, *288*, 2042-5.
- (6) Ernst, J. T.; Kutzki, O.; Debnath, A. K.; Jiang, S.; Lu, H.; Hamilton, A. D. *Angew. Chem. Int. Ed.* **2002**, *41*, 278-81.
- (7) Jones, S.; Thornton, J. M. *Proc. Natl. Acad. Sci.* **1996**, *93*, 13-20.
- (8) Larsen, T. A. O., Arthur J.; Goodsell, David S. *structure* **1998**, *6*, 421-427.
- (9) Bodmer, J.-L.; Schneider, P.; Tschopp, J. *TRENDS in Biochem. Sci.* **2002**, *27*, 19-26.
- (10) Liu, Y.; Hong, X.; Kappler, J.; Jiang, L.; Zhang, R.; Xu, L.; Pan, C.; Martin, W.; Murphy, R.; Shu, H.; Dai, S.; Zhang, G. *Nature* **2003**, *423*.
- (11) MacEwan, D. J. *British Journal of Pharmacology* **2002**, *135*, 855-875.
- (12) Locksley, R.; Killeen, N.; Lenardo, M. J. *Cell* **2001**, *104*, 487-501.
- (13) Zhang, G. *Cur. Opin. Struct. Bio.* **2004**, *14*, 154-160.
- (14) Aggarwal, B. B. *Nature Reviews* **2003**, *3*, 745-756.
- (15) Smith, C. A.; Farrah, T.; Goodwin, R. G. *Cell* **1994**, *76*, 959-62.
- (16) Ostade, X. V.; Vandenabeele, P.; Everaerd, B.; Loetscher, H.; Gentz, R.; Brockhaus, M.; Lessiauer, W.; Tavernier, J.; Brouckaert, P.; Fiers, W. *Nature* **1993**, *361*, 266-9.
- (17) Lewit-Bentley, A.; Fourme, R.; Kahn, R.; Prange, T.; Vachette, P.; Tavernier, J.; Hauquier, G.; Fiers, W. *J. Mol. Biol.* **1988**, *199*, 389-92.

- (18) Totpal, K.; LaPushin, R.; Kohno, T.; Darnay, B.; Aggarwal, B. B. *J. Immunol* **1994**, *153*, 2248.
- (19) Barbara, J. A. J.; Smith, W. B.; Gamble, J. R.; Ostade, X. V.; Vandenabeele, P.; Tavernier, J.; Fiers, W.; Vadas, M. A.; Lopez, A. F. *The EMBO Journal* **1994**, *13*, 842-50.
- (20) Camussi, G.; Lupia, E. *Drugs* **1998**, *55*, 613-20.
- (21) Carter, B. D.; Kaltschmidt, C.; Kaltschmidt, B.; Offenhäuser, N.; Böhm-Matthaei, R.; Baeuerle, P. A.; Barde, Y.-A. *Science* **1996**, *272*, 542-5.
- (22) Khursigara, G.; Orlinick, J. R.; Chao, M. V. *J. Biol. Chem.* **1999**, *274*, 2597-600.
- (23) Barbara, J. A. J.; Ostade, X. V.; Lopez, A. F. *Immunology and Cell Biology* **1996**, *74*, 434-43.
- (24) Takasaki, W.; Kajino, Y.; Kajino, K.; Murali, R.; Greene, M. I. *Nature Biotechnology* **1997**, *15*, 1266-70.
- (25) Chen, P. C.-H.; DuBois, G. C.; Chen, M.-J. *J. Biol. Chem.* **1995**, *270*, 2874-8.
- (26) Zhang, X.-M.; Weber, I.; Chen, M.-J. *J. Biol. Chem.* **1992**, *267*, 24069-75.
- (27) Bibel, M.; Barde, Y.-A. *Genes & Development* **2000**, *14*, 2919-37.
- (28) Eide, F. F.; Lowenstein, D. H.; Reichardt, L. F. *Experimental Neurology* **1993**, *121*, 200-14.
- (29) McInnes, C.; Sykes, B. D. *Biopolymers* **1998**, *43*, 339-66.
- (30) Maness, L. M.; Kastin, A. J.; Weber, J. T.; Banks, W. A.; Beckman, B. S.; Zadina, J. E. *Neurosci. and Biobehavioral Rev.* **1994**, *18*, 145-59.
- (31) Conner, J. M.; Tuszynski, M. H. *Mental Retardation and Developmental Disabilities Research Reviews* **1998**, *4*, 212-22.
- (32) Gao, W.-Q.; Weil, R. J.; Dugich-Djordjevic, M.; Lu, B. *Exp. Opin. Ther. Patents* **1997**, *7*, 325-8.
- (33) Patapoutian, A.; Reichardt, L. F. *Curr. Opin. Neurobiol.* **2001**, *11*, 272-80.
- (34) Lee, F. S.; Kim, A. H.; Khursigara, G.; Chao, M. V. *Cur. Opin. Neurobio.* **2001**, *11*, 281-6.
- (35) Kaplan, D. R.; Hempstead, B. L.; Martin-Zanca, D.; Chao, M. V.; Parada, L. F. *Science* **1991**, *252*, 554-8.
- (36) Lamballe, F.; Klein, R.; Barbacid, M. *Cell* **1991**, *66*, 967-79.

- (37) Barbacid, M. *J. Neurobiol.* **1994**, *25*, 1386-403.
- (38) Chao, M. V.; Hempstead, B. L. *Trends Neurosci.* **1995**, *18*, 321-26.
- (39) Rodriguez-Tebar, A.; Dechant, G.; Gotz, R.; Barde, Y. A. *Eur. Mol. Biol. Org. J.* **1992**, *11*, 917-22.
- (40) Meakin, S. O.; Shooter, E. M. *Trends Neurosci.* **1992**, *15*, 323-31.
- (41) Ibáñez, C. F. *Trends Biotechnol.* **1995**, *13*, 217-27.
- (42) Ibáñez, C. F. *Trends Neurosci.* **1998**, *21*, 438-44.
- (43) Schneider, R.; Schweiger, M. *Oncogene* **1991**, *6*, 1807-11.
- (44) Kaplan, D. R.; Stephens, R. M. *J. Neurobiology* **1994**, *25*, 1404-17.
- (45) Chao, M.; Casaccia-Bonnel, P.; Carter, B.; Chittka, A.; Kong, H.; Yoon, S. O. *Brain Research Reviews* **1998**, *26*, 295-301.
- (46) Friedman, W. J.; Greene, L. A. *Experimental Cell Research* **1999**, *253*, 131-142.
- (47) Sofroniew, M. V.; Howe, C. L.; Mobley, W. C. *Annu. Rev. Neurosci.* **2001**, *24*, 1217-1281.
- (48) Xie, Y.; Tisi, M. A.; Yeo, T. T.; Longo, F. M. *J. Biol. Chem.* **2000**, *275*, 29868-74.
- (49) Pang, L.; Sawada, T.; Decker, S. J.; Saltiel, A. R. *J. Bio. Chem.* **1995**, *270*, 13585-8.
- (50) Perron, J. C.; Bixby, J. L. *Molecular and Cellular Neuroscience* **1999**, *13*, 362-78.
- (51) Alessi, D. R.; Cuenda, A.; Cohen, P.; Dudley, D. T.; Saltiel, A. R. *J. Bio. Chem.* **1995**, *270*, 27489-94.
- (52) Bamji, S. X.; Majdan, M.; Belliveau, C. D.; Aloyz, D. J.; Kohn, R.; Causing, C. G.; Miller, F. D. *J. Cell Biol.* **1998**, *140*, 911-23.
- (53) Bredesen, D. E.; Rabizadeh, S. *Trends Neurosci.* **1997**, *20*, 287-90.
- (54) Carter, B. D.; Lewin, G. R. *Neuron* **1997**, *18*, 187-90.
- (55) Zaccaro, M.; Ivanisevic, L.; Perez, P.; Meakin, S.; Saragovi, H. *J. Biol. Chem.* **2001**, *276*, 31023-9.
- (56) Twiss, J. L.; Wada, H. G.; Fok, K. S.; Chan, S. D. H.; Verity, A. N.; Baxter, G. T.; Shooter, E. M.; Sussman, H. H. *J. Neurosci. Res.* **1998**, *51*, 442-53.
- (57) Drinkwater, C. C.; Barker, P. A.; Suter, U.; Shooter, E. M. *J. Biol. Chem.* **1993**, *268*, 23202-23207.

- (58) Ibáñez, C. F.; Ebendal, T.; Barbany, G.; Murray-Rust, J.; Blundell, T. L.; Persson, H. *Cell* **1992**, *69*, 329-41.
- (59) Ibáñez, C. F.; Ebendal, T.; Persson, H. *Eur. Mol. Biol. Org. J.* **1990**, *9*, 1477-83.
- (60) Ibáñez, C. F.; Ilag, L. L.; Murray-Rust, J.; Persson, H. *Eur. Mol. Biol. Org. J.* **1993**, *12*, 2281-93.
- (61) Kahle, P.; Burton, L. E.; Schmelzer, C. H.; Hertel, C. *J. Biol. Chem.* **1992**, *267*, 22707-10.
- (62) Kullander, K.; Kylberg, A.; Ebendal, T. *J. Neurosci. Res.* **1997**, *50*, 496-503.
- (63) Shih, A.; Laramée, G. R.; Schmelzer, C. H.; Burton, L. E.; Winslow, J. W. *J. Biol. Chem.* **1994**, *269*, 27679-86.
- (64) Kruttgen, A.; Jr., J. V. H.; Kahle, P. J.; Shooter, E. M. *J. Biol. Chem.* **1997**, *272*, 29222-8.
- (65) Rydén, M.; Ibanez, C. F. *J. Biol. Chem.* **1997**, *272*, 33085-91.
- (66) Guo, M.; Meyer, S. L.; Kaur, H.; Gao, J.-J.; Neet, K. E. *Protein Sci.* **1996**, *5*, 447-55.
- (67) Ibáñez, C. F.; Ebendal, T.; Persson, H. *Eur. Mol. Biol. Org. J.* **1991**, *10*, 2105-10.
- (68) Ilag, L. L.; Lonnerberg, P.; Persson, H.; Ibanez, C. F. *J. Biol. Chem.* **1994**, *269*, 19941-19946.
- (69) Kullander, K.; Ebendal, T. *J. Neurosci. Res.* **1994**, *39*, 195-210.
- (70) McDonald, N. Q.; Lapatto, R.; Murray-Rust, J.; Gunning, J.; Wlodawer, A.; Blundell, T. L. *Nature* **1991**, *345*, 411-4.
- (71) Holland, D. R.; Cousens, L. S.; Meng, W.; Matthews, B. W. *J. Mol. Biol.* **1994**, *239*, 385-400.
- (72) Wiesmann, C.; Ultsch, M. H.; Bass, S. H.; de Vos, A. M. *Nature* **1999**, *401*, 184-8.
- (73) Urfer, R.; Tsoulfas, P.; Soppet, D.; Escandon, E.; Parada, L. F.; Presta, L. G. *Eur. Mol. Biol. Org. J.* **1994**, *13*, 5896-909.
- (74) Rydén, M.; Murray-Rust, J.; Glass, D.; Illag, L. L.; Trupp, M.; Yancouopoulos, G. D.; McDonald, N. Q.; Ibanez, C. F. *Eur. Mol. Biol. Org. J.* **1995**, *14*, 1979-90.
- (75) Urfer, R.; Tsoulfas, P.; O'Connell, L.; Presta, L. G. *Biochemistry* **1997**, *36*, 4775-81.

- (76) Butte, M. J.; Hwang, P. K.; Mobley, W. C.; Fletterick, R. J. *Biochemistry* **1998**, *37*, 16846-52.
- (77) Hughes, R. A.; O'Leary, P. D. *Clinical and Experimental Pharmacology and Physiology* **1996**, *23*, 965-9.
- (78) Ito, M.; Sakai, N.; Ito, K.; Mizobe, F.; Hanada, K.; Mizoue, K.; Bhandari, R.; Eguchi, T.; Kakinuma, K. *J. Antibiotics* **1999**, *52*, 224-30.
- (79) Labie, C.; Lafon, C.; Marmouget, C.; Saubusse, P.; Fournier, J.; Keane, P. E.; Fur, G. L.; Soubrie, P. *British Journal of Pharmacology* **1999**, *127*, 139-44.
- (80) Steiner, J. P.; Connolly, M. A.; Valentine, H. L.; Hamilton, G. S.; Dawson, T. M.; Hester, L.; Snyder, S. H. *Nature Med.* **1997**, *3*, 421-8.
- (81) Steiner, J. P.; Hamilton, G. S.; Ross, D. T.; Valentine, H. L.; Guo, H.; Connolly, M. A.; Liang, S.; Ramsey, C.; Li, J.-H. J.; Huang, W.; Howorth, P.; Soni, R.; Fuller, M.; Sauer, H.; Nowotnik, A. C.; Suzkak, P. D. *Proc. Natl. Acad. Sci. USA* **1997**, *94*, 2019-24.
- (82) Jaen, J. C.; Laborde, E.; Bucsh, R. A.; Caprathe, B. W.; Sorenson, R. J.; Fergus, J.; Spiegel, K.; Marks, J.; Dickerson, M. R.; Davis, R. E. *J. Med. Chem.* **1995**, *38*, 4439-45.
- (83) Lazarovici, P.; Rasouly, D.; Friedman, L.; Tabekman, R.; Ovadia, H.; Matsuda, Y. *Adv. Exp. Med. Biol.* **1996**, *391*, 367-77.
- (84) Owolabi, J. B.; Rizkalla, G.; Tehim, A.; Ross, G. M.; Riopelle, R. J.; Kamboj, R.; Ossipov, M.; Bian, D.; Wegert, S.; Porreca, F.; Lee, D. K. H. *J. Pharm. Expt. Ther.* **1999**, *289*, 1271-6.
- (85) LeSauter, L.; Malartchouk, S.; LeJeune, H.; Quirion, R.; Saragovi, H. U. *J. Neurosci.* **1996**, *16*, 1308-16.
- (86) Hopkins, M. A.; Rosser, M. P.; Fernandes, P. B.; Bursuker, I. *J. Neurosci. Methods* **1997**, *72*, 167-74.
- (87) Saragovi, H. U.; Gehring, K. In *Peptidomimetics and Small Molecule Design: Accelerating Drug Discovery*; Hori, W., Ed.; IBC Publications: Cambridge, U.K., 1997, p 3-25.
- (88) Estenne-Bouhtou, G.; Kullander, K.; Karlsson, M.; Ebendal, T.; Hacksell, U.; Luthman, K. *Int. J. Peptide Protein Res.* **1996**, *48*, 337-46.

- (89) O'Leary, P. D.; Hughes, R. A. *J. Neurochem.* **1998**, *70*, 1712-21.
- (90) Rashid, R.; Van der Zee, C. E. E. M.; Ross, G. M.; Chapman, C. A.; Stanisiz, J.; Riopelle, R. J.; Racine, R. J.; Fahnestock, M. *Proc. Natl. Acad. Sci.* **1995**, *92*, 9495-9.
- (91) Longo, F. M.; Manthorpe, M.; Xie, Y. M.; Varon, S. *J. Neurosci. Res.* **1997**, *48*, 1-17.
- (92) Saragovi, H. U.; Greene, M. I. *Immunomethods* **1992**, *1*, 5-9.
- (93) Saragovi, H. U.; Greene, M. I.; Chrusciel, R. A.; Kahn, M. *Biotechnology* **1992**, *10*, 773-8.
- (94) Wilczak, N.; Kuhl, N.; Chesik, D.; Geerts, A.; Luiten, P.; De Keyser, J. *Journal of Neurochemistry* **2002**, *82*, 430-438.
- (95) Siwanowicz, I.; Popowicz Grzegorz, M.; Wisniewska, M.; Huber, R.; Kuenkele, K.-P.; Lang, K.; Engh Richard, A.; Holak Tad, A. *Structure* **2005**, *13*, 155-67.
- (96) Vajdos, F. F.; Ultsch, M.; Schaffer, M. L.; Deshayes, K. D.; Liu, J.; Skelton, N. J.; de Vos, A. M. *Biochemistry* **2001**, *40*, 11022-11029.
- (97) Liu, X.; Linnington, C.; Webster, H. D.; Lassmann, S.; Yao, D. L.; Hudson, L. D.; Wekerle, H.; Kreutzberg, G. W. *J Neurosci Res* **1997**, *47*, 531-8.
- (98) Clemmons, D. R. *Endocr. Rev.* **2001**, *22*, 800-17.
- (99) Voutilainen, R.; Ranks, S.; Mason, H. D.; Martikainen, H. *Journal of Clinical Endocrinology and Metabolism* **1996**, *81*, 1003-8.
- (100) Sesti, G.; Federici, M.; Lauro, D.; Sbraccia, P.; Lauro, R. *Diabetes Metab Res Rev* **2001**, *17*, 363-373.
- (101) De Meyts, P.; Whittaker, J. *Nat. Rev. Drug Discov.* **2002**, *1*, 769-83.
- (102) Siddle, K.; Urso, B.; Niesler, C. A.; Cope, D. L.; Molina, L.; Surinya, K. H.; Soos, M. A. *Biochem. Soc. Trans.* **2001**, *29*, 513-25.
- (103) Chou, P. Y.; Fasman, G. D. *J. Mol. Biol.* **1977**, *115*, 135-75.
- (104) Wilmot, C. M.; Thornton, J. M. *J. Mol. Biol.* **1988**, *203*, 221-32.
- (105) Venkatachalam, C. M. *Biopolymers* **1968**, *6*, 1425-36.
- (106) Thornton, J. M.; Sibanda, B. L.; Edwards, M. S.; Barlow, D. J. *Bioassays* **1988**, *8*, 63-9.

- (107) Hanessian, S.; McNaughton-Smith, G.; Lombart, H.-G.; Lubell, W. D. *Tetrahedron* **1997**, *53*, 12789-854.
- (108) Burgess, K. *Acc. Chem. Res.* **2001**, *34*, 826-35.
- (109) Kyle, D. J.; Green, L. M.; Blake, P. R.; Smithwick, D.; Summers, M. F. *Peptide Research* **1992**, *5*, 206-09.
- (110) Virgilio, A. A.; Bray, A. A.; Zhang, W.; Trinh, L.; Snyder, M.; Morrissey, M. M.; Ellman, J. A. *Tetrahedron* **1997**, *53*, 6635-44.
- (111) Eguchi, M.; Lee, M. S.; Nakanishi, H.; Stasiak, M.; Lovell, S.; Kahn, M. *J. Am. Chem. Soc.* **1999**, *121*, 12204-5.
- (112) Kitagawa, O.; Velde, D. V.; Dutta, D.; Morton, M.; Takusagawa, F.; Aubé, J. *J. Am. Chem. Soc.* **1995**, *117*, 5169-78.
- (113) Wang, W.; Yang, J.; Ying, J.; Xiong, C.; Zhang, J.; Cai, C.; Hruby, V. J. *J. Org. Chem.* **2002**, *67*, 6353-60.
- (114) Johannesson, P.; Lindeberg, G.; Tong, W.; Gogoll, A.; Karlen, A.; Hallberg, A. *J. Med. Chem.* **1999**, *42*, 601-8.
- (115) Mueller, R.; Revesz, L. *Tetrahedron Lett.* **1994**, *35*, 4091-2.
- (116) Shuker, S. B.; Hajduk, P. J.; Meadows, R. P.; Fesik, S. W. *Science* **1996**, *274*, 1531-4.
- (117) Hajduk, P. J.; Sheppard, G.; Nettlesheim, D. G.; Olejniczak, E. T.; Shuker, S. B.; Meadows, R. P.; Steinman, D. H.; Carrera, G. M.; Marcotte, P. A.; Severin, J.; Walter, K.; Smith, H.; Gubbins, E.; Simmer, R.; Holzman, T. F.; Morgan, D. W.; Davidsen, S. K.; Summers, J. B.; Fesik, S. W. *J. Am. Chem. Soc.* **1997**, *119*, 5818-27.
- (118) Olejniczak, E. T.; Hajduk, P. J.; Marcotte, P. A.; Nettlesheim, D. G.; Meadows, R. P.; Edalji, R.; Holzman, T. F.; Fesik, S. W. *J. Am. Chem. Soc.* **1997**, *119*, 5828-32.
- (119) Hajduk, P. J.; Olejniczak, E. T.; Fesik, S. W. *JACS* **1997**, *119*, 12257-61.
- (120) Livnah, O.; Stura, E. A.; Johnson, D. L.; Middleton, S. A.; Mulcahy, L. S.; Wrighton, N. C.; Dower, W. J.; Jolliffe, L. K.; A. Wilson, I. *Science* **1996**, *273*, 464-71.

- (121) Wrighton, N. C.; Balasubramanian, P.; Barbone, F. P.; Kashyap, A. K.; Farrell, F. X.; Jolliffe, L. K.; Barrett, R. W.; Dower, W. J. *Nature Biotechnology* **1997**, *15*, 1261-5.
- (122) Wrighton, N. C.; Farrell, F. X.; Chang, R.; Kashyap, A. K.; Barbone, F. P.; Mulcahy, L. S.; Johnson, D. L.; Barrett, R. W.; Jolliffe, L. K.; Dower, W. J. *Science* **1996**, *273*, 458-63.
- (123) Cwirla, S. E.; Balasubramanian, P.; Duffin, D. J.; Wagstrom, C. R.; Gates, C. M.; Singer, S. C.; Davis, A. M.; Tansik, R. L.; Mattheakis, L. C.; Boytos, C. M.; Schatz, P. J.; Baccanari, D. P.; Wrighton, N. C.; Barrett, R. W.; Dower, W. J. *Science* **1997**, *276*, 1696-9.
- (124) Xie, Y.; Longo, F. M. *Progress in Brain Research* **2000**, *128*, 333-47.
- (125) Beglova, N.; Maliartchouk, S.; Ekiel, I.; Zaccaro, M. C.; Saragovi, H. U.; Gehring, K. *J. Med. Chem.* **2000**, *43*, 3530-40.
- (126) Nishino, N.; Mihara, H.; Tanaka, Y.; Fujimoto, T. *Tetrahedron Lett.* **1992**, *33*, 5767-5770.
- (127) Stigers, K. D.; Soth, M. J.; Nowick, J. S. *Curr. Opin. Chem. Biol.* **1999**, *3*, 714-23.
- (128) Moree, W. J.; Marel, G. A.; Liskamp, R. M. J. *Tetrahedron Lett.* **1992**, *33*, 6389-92.
- (129) Pattarawarapan, M.; Zaccaro, M. C.; Saragovi, U.; Burgess, K. *J. Med. Chem.* **2002**, *45*, 4387-90.
- (130) Reyes, S. J.; Burgess, K. *Tetrahedron: Asymm.* **2005**, *16*, 1061-1069.
- (131) Kessler, H. *Angew. Chem. Int. Ed.* **1993**, *32*, 543-4.
- (132) Wels, B.; Kruijtzter, J. A. W.; Liskamp, R. M. J. *Org. Lett.* **2002**, *4*, 2173-6.
- (133) Patch, J. A.; Kirshenbaum, K.; Seuryneck, S. L.; Zuckermann, R. N.; Barron, A. E. In *Pseudo-Peptides in Drug Discovery*; Nielsen, P. E., Ed.; Wiley-VCH: Weinheim, Germany, 2004, p 1-31.
- (134) Alluri, P. G.; Reddy, M. M.; Bachhawat-Sikder, K.; Olivos, H. J.; Kodadek, T. *J. Am. Chem. Soc.* **2003**, *125*, 13995-14004.
- (135) Peretto, I.; Sanchez-Martin, R. M.; Wang, X.; Ellard, J.; Mittoo, S.; Bradley, M. *Chem. Commun.* **2003**, *18*, 2312-2313.

- (136) Meier, C.; Engels, J. W. *Angew. Chem. Int. Ed.* **1992**, *31*, 1008-10.
- (137) Shin, I.; Park, K. *Organic Letters* **2002**, *4*, 869-872.
- (138) Goff, D. A.; Zuckermann, R. N. *JOC* **1995**, *60*, 5744-5.
- (139) Kumpaty, H. J.; Bhattacharyya, S. *Synthesis* **2005**, 2205-2209.
- (140) Kruijtzter, J. A. W.; Liskamp, R. M. J. *Tetrahedron Lett.* **1995**, *36*, 6969-72.
- (141) Mouna, A. M.; Nguyen, C.; Rage, I.; Xie, J.; Nee, G.; Mazaleyrat, J. P.; Wakselman, M. *Synthetic Communications* **1994**, *24*, 2429-35.
- (142) Zuckermann, R. N.; Kerr, J. M.; Kent, S. B. H.; Moos, W. H. *J. Am. Chem. Soc.* **1992**, *114*, 10646-7.
- (143) Kruijtzter, J. A. W.; Hofmeyer, L. J. F.; Heerma, W.; Versluis, C.; Liskamp, R. M. *J. Chemistry--A European Journal* **1998**, *4*, 1570-1580.
- (144) Simon, R. J.; Kania, R. S.; Zuckermann, R. N.; Huebner, V. D.; Jewell, D. A.; Banville, S.; Ng, S.; Wang, L.; Rosenberg, S.; Marlowe, C. K. *Proc. Natl. Acad. Sci.* **1992**, *89*, 9367-71.
- (145) Kodadek, T.; Reddy, M. M.; Olivos, H. J.; Bachhawat-Sikder, K.; Alluri, P. G. *Acc. Chem. Res.* **2004**, *37*, 711-718.
- (146) Gordon, E. M.; Barrett, R. W.; Dower, W. J.; Fodor, S. P. A.; Gallop, M. A. *J. Med. Chem.* **1994**, *37*, 1385-401.
- (147) Olivos, H. J.; Alluri, P. G.; Reddy, M. M.; Salony, D.; Kodadek, T. *Org. Lett.* **2002**, *4*, 4057-4059.
- (148) Gorske, B. C.; Jewell, S. A.; Guerard, E. J.; Blackwell, H. E. *Org. Lett.* **2005**, *7*, 1521-1524.
- (149) Fukuyama, T.; Jow, C.-K.; Cheung, M. *Tetrahedron Lett.* **1995**, *36*, 6373-4.
- (150) Chevallet, P.; Garrouste, P.; Malawska, B.; Martinez, J. *Tetrahedron Lett.* **1993**, *34*, 7409-12.
- (151) Zhang, Y.; Kennan, A. J. *Org. Lett.* **2001**, *3*, 2341-4.
- (152) Gardner, A. R. K., R.; Wang, C.; Phanstiel, O. *JOC* **2004**, *69*, 3530-3537.
- (153) Reddy, G. V. S. R., G. Venkat; Subramanyam, R. V. K.; Iyengar, D. S. *Synthetic Communications* **2000**, *30*, 2233-2237.
- (154) Park, C.; Burgess, K. *J. Comb. Chem.* **2001**, *3*, 257-66.

- (155) Holder, J. R. B., Rayna; Xiang, Zhimin; Scott, Joseph; Haskell-Luevano, Carrie *Bioorg. & Med. Chem. Lett.* **2003**, *13*, 4505-9.
- (156) Ohnishi, M.; Urry, D. W. *Biochem. and Biophys. Res. Commun.* **1969**, *36*, 194-202.
- (157) Williamson, M. P.; Waltho, J. P. *Chem. Soc. Rev.* **1992**, 227-36.
- (158) Sefler, A. M.; Lauri, G.; Bartlett, P. A. *Int. J. Peptide Protein Res.* **1996**, *48*, 129-38.
- (159) Narutis, V. P.; Kopple, K. D. *Biochemistry* **1983**, *22*, 6233-9.
- (160) Smith, J. A.; Pease, L. G. *CRC Crit. Rev. Biochem.* **1980**, *8*, 315-99.
- (161) Englander, S. W.; Downer, N. W.; Teitelbaum, H. *Annu. Rev. Biochem* **1972**, *41*, 903-24.
- (162) Perczel, A.; Hollosi, M. In *Circular Dichroism and the Conformational Analysis of Biomolecules*; Fasman, G. D., Ed.; Plenum Press: New York, 1996, p 362-4.
- (163) Woody, R. W. In *Circular Dichroism Principles and Applications*; Nakanishi, K., Berova, N., Woody, R. W., Eds.; VCH: New York, 1994, p 473-96.
- (164) Manning, M. C.; Illangasekare, M.; Woody, R. W. *Biophys. Chem.* **1988**, *31*, 77-86.
- (165) Woody, R. W. In *Peptides, Polypeptides and Proteins*; Blout, E. R., Bovey, F. A., Goodman, M., Lotan, N., Eds.; Wiley: New York, 1974, p 338-50.
- (166) Bush, C. A.; Sarkar, S. K.; Kopple, K. D. *Biochemistry* **1978**, *17*, 4951-4.
- (167) Greenfield, N.; Fasman, G. D. *Biochemistry* **1969**, *8*, 4108-16.
- (168) Bandekar, J.; Evans, D. J.; Krimm, S.; Leach, S. J.; Lee, S.; McQuie, J. R.; Minasian, E.; Nemethy, G.; Pottle, M. S.; Scheraga, H. A.; Stimson, E. R.; Woody, R. W. *Int. J. Peptide Protein Res.* **1982**, *19*, 187-205.
- (169) Pettitt, B. M.; Matsunaga, T.; Al-Obeidi, F.; Gehrig, C.; Hruby, V. J.; Karplus, M. *Biophys. J. Biophys. Soc.* **1991**, *60*, 1540-4.
- (170) O'Connor, S. D.; Smith, P. E.; Al-Obeidi, F.; Pettitt, B. M. *J. Med. Chem.* **1992**, *35*, 2870-81.
- (171) Saragovi, H. U.; Zheng, W.; Maliartchouk, S.; DiGugliemo, G. M.; Mawal, Y. R.; Kamen, A.; Woo, S. B.; Cuello, A. C.; Debeir, T.; Neet, K. E. *J Biol Chem* **1998**, *273*, 34933-40.

- (172) Knight, E., Jr.; Connors, T. J.; Maroney, A. C.; Angeles, T. S.; Hudkins, R. L.; Dionne, C. A. *Anal Biochem* **1997**, *247*, 376-81.
- (173) Carmignani, M.; Volpe, A. R.; Botta, B.; Espinal, R.; De Bonnevaux, S. C.; De Luca, C.; Botta, M.; Corelli, F.; Tafi, A.; Rosario, S.; Monache, G. D.; *J. Med. Chem.* **2001**, *44*, 2950-8.
- (174) Feng, Y.; Pattarawarapan, M.; Wang, Z.; Burgess, K.; *Org. Lett.* **1999**, *1*, 121-4

APPENDIX

EXPERIMENTAL SECTION FOR CHAPTER II

General Methods

NMR spectra were recorded on INOVA 500 (500 MHz for ^1H and 125 MHz ^{13}C) and Mercury 300 (300 MHz for ^1H) spectrometers. NMR chemical shifts are expressed in ppm relative to internal solvent peaks, and coupling constants were measured in Hz. ESI and MALDI mass spectra were obtained from the Mass Spectrometry Applications Laboratory at Texas A&M University. Thin layer chromatography was performed using silica gel 60 F254 plates. Flash chromatography was performed using silica gel (230-600 mesh). All chemicals were purchased from commercial supplier and used as received. For solid phase synthesis at room temperature, a manual control shaking apparatus and standard Fmoc and peptoid chemistry were used throughout. A fritted polypropylene syringe (5-10 mL capacity) purchased from Torviq was used as the reaction vessel. A CEM Discover microwave reactor was used for the peptoid synthesis with magnetic stirring at atmospheric pressure. A 10 mL microwave reaction tube from CEM was used for the microwave reactions. All the α -amino acids used had the L-configuration and were obtained from Advanced ChemTech except where otherwise indicated. All primary amines are from Aldrich and Fluka. Reverse phase high performance liquid chromatography (RP-HPLC) was carried out on Vydac C-18 columns (25 x 0.46 cm for analysis, 25 x 2.2 cm for preparative work) using Beckman system with the 32 Karat software. The Sedex 55 was used for ELS detection, while the UV detectors used were Beckman System Gold 166 (215 and 254 nm) and System Gold 166P (215 nm) for analytical and preparative HPLC analyses respectively. All HPLC analyses were done using gradient conditions. The eluents used were solvent A (H_2O with 0.1 % TFA) and solvent B (CH_3CN with 0.1 % TFA). Flow rates applied were 1 mL/min and 10 mL/min for analytical and preparative HPLC respectively.

Preparation of Protected Amines and Templates

***N*-(2-*tert*-Butoxyethyl)-2-nitrobenzenesulfonamide (3).** A solution of nosyl chloride (3.63 g, 16.37 mmol) in ethanol (10 mL) was added dropwise to a solution of aminoethanol (1.00 g, 16.37 mmol) in ethanol (15 mL). The mixture was stirred at 25 °C for 2 h and monitored with TLC and ninhydrin. The solvent was evaporated. ¹H NMR analysis of the crude *N*-nosylaminoethanol indicated that it was sufficiently pure for the next step, so it was used for the next step without purification. This product was dissolved in dichloromethane (25 mL) and cooled to -78 °C, then 0.25 mL of H₃PO₄ dried over P₂O₅ was added to the solution, stirred, and, while stirring, 0.5 mL of BF₃·Et₂O was added. *Isobutene* (13 mL) was collected onto a 25 mL flask in a dry ice bath and added into the reaction mixture. The reaction mixture was stirred in dry ice for 1.5 h and then allowed to stir overnight at room temperature. The reaction mixture was poured into a 2 M ammonium hydroxide solution (50 mL) and extracted with dichloromethane. The organic solution was dried over sodium sulfate, concentrated, and flash columned with 50 % ethyl acetate in hexane eluent. The product was dried to obtain a yellow powder (3.5 g, 69 %). R_f = 0.78 (50 % ethyl acetate in hexane); ¹H NMR (300 MHz, CDCl₃) δ 8.40-8.36 (m, 1H), 7.97-7.93 (1, 2H), 7.72-7.69(m, 2H), 3.41 (t, *J* = 5.0 Hz, 2H), 3.23 (t, *J* = 5.25 Hz), 2.01 (s, 1H), 1.09 (s, 9H); ¹³C NMR (75 MHz, DMSO-*d*₆) δ 130.6, 130.1, 117.6, 115.2, 155.0, 106.8, 65.6, 54.2, 42.5, 18.3; MS (ESI) calc'd for C₁₂H₁₈N₂O₅S (M+Na)⁺ 325, found 325.

***N*-(2-*tert*-Butoxypropyl)-2-nitrobenzenesulfonamide (4).** This compound was prepared via a procedure similar to that described above. R_f = 0.59 (30 % ethyl acetate in hexane); ¹H NMR (300 MHz, CDCl₃) δ 8.10 (d, *J* = 3.0 Hz, 1H), 7.85-7.83 (m, 1H), 7.74-7.70 (m, 2H), 3.29-3.23 (m, 3H), 1.96 (s, 1H), 1.18 (s, 9H), 1.11 - 0.99 (m, 3H); ¹³C NMR (75 MHz, DMSO-*d*₆) 130.6, 117.6, 115.3, 115.1, 106.8, 100.8, 65.5, 55.7, 54.2, 21.6, 18.5; MS (ESI) calc'd for C₁₃H₂₀N₂O₅S (M+Li⁺) 323, found 323.

1-Amino-4-[N^2, N^3 -bis(*tert*-butoxycarbonyl)guanidino] propane (5). A solution of 1,3-diaminopropane (0.26 g) was prepared in 5% N,N' -diisopropylethylamine in THF (10 mL). Then a solution of N,N' -bis(*tert*-butoxycarbonyl)-1*H*-pyrazole-1-carboxamidine¹⁵¹ (0.51 g) in THF (10 mL) was added dropwise with vigorous stirring. The mixture was stirred at 25 °C overnight. The solvent was evaporated and the product recrystallized in ethanol to obtain white crystals (0.29 g, 58 %), mp = 168-170 °C. R_f = 0.37 (10 % methanol, 1.0 % ammonium hydroxide, in chloroform). The ¹H NMR corresponds to the NMR reported in the literature.¹⁷³ ¹H NMR (300 MHz, CDCl₃) δ 7.56 (d, J = 2.1 Hz, 1H), 6.29 (s, 1H), 3.33 (t, J = 5.85 Hz, 4H), 1.87 (m, 2H), 1.42 (s, 18H).

(4-Aminobutyl)carbamic acid *tert*-butyl ester (6). Compound was synthesized as reported by Gardner *et.al.*¹⁵² R_f = 0.67 (10 % methanol, 1.0 % ammonium hydroxide, in chloroform); ¹H NMR (300 MHz, CDCl₃) δ 4.92 (s, 1H), 2.99 (t, J = 6.2 Hz, 2H), 2.60 (t, J = 6.5 Hz, 2H), 1.35 (s, 9H), 1.34 – 1.19 (m, 4H).

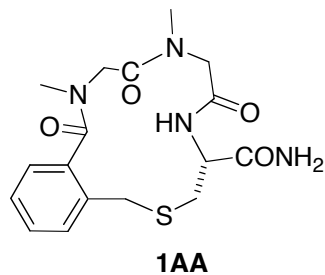
4-Aminomethylphenol (7). Compound synthesized as reported by Reddy *et al.*¹⁵³ R_f = 0.49 (20 % ethyl acetate, in hexane); ¹H NMR (300 MHz, CDCl₃) δ 7.35-7.23 (m, 4H), 4.54 (s, 2H), 3.75 (bs, 2H);

2-bromomethyl-benzoic acid (8). This compound was synthesized following a procedure that was developed in our group.¹⁷⁴ ¹H NMR (300 MHz, CdCl₃) δ 8.03 (d, J = 7.5 Hz, 1H), 7.59 – 7.57 (m, 2H), 7.48 (d, J = 7.0 Hz, 1H), 5.01 (s, 2H)

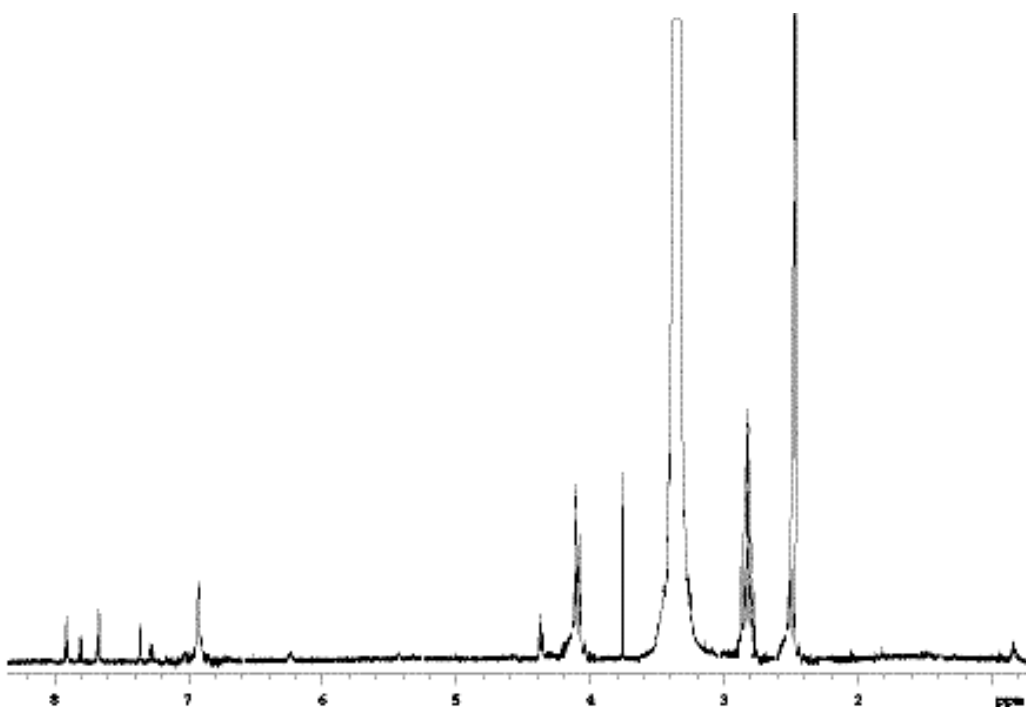
2-bromomethyl-5-nitrobenzoic acid (9). This compound was synthesized following a procedure that was developed in our group.¹⁷⁴ ¹H NMR (300 MHz, CdCl₃) δ 8.93 (s, 1H), 8.29 (d, J = 7.0 Hz, 1H), 7.88 (d, J = 7.0 Hz, 1H), 5.23 (s, 2H)

Synthesis Procedures and Spectral Data for Compounds 1

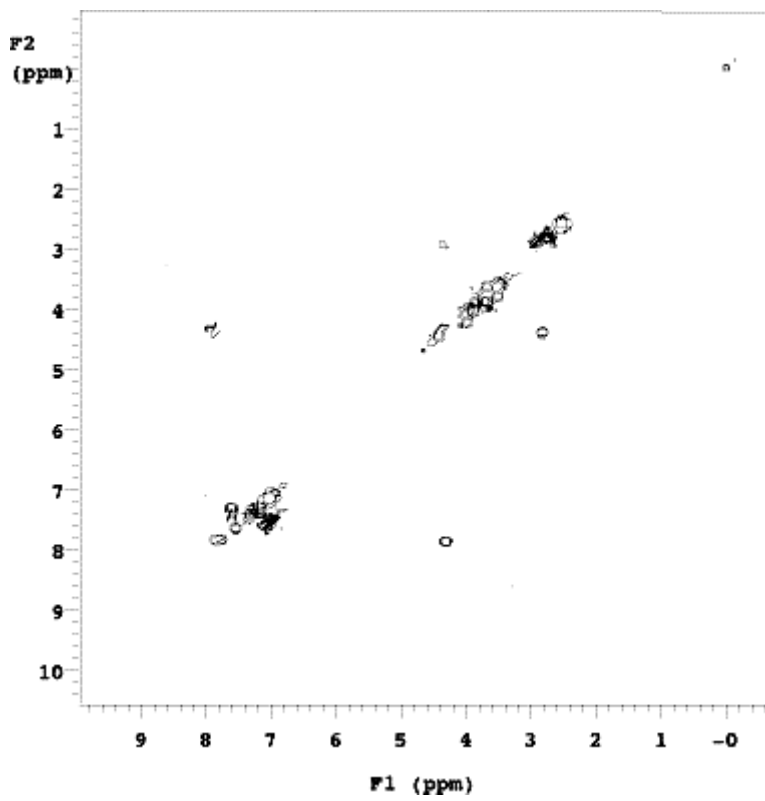
Rink amide MBHA resin (0.100 g, 0.72 mmol/g loading) was swelled with CH_2Cl_2 (10 mL/g) in a 3 mL fritted syringe for 30 min. The Fmoc protecting group on the Rink handle was removed by treating the resin with 20 % piperidine in DMF (2 x *ca* 1.5 mL, 10 min and then 15 min). The resin was then washed with DMF (3x), MeOH (3x), DMF (1x), MeOH (1x), CH_2Cl_2 (2x), MeOH (2x), and CH_2Cl_2 (3x), after which, Fmoc-Cys(Mmt)-OH (3 equiv.), DIC (3 equiv.), HOBt (3 equiv.), and DIEA (5 equiv.) in DMF (1.5 mL) were added. After gentle shaking for 2 h, the reaction mixture was then drained and the resin was subjected to the washing cycle and Fmoc deprotection as previously described. The resin was washed again, transferred to the microwave reaction vessel, and treated with bromoacetic acid (2M), DIC (2M), in DMF (*ca* 1.5 mL). The vessel was placed in a microwave reactor and irradiated at 50 °C, 1 atm (open vessel), for 1 min. After washing with DMF (9x), the resin was then treated with primary amine (2 M), in DMF or DMSO (1.5 mL), and microwaved at 50 °C, 1 atm (open vessel), for 1 min. The washing cycle with DMF were repeated. The two microwave reactions and washing cycles were repeated. Then the resin was transferred back to the syringe. The 2-bromomethylbenzoic acid moiety was introduced by treating the resin with 2-bromomethylbenzoyl chloride (3 equiv.) and DIEA (3 equiv.) in CH_2Cl_2 (1.5 mL) for 40 min. The Mmt protecting group of the cysteine was removed by treatment with 1 % TFA and 5 % TIS in CH_2Cl_2 (2 mL, 7x 2 min each, or until yellow color disappeared). After the resin was washed, macrocyclization was affected by adding K_2CO_3 (10 equiv.) in DMF and microwaving at 50 °C, 1 atm (open vessel), for 10 min. The reaction mixture was then drained and the resin was washed with H_2O (5x), DMF (3x), MeOH (3x), DMF (1x), MeOH (1x), CH_2Cl_2 (2x), MeOH (2x), and CH_2Cl_2 (3x) and then dried under vacuum for 4 h. The peptide was cleaved from the resin by treatment with a mixture of 90 % TFA, 5 % TIS, and 5 % H_2O . The cleavage solution was separated from the resin by filtration. After most of the cleavage cocktail was evaporated *in vacuo*, the crude peptide was triturated using anhydrous ethyl ether. The crude peptide was then dissolved in $\text{H}_2\text{O}/\text{CH}_3\text{CN}$ mixture (1:1, 2 mL), purified via preparative HPLC and then lyophilized to give a powder obtained as a TFA salt.



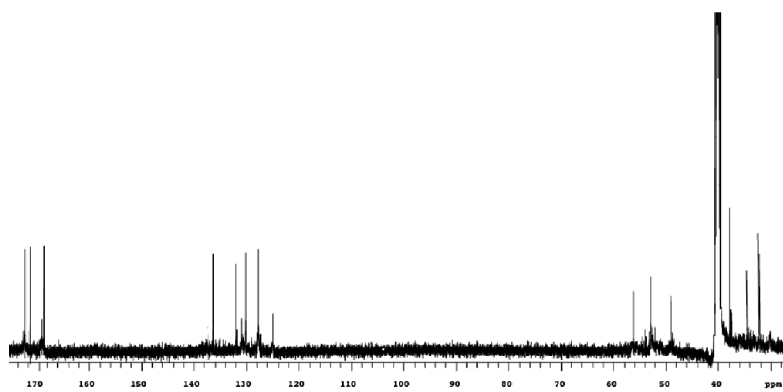
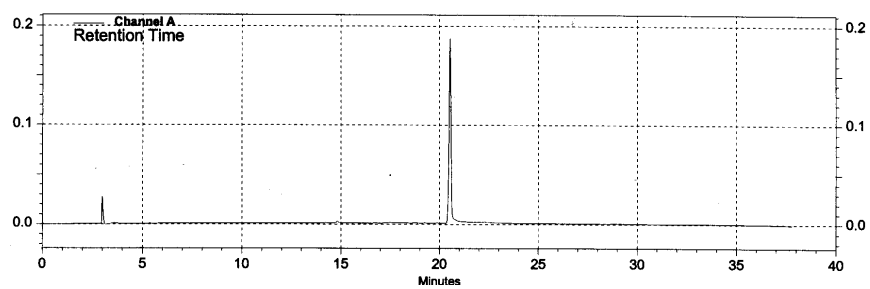
^1H NMR (500 MHz, DMSO- d_6) δ 7.96 (d, J = 6.5 Hz, 1H), 7.85 (d, J = 7.0 Hz, 1H), 7.68 (dd, J = 7.0, 2.5 Hz), 7.39 (d, J = 7.8 Hz), 7.32 (dd, J = 2.5, 7.8 Hz, 1H), 6.96 (s, 2H), 4.39-4.35 (m, 1H), 4.18-4.06 (m, 4H), 3.78 (s, 2H), 2.87-2.76 (m, 8H); ^{13}C NMR (125 MHz, DMSO- d_6) δ 172.6, 171.6, 169.0, 168.6, 136.5, 131.9, 130.9, 130.1, 127.7, 124.9, 56.2, 53.0, 49.0, 37.8, 37.6, 34.4, 32.2; LRMS (APCI) calc'd for $\text{C}_{17}\text{H}_{22}\text{N}_4\text{O}_4\text{S}$ ($\text{M}+\text{H}^+$) 379, found 379; analytical HPLC homogeneous single peak, retention time = 20.9 min (5-70% B in 30 min).



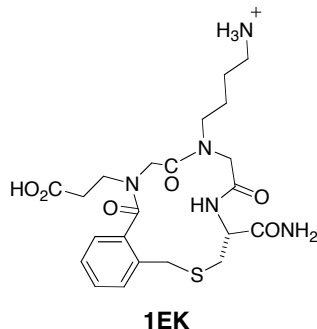
^1H NMR



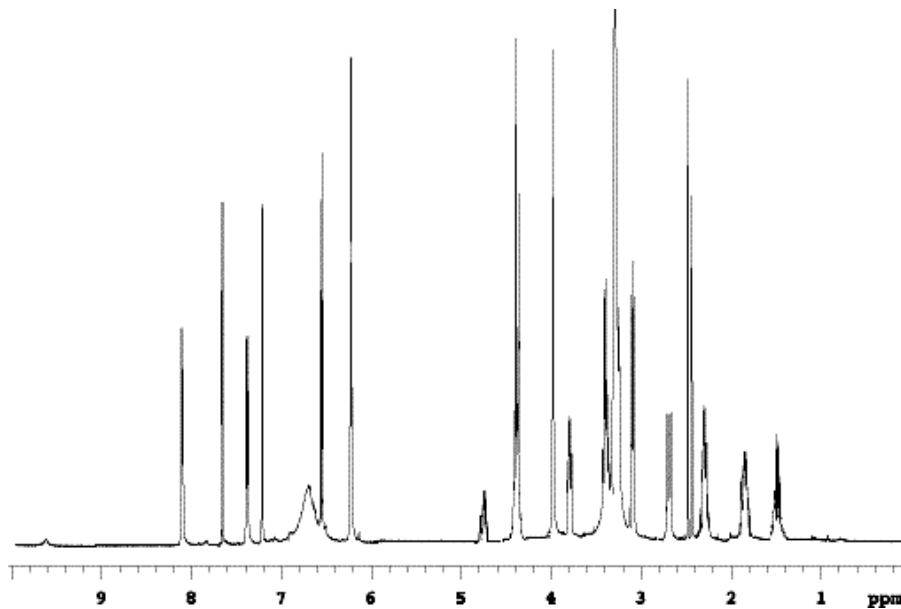
COSY

¹³C NMR

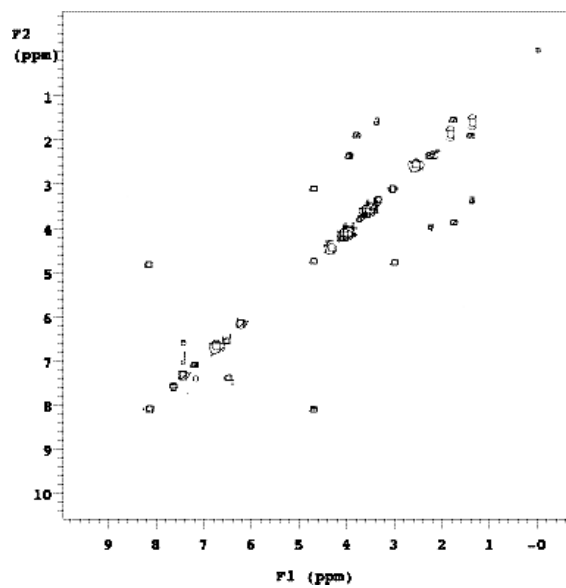
HPLC



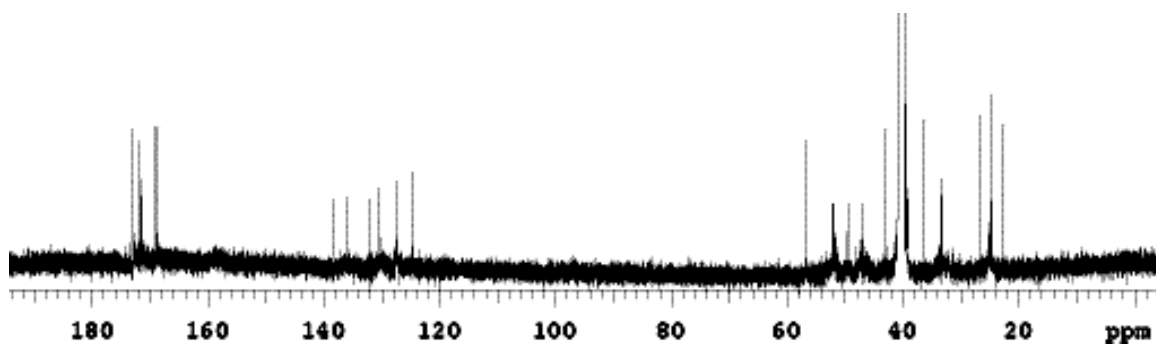
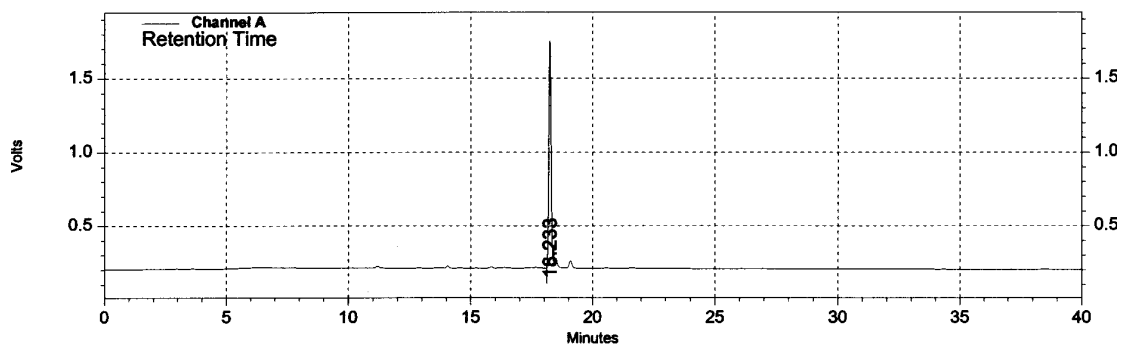
^1H NMR (500 MHz, DMSO- d_6) δ 8.17 (d, $J=8.0$ Hz, 1H), 7.65 (d, $J=7.8$, 1H), 7.40 (dd, $J=7.7$, 2.5 Hz, 3H), 7.20 (d, $J=7.7$, 1H), 6.70 (bs, 3H), 6.56 (dd, $J=7.8$, 2.5 Hz, 1H), 6.19 (s, 2H), 4.79-4.71 (m, 1H), 4.40-4.32 (m, 4H), 3.99 (s, 4H), 3.80 (t, $J=6.0$ Hz, 2H), 3.41-3.34 (m, 2H), 3.13 (t, $J=5.0$ Hz, 2H), 2.76 (d, $J=7.0$ Hz, 2H), 2.29 (t, $J=6.0$ Hz, 2H), 1.91-1.81 (m, 2H), 1.58-1.42 (m, 2H); ^{13}C NMR (125 MHz, DMSO- d_6) δ 172.9, 171.8, 171.5, 169.2, 168.8, 138.8, 135.9, 132.0, 130.6, 127.8, 124.7, 56.8, 52.2, 51.8, 49.5, 46.9, 43.2, 36.5, 33.3, 26.5, 24.8, 22.9; MS (ESI) calc'd for $\text{C}_{22}\text{H}_{31}\text{N}_5\text{O}_6\text{S}(\text{M}+\text{H}^+)$ 493, found 494; analytical HPLC: retention time = 18.2 min (8-70% B in 30 min), purity = 98 %.



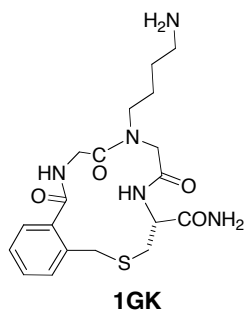
^1H NMR



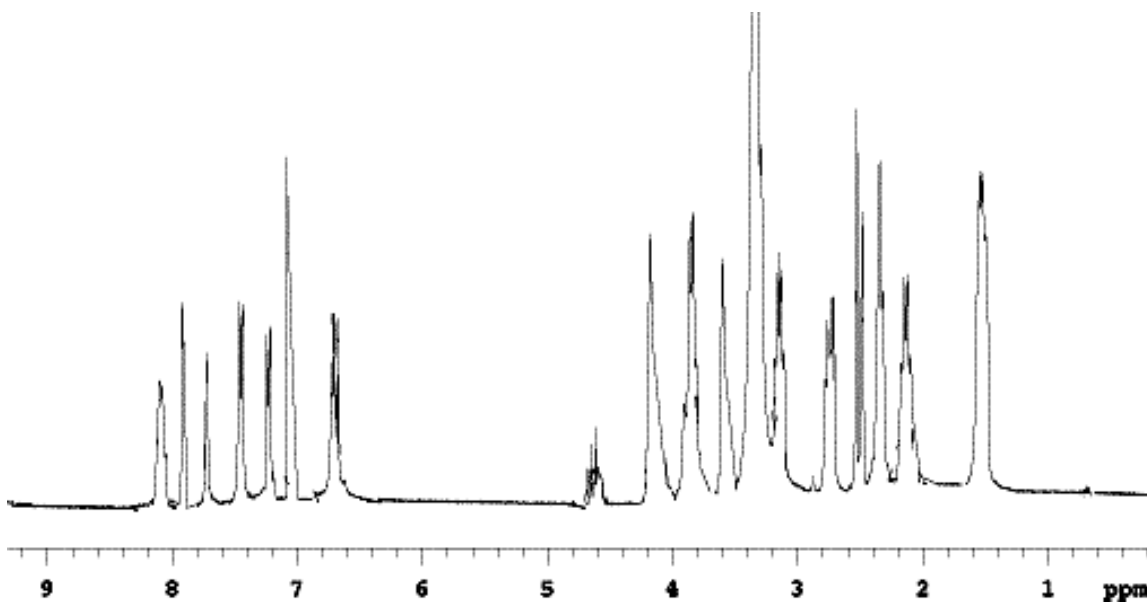
COSY

¹³C NMR

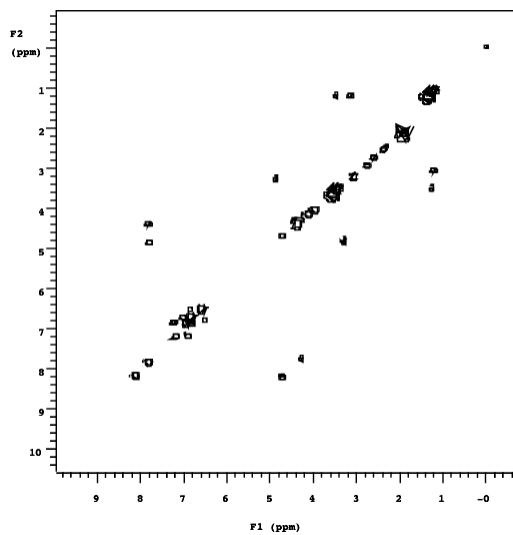
HPLC



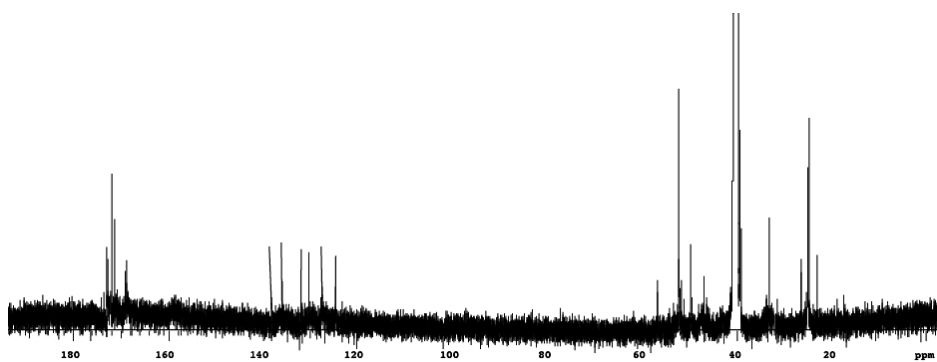
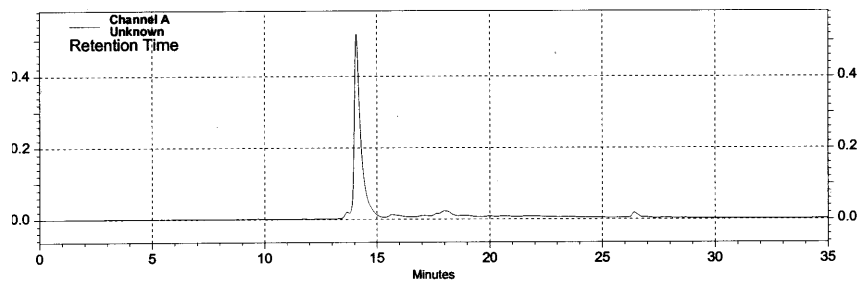
^1H NMR (500 MHz, DMSO-d_6) δ 8.17 (t, $J = 7.6$ Hz, 1H), 7.95 (d, $J = 8.0$ Hz, 1H), 7.74 (d, $J = 8.5$ Hz, 1H), 7.45 (dd, $J = 8.5, 3.8$ Hz, 1H), 7.23 (d, $J = 7.0$ Hz, 2H), 7.02 (s, 2H), 6.75 (dd, $J = 3.8, 7.0$ Hz, 1H), 4.71-4.58 (m, 1H), 4.21 (s, 2H), 3.82 (d, $J = 7.6$ Hz, 2H), 3.58 (s, 2H), 3.18 (t, $J = 7.4$ Hz, 2H), 2.75 (d, $J = 7.0$ Hz, 2H), 2.31 (m, 2H), 2.14 (bs, 2H), 1.57 (m, 4H); ^{13}C NMR (125 MHz, DMSO-d_6) δ 173.8, 172.6, 172.4, 169.2, 138.1, 135.9, 131.6, 130.2, 127.5, 124.7, 56.8, 52.2, 49.5, 46.9, 33.2, 26.5, 25.0, 24.9, 23.0; LRMS (ESI) calc'd for $\text{C}_{19}\text{H}_{27}\text{N}_5\text{O}_4\text{S}$ ($\text{M}+\text{H}^+$) 422, found 422; analytical HPLC: purity = 94 %, retention time = 14.1 min (5-95% B in 30 min).



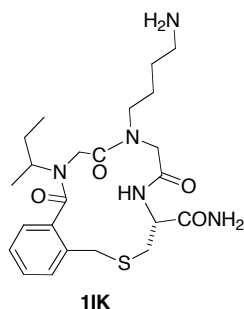
^1H NMR



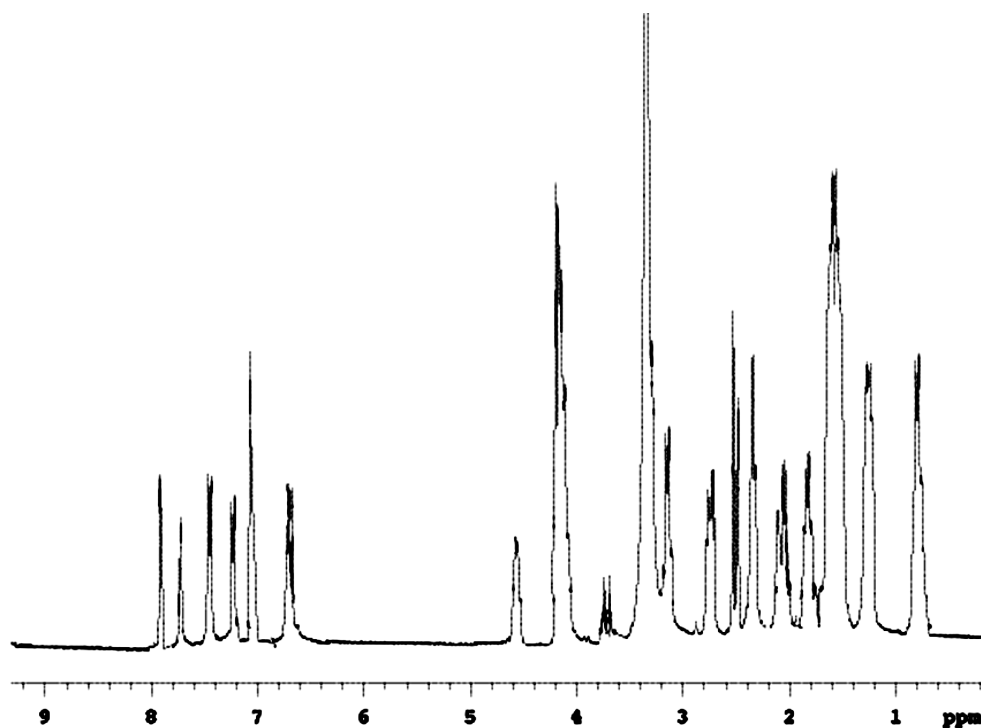
COSY

¹³C NMR

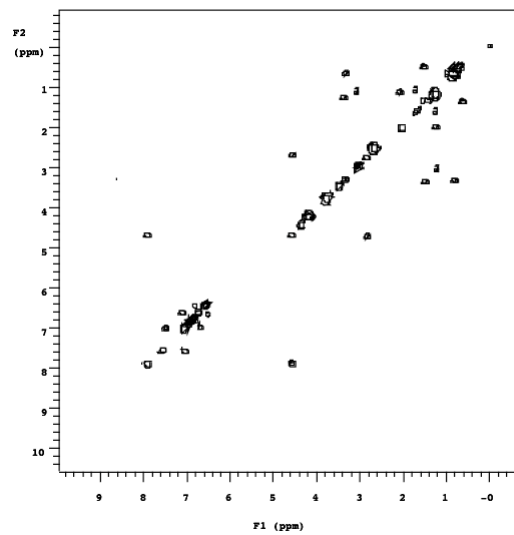
HPLC



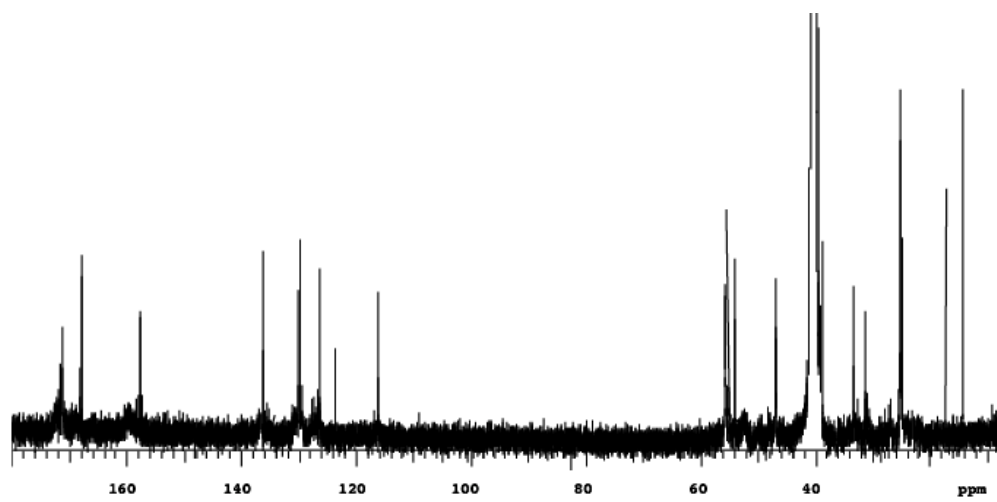
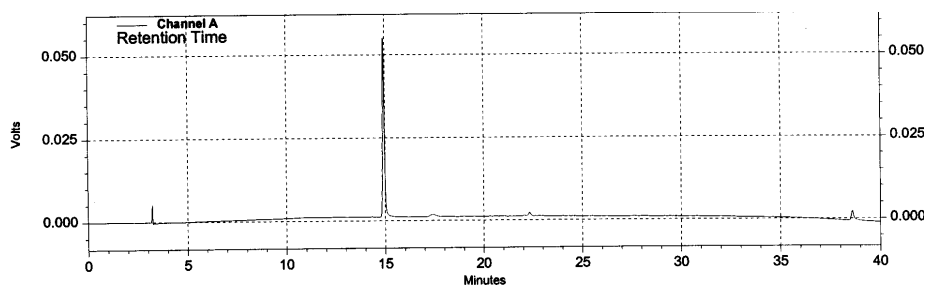
^1H NMR (300 MHz, DMSO-d_6) δ 7.95(d, $J = 5.2$ Hz, 1H), 7.76 (d, $J = 5.3$ Hz, 1H), 7.44 (dd, $J = 5.3, 3.0$ Hz, 1H), 7.21 (d, $J = 6.7$ Hz, 1H), 7.01 (s, 2H), 6.71 (dd, $J = 3.0, 6.7$ Hz, 1H), 4.60 (m, 1H), 4.24 (s, 2H), 4.15 (s, 4H), 3.75 (m, 1H), 3.17 (m, 2H), 2.76 (d, $J = 6.5$ Hz, 2H), 2.20-2.00 (m, 2H) 1.84 (bs, 2H), 1.71-1.52 (m, 6H), 1.24 (d, $J = 6.5$ Hz, 3H), 0.81 (t, $J = 6.8$ Hz, 3H); ^{13}C NMR (125 MHz, DMSO-d_6) δ 171.1, 167.9, 157.8, 157.5, 136.2, 130.1, 129.6, 127.2, 126.4, 116.1, 55.9, 55.7, 54.2, 46.9, 39.4, 38.9, 33.6, 31.9, 25.3, 25.1, 24.8, 17.4, 14.2; LRMS (ESI) calc'd for $\text{C}_{23}\text{H}_{35}\text{N}_5\text{O}_4\text{S}$ ($\text{M}+\text{H}^+$) 478, found 478; analytical HPLC: purity = 97 %, retention time = 14.9 min (5-95% B in 30 min).



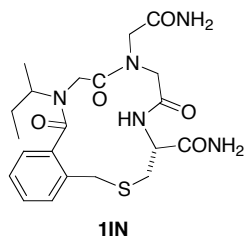
^1H NMR



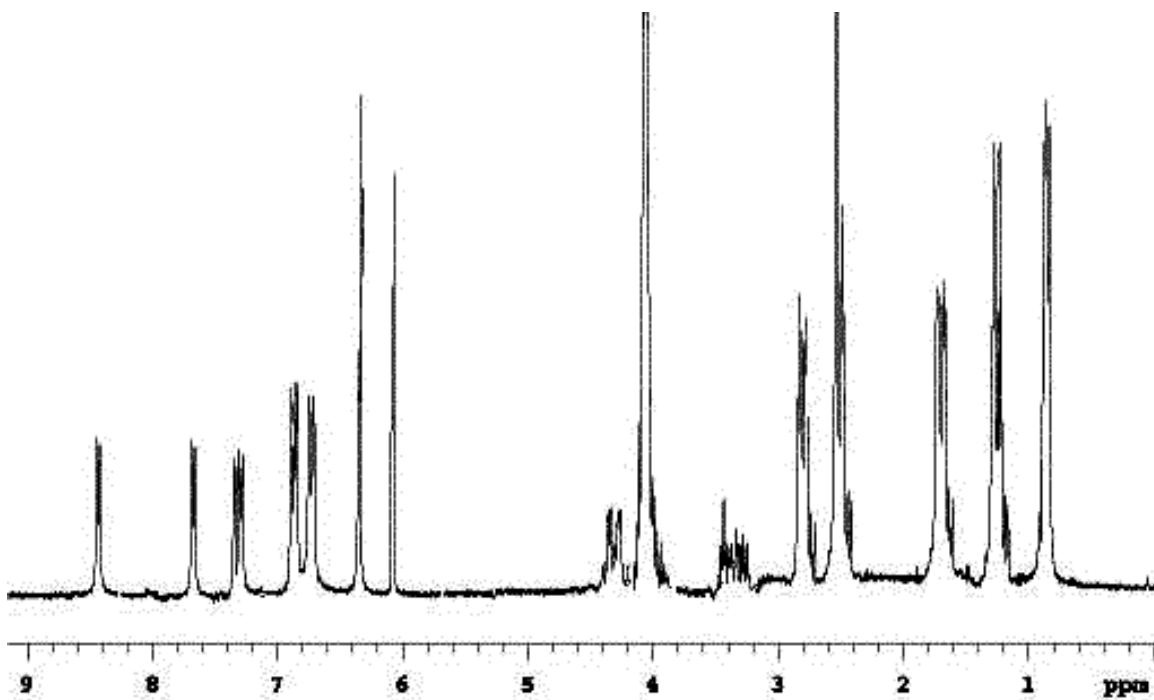
COSY

¹³C NMR

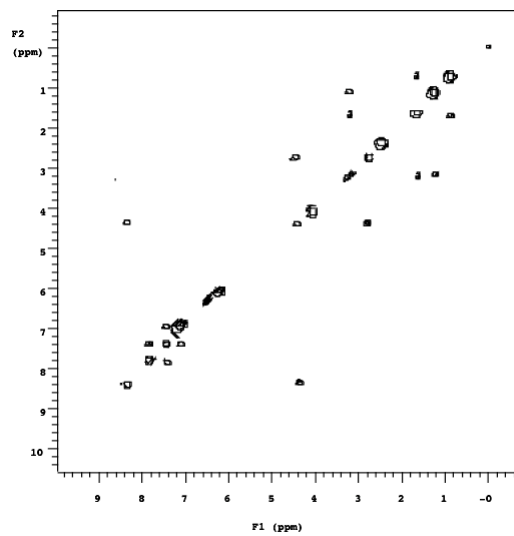
HPLC



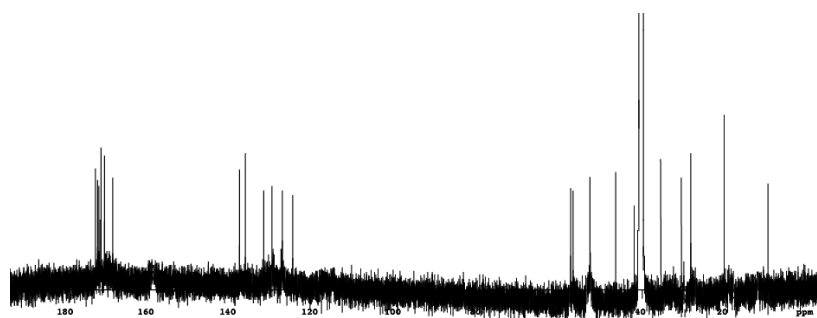
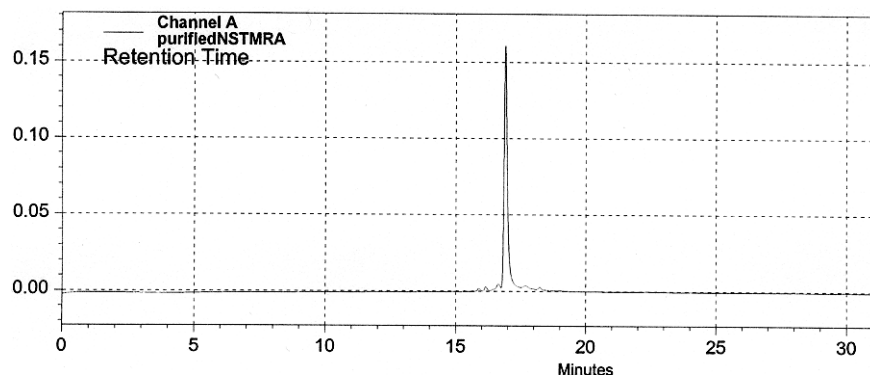
11n: ^1H NMR (500 MHz, DMSO-d_6) δ 8.45 (d, $J = 7.2$ Hz, 1H), 7.72 (d, $J = 7.0$ Hz, 1H), 7.36 (dd, $J = 7.0, 2.5$ Hz, 1H), 6.89 (dd, $J = 2.5, 7.4$ Hz, 1H), 6.77 (d, $J = 7.4$ Hz, 1H), 6.36 (s, 2H), 6.03 (s, 2H), 4.22-4.41 (m, 1H), 4.18-3.97 (m, 6H), 3.45-3.21 (m, 3H), 2.77 (d, $J = 9.5$ Hz, 2H), 1.84-1.72 (m, 2H), 1.28 (d, $J = 7.5$, 3H), 0.83 (t, $J = 7.0$ Hz, 3H); ^{13}C NMR (125 MHz, DMSO-d_6) δ 173.1, 172.3, 171.7, 170.9, 168.8, 137.8, 136.5, 132.7, 129.9, 127.4, 125.0, 57.2, 56.7, 52.7, 46.4, 41.8, 35.7, 31.4, 27.9, 19.9, 9.3; LRMS (ESI) calc'd for $\text{C}_{21}\text{H}_{29}\text{N}_5\text{O}_5\text{S}$ ($\text{M}+\text{H}^+$) 464, found 464; analytical HPLC: homogeneous single peak, retention time = 16.8 min (8-70% B in 30 min).



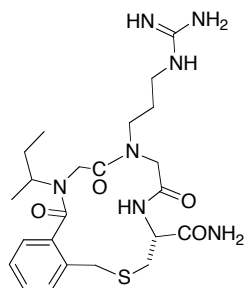
^1H NMR



COSY

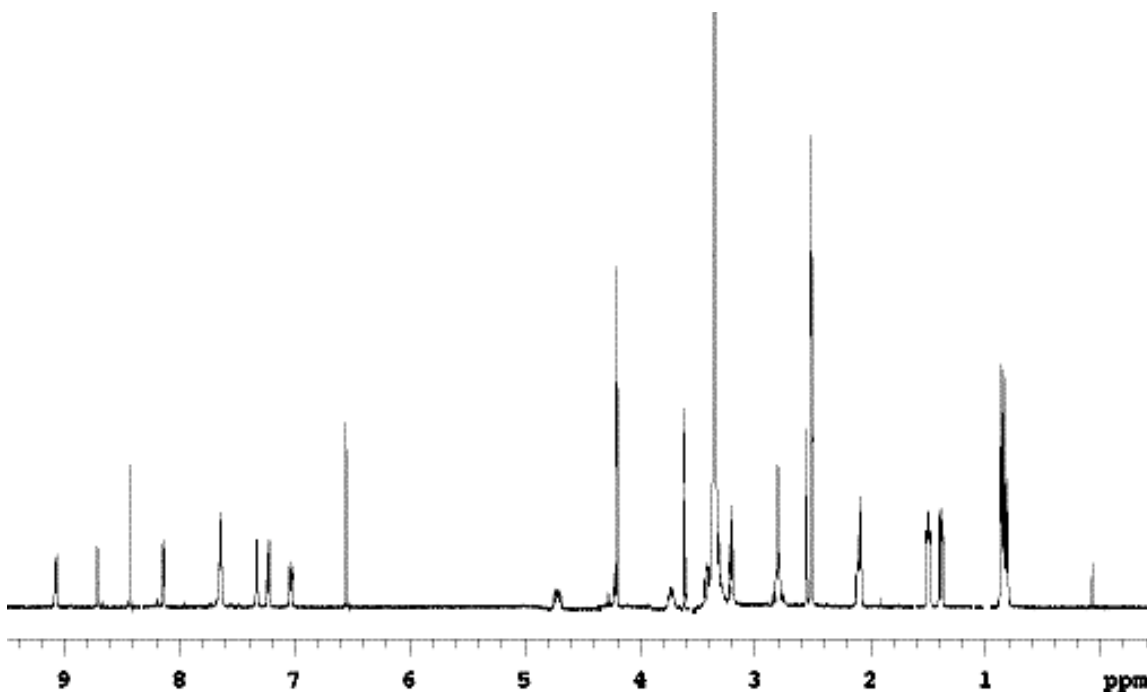
¹³C NMR

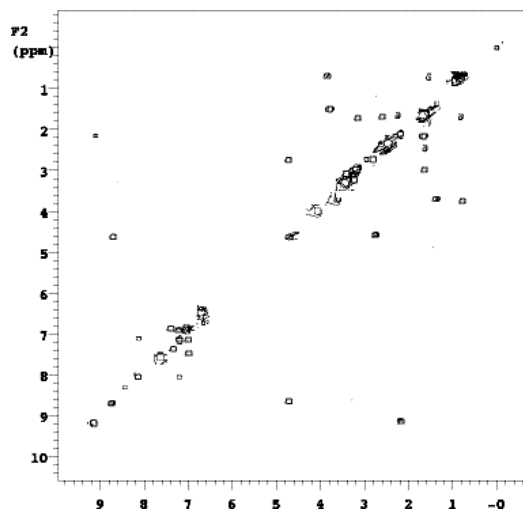
HPLC



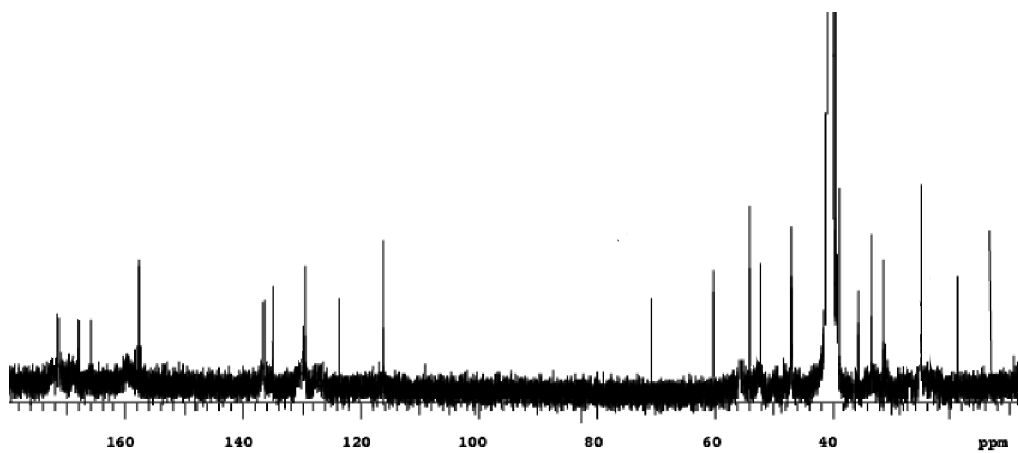
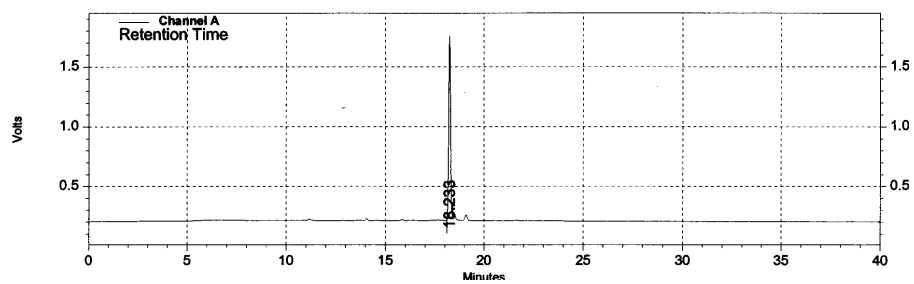
11R

^1H NMR (500 MHz, DMSO- d_6) δ 9.11 (t, $J = 8.0$ Hz, 1H), 8.76 (d, $J = 7.5$ Hz, 1H), 8.41 (s, 1H), 8.17 (d, $J = 7.6$ Hz, 1H), 7.64 (s, 2H), 7.38 (d, $J = 7.0$ Hz, 1H), 7.23 (dd, $J = 7.6$, 3.4 Hz, 1H), 7.06 (dd, $J = 3.4$, 7.0 Hz, 1H), 6.58 (s, 2H), 4.79-4.68 (m, 1H), 4.22-4.19 (m, 4H), 3.79-3.71 (m, 1H), 3.61 (s, 2H), 3.19 (t, $J = 7.2$ Hz, 2H), 2.80 (d, $J = 7.8$ Hz, 2H), 2.15-2.10 (m, 2H), 1.58-1.52 (m, 4H), 1.40-1.37 (m, 2H), 0.88-0.79 (6, 4H); ^{13}C NMR (125 MHz, DMSO- d_6) δ 172.0, 171.9, 168.9, 165.8, 157.9, 137.8, 137.4, 135.6, 130.1, 123.7, 116.4, 70.8, 60.1, 54.1, 52.2, 47.3, 39.2, 35.7, 33.6, 31.7, 25.7, 18.6, 13.5; MALDI MS calc'd for ($\text{M}+\text{H}^+$) 506, found 506, ($\text{M}+\text{K}^+$) 544 found 544; analytical HPLC purity = 97 %, retention time = 18.2 min (5-95% B in 30 min).

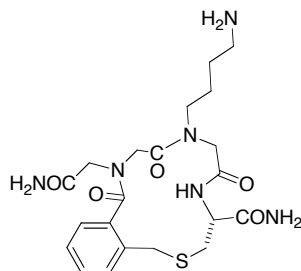
 ^1H NMR



COSY

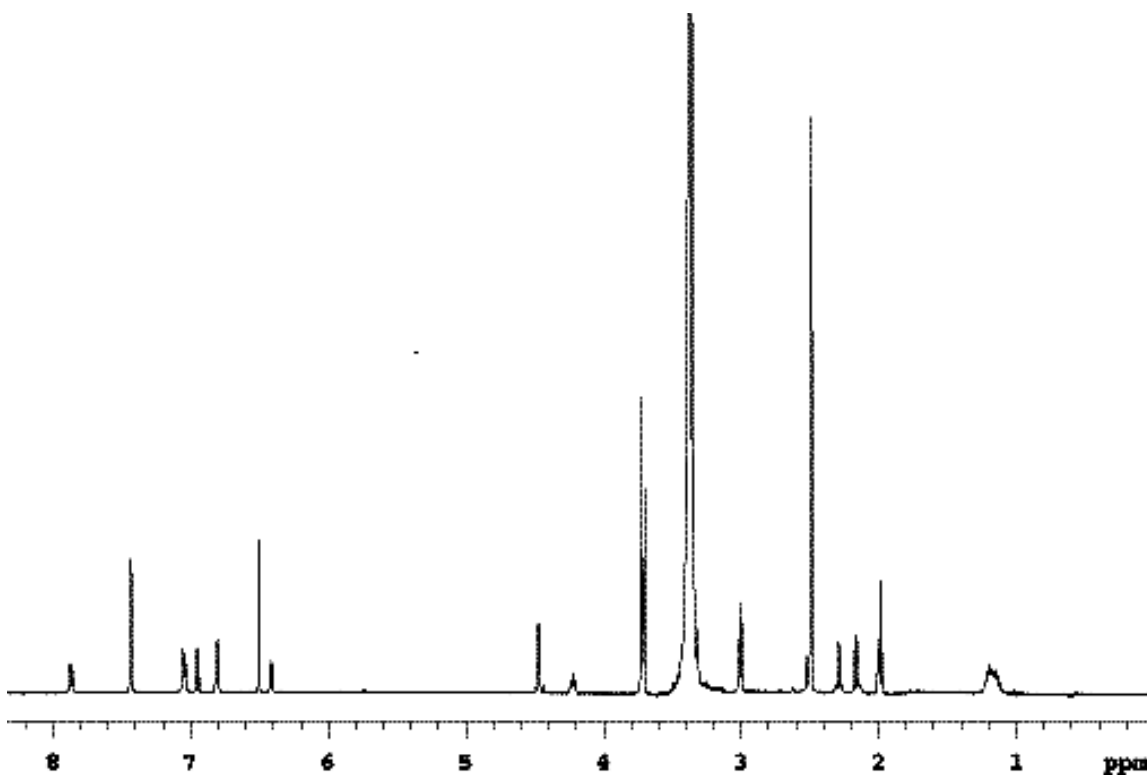
¹³C NMR

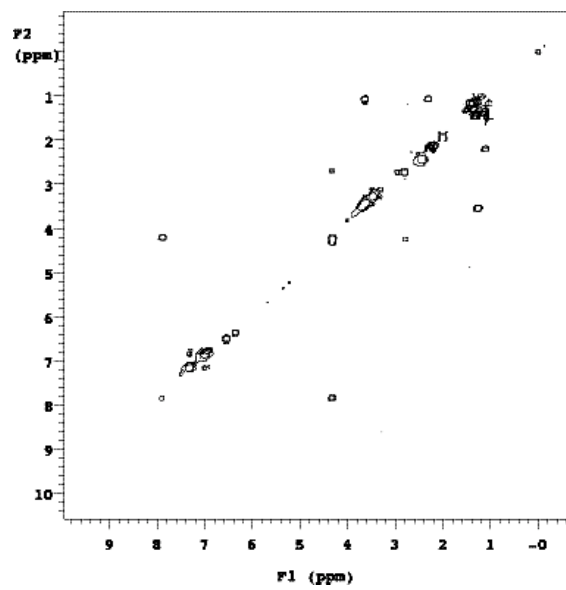
HPLC



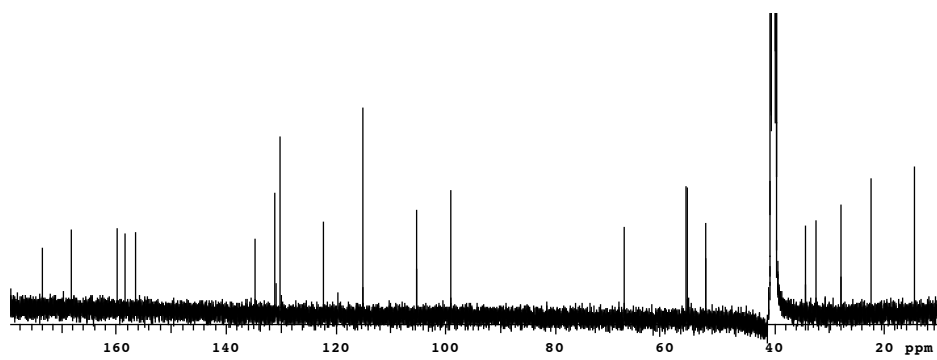
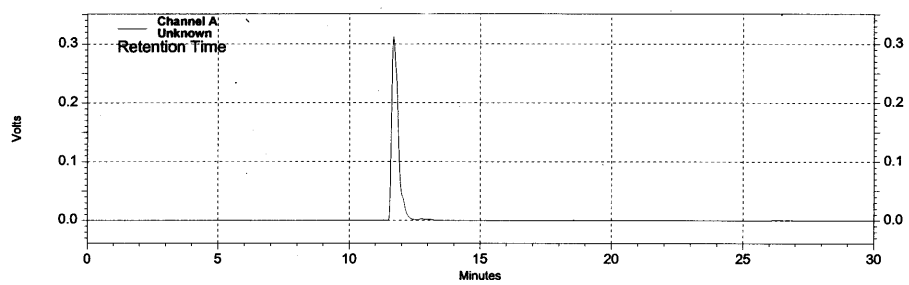
1NK

^1H NMR (500 MHz, DMSO- d_6) δ 7.88 (d, $J = 8.5$, 1H), 7.43 (s, 2H), 7.05 (d, $J = 8.5$ Hz, 1H), 6.96 (dd, $J = 8.5, 4.8$ Hz, 1H), 6.82 (d, $J = 8.0$ Hz, 2H), 6.51 (s, 2H), 6.43 (dd, $J = 4.8, 8.0$ Hz, 1H), 4.47 (s, 2H), 4.23 (m, 1H), 3.72 (s, 6H), 3.00 (t, $J = 6.8$ Hz, 2H), 2.37-2.32 (m, 2H), 2.21-2.17 (m, 2H), 2.07 (d, 7.4 Hz, 2H), 1.23-1.12 (m, 4H); ^{13}C NMR (125 MHz, DMSO- d_6) δ 174.0, 168.2, 159.7, 158.3, 156.5, 134.7, 130.9, 130.0, 122.2, 115.0, 105.1, 99.0, 67.4, 56.0, 55.8, 52.5, 34.4, 32.4, 27.9, 22.5, 14.5; LRMS (ESI) calc'd ($\text{M}+\text{H}^+$) 479, found 479; analytical HPLC homogeneous single peak, retention time = 11.8 min (8-70% B in 30 min).

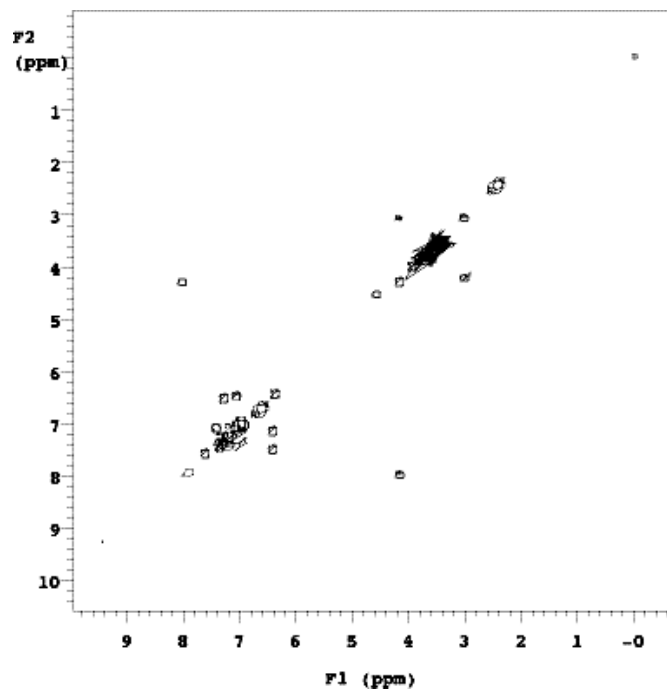
 ^1H NMR



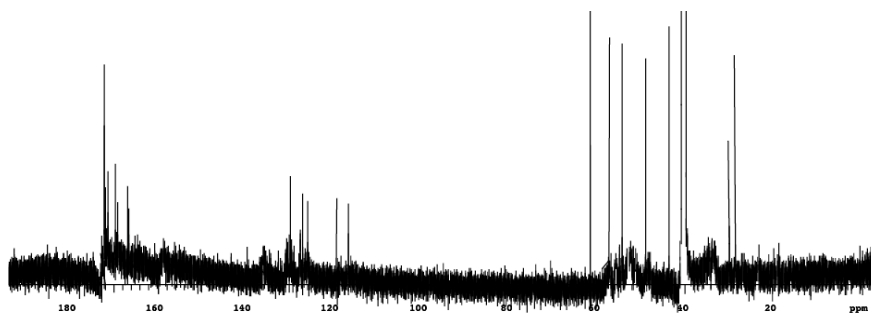
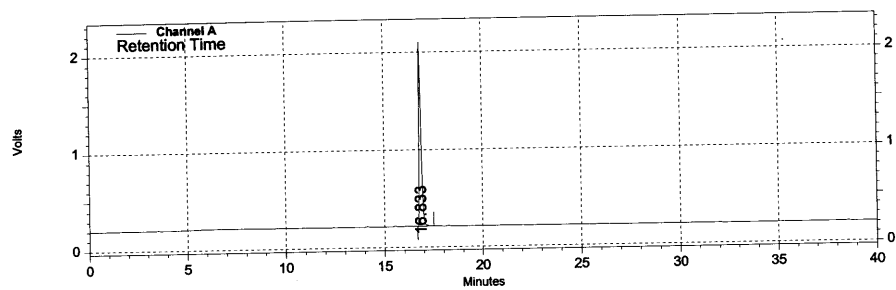
COSY

¹³C NMR

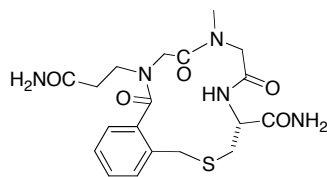
HPLC



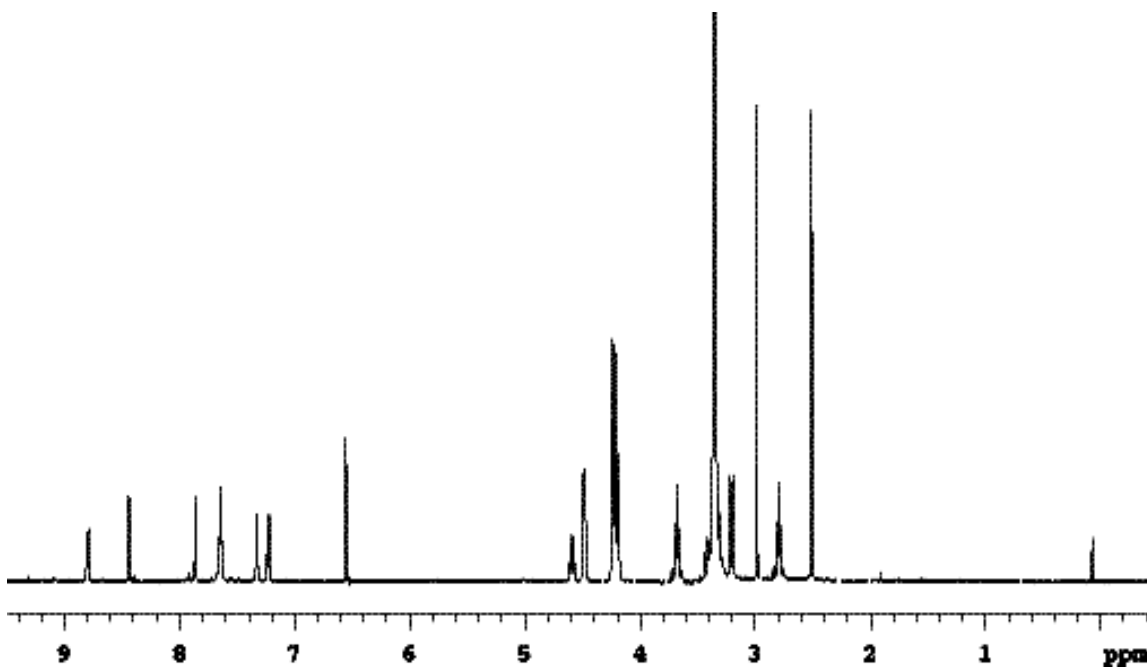
COSY

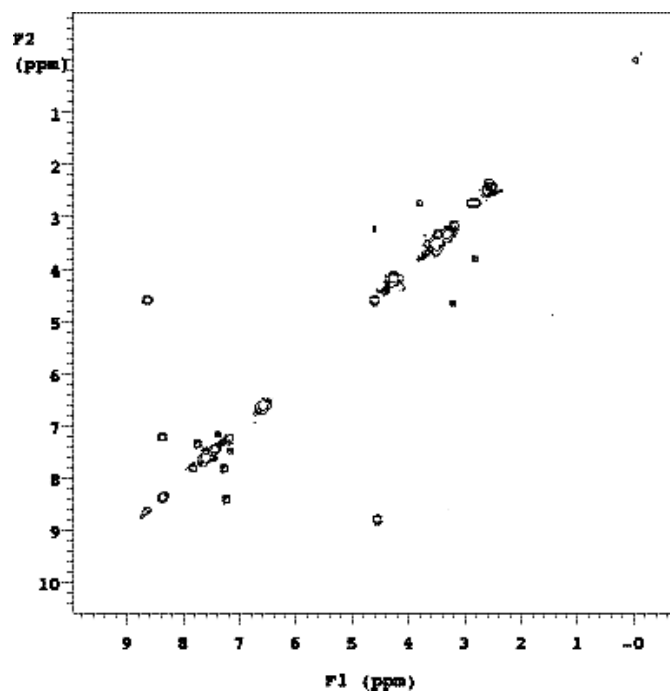
¹³C NMR

HPLC

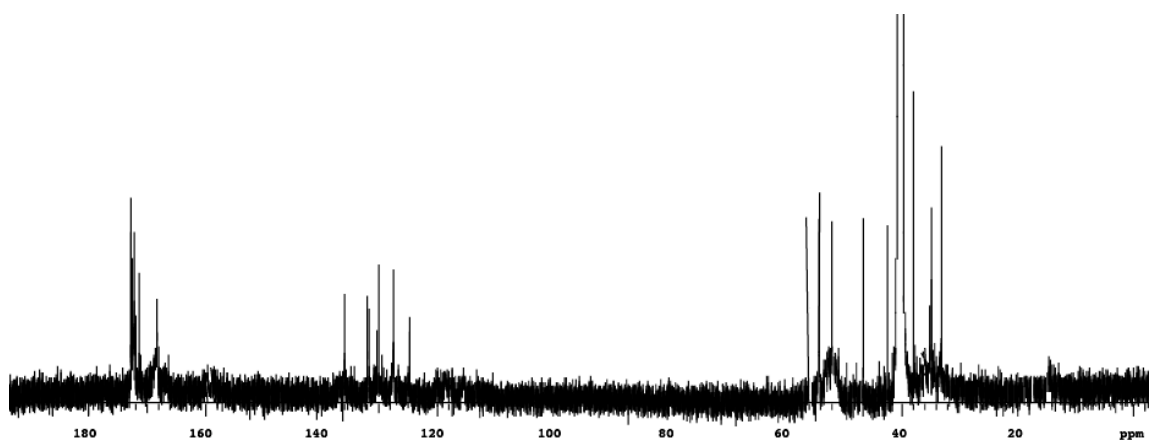
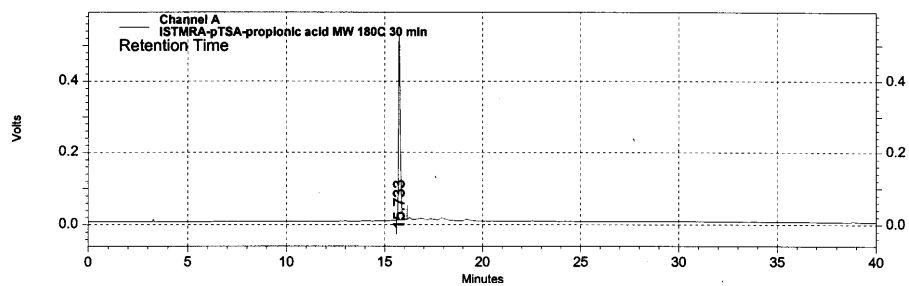
**1QA**

^1H NMR (500 MHz, DMSO- d_6) δ 8.80 (d, $J = 8.0$ Hz, 1H), 8.41 (d, $J = 7.8$ Hz, 1H), 7.86 (dd, $J = 4.0, 7.5$ Hz, 1H), 7.68 (s, 2H), 7.37 (d, $J = 7.5$ Hz, 1H), 7.22 (dd, $J = 4.0, 7.8$ Hz, 1H), 6.58 (s, 2H), 4.62-4.38 (m, 1H), 4.49 (s, 2H), 4.26-4.21 (m, 4H), 3.74 (t, $J = 7.4$ Hz, 2H), 3.21 (d, $J = 8.5$ Hz, 2H), 3.00 (s, 3H), 2.81 (t, $J = 7.4$ Hz, 2H); ^{13}C NMR (125 MHz, DMSO- d_6) δ 172.7, 172.5, 172.2, 171.5, 168.3, 136.1, 132.0, 131.9, 130.2, 127.4, 125.1, 55.7, 54.2, 50.5, 45.1, 42.5, 37.8, 34.9, 33.6; MS (ESI) calc'd for $\text{C}_{19}\text{H}_{25}\text{N}_5\text{O}_5\text{S}$ ($\text{M}+\text{H}^+$) 436, found 436; analytical HPLC purity = 98 %, retention time = 15.7 min (5-95% B in 30 min).

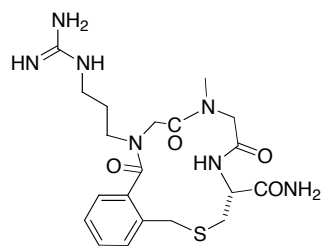
 ^1H NMR



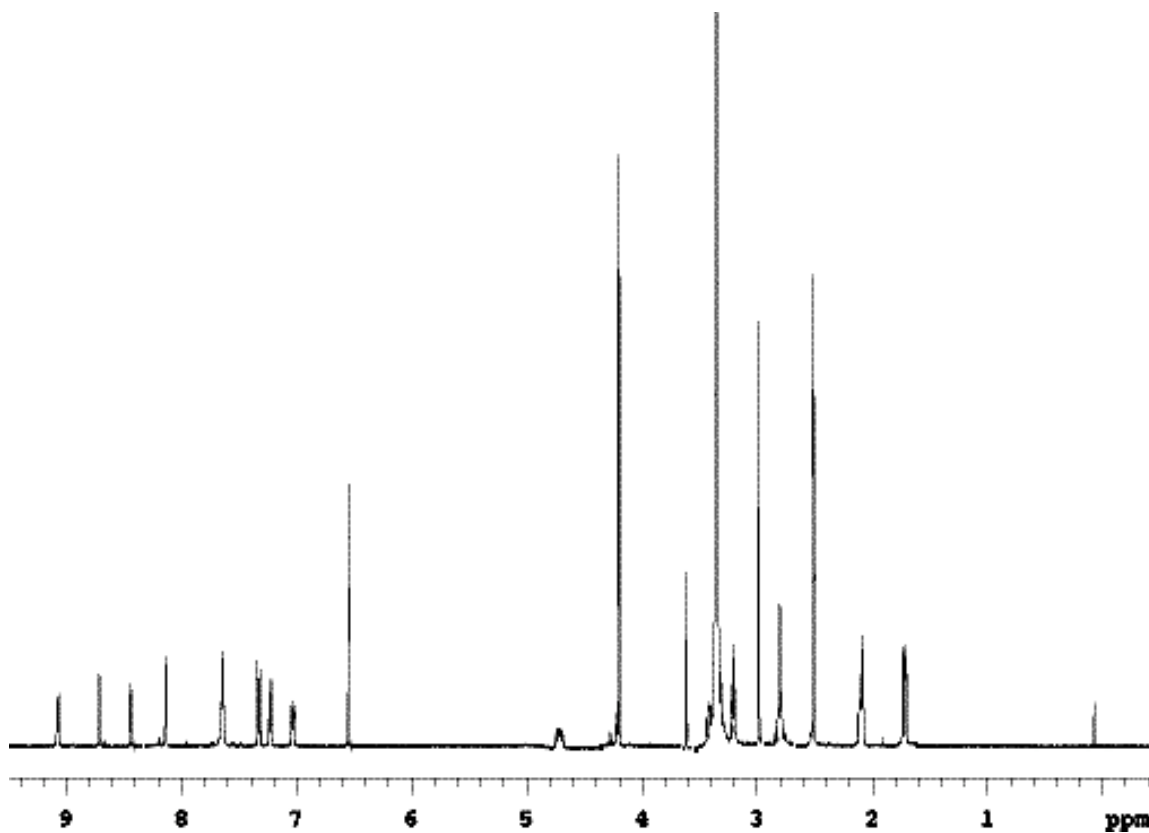
COSY

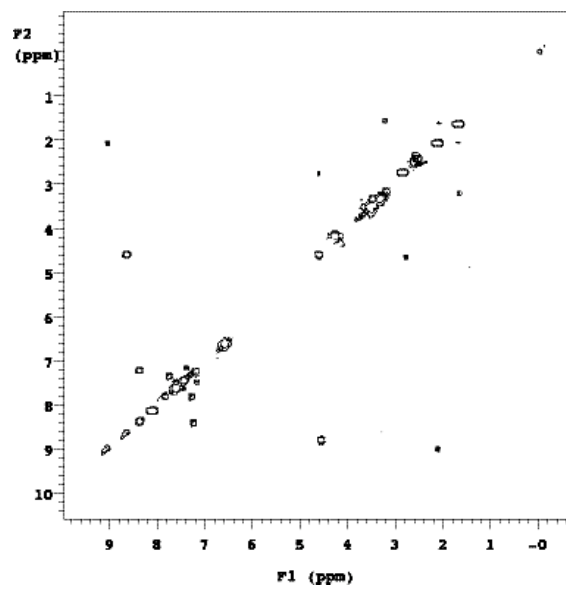
¹³C NMR

HPLC

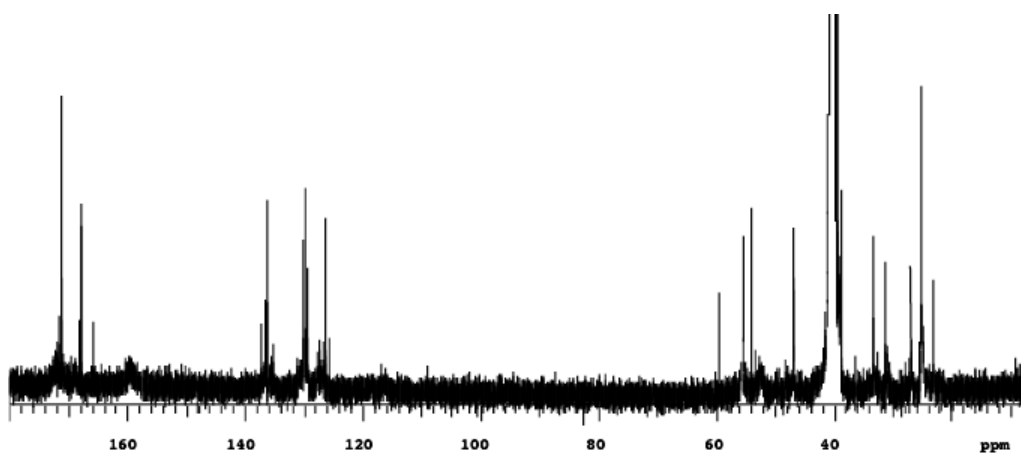
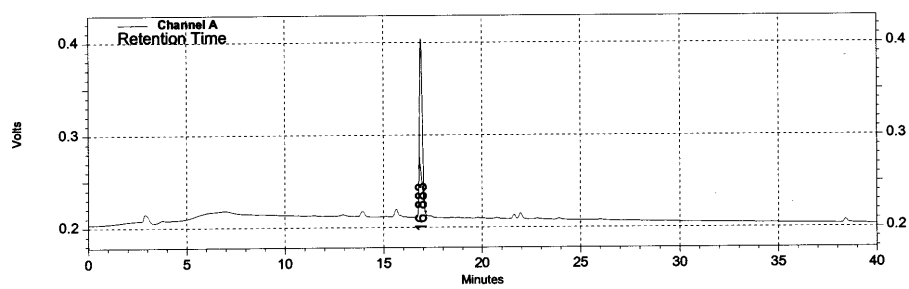
**1RA**

^1H NMR (500 MHz, DMSO-d_6) δ 9.09 (t, $J = 7.2$ Hz, 1H), 8.71 (d, $J = 7.8$ Hz, 1H), 8.44 (d, $J = 8.0$ Hz, 1H), 8.18 (s, 1H), 7.65 (s, 2H), 7.37 (dd, $J = 8.0, 5.5$ Hz, 1H), 7.21 (d, $J = 8.5$ Hz, 1H), 7.06 (dd, $J = 8.5, 5.5$ Hz, 1H), 6.60 (s, 2H), 4.72-4.78 (m, 1H), 4.22-4.19 (m, 4H), 3.64 (s, 2H), 3.18 (t, $J = 7.5$ Hz, 2H), 2.99 (s, 3H), 2.80 (t, $J = 7.0$ Hz, 2H), 2.15 (m, 2H), 1.74 (m, 2H); ^{13}C NMR (125 MHz, DMSO-d_6) δ 172.0, 171.9, 168.1, 168.0, 166.3, 137.8, 137.1, 130.1, 130.0, 129.9, 126.8, 59.8, 55.7, 54.0, 47.2, 33.4, 31.7, 27.9, 25.6, 23.7; LRMS (MALDI) calc'd $(\text{M}+\text{H})^+$ 464, found 464; analytical HPLC: purity = 91 %, retention time = 15.9 min (5-95% B in 30 min).

 ^1H NMR



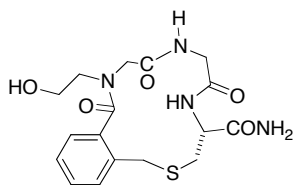
COSY

¹³C NMR

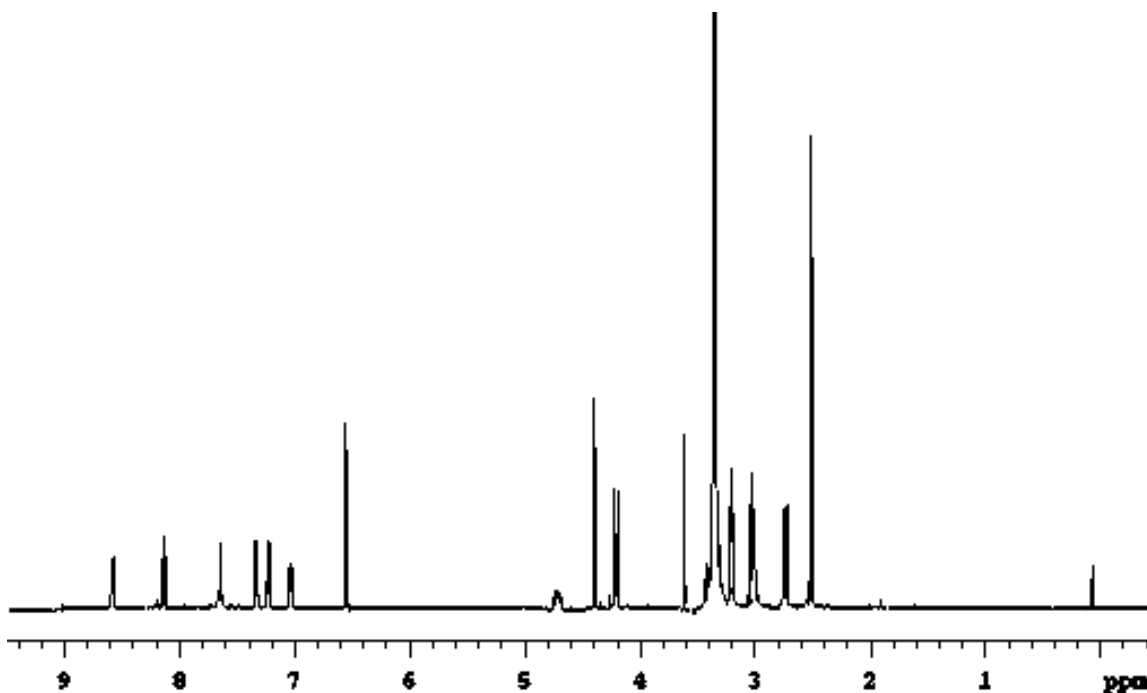
HPLC

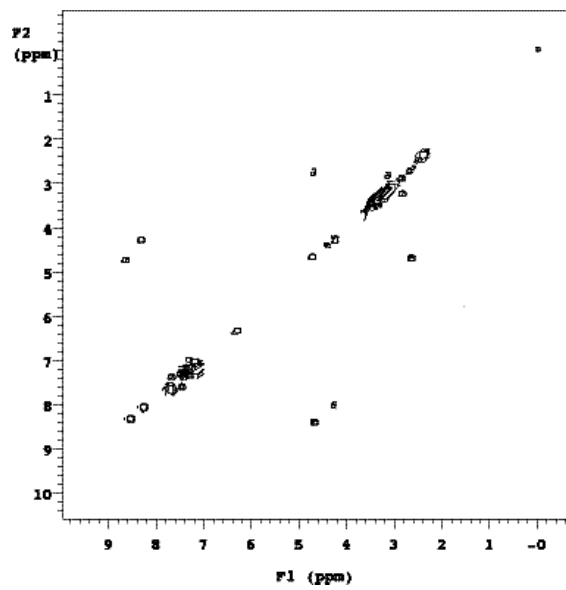
Procedure for solid phase synthesis of Peptidomimetics 1sg, sy, and tg: Rink amide HMBA resin (0.100 g, 0.72 mmol/g loading) was swelled with CH_2Cl_2 (10 mL/g) in a 3 mL fritted syringe for 30 min. The Fmoc protecting group on the Rink handle was removed by treating the resin with 20 % piperidine in DMF (2 x 1.5 mL, 10 min and then 15 min). The resin was then washed with DMF (3x), MeOH (3x), DMF (1x), MeOH (1x), CH_2Cl_2 (2x), MeOH (2x), and CH_2Cl_2 (3x), after which, Fmoc-Cys(Mmt)-OH (3 equiv.), DIC (3 equiv.), HOBt (3 equiv.), and DIEA (5 equiv.) in DMF (1.5 mL) were added. After gentle shaking for 2 h, the reaction mixture was then drained and the resin was subjected to the washing cycle and Fmoc deprotection as previously described. The resin was washed again, transferred to the microwave reaction vessel, then treated with bromoacetic acid (2M), DIC (2M.), in DMF (1.5 mL) and microwaved at 50 °C, 1 atm (open vessel), for 1 min. After washing with DMF (9x), the resin was treated with primary amine (2 M), in DMF or DMSO (1.5 mL), and microwaved at 50 °C, 1 atm (open vessel), for 1 min. The washing cycle with DMF were repeated. The microwave acylation reaction with bromoacetic acid was repeated and washed. The resin bound product was treated with *N*-(2-*tert*-Butoxyalkyl)-2'-nitrobenzenesulfonamide (2 M) in DMSO and K_2CO_3 (10 equiv.). The vessel was irradiated with microwave at 50 °C for 2 min. The resin was transferred back to the syringe and washed. Then 2-mecaptoethanol (5 equiv.), and DBU (5 equiv.) in DMF (1.5 mL) were added to the syringe and shaken for 30 min. The process was repeated for another 30 min and then the resin was washed with DMF (3x), MeOH (3x), DMF (1x), MeOH (1x), CH_2Cl_2 (2x), MeOH (2x), and CH_2Cl_2 (3x). The 2-bromomethylbenzoic acid moiety was introduced by treating the resin with 2-bromomethylbenzoyl chloride (3 equiv.) and DIEA (3 equiv.) in CH_2Cl_2 (1.5 mL) for 40 min. The Mmt protecting group of the cysteine was removed by treatment with 1 % TFA and 5 % TIS in CH_2Cl_2 (2 mL, 2 min 7x, or until yellow color disappeared). After the resin was washed, macrocyclization was affected by adding K_2CO_3 (10 equiv.) in DMF and microwaved at 50 °C, 1 atm (open vessel), for 10 min. The reaction mixture was then drained and the resin was washed with H_2O (5x), DMF (3x), MeOH (3x), DMF (1x), MeOH (1x), CH_2Cl_2 (2x), MeOH (2x), and CH_2Cl_2 (3x) and then dried under vacuum for 4 h. The peptide was cleaved from the resin by treatment with a mixture of 90 % TFA, 5 % TIS, and 5 % H_2O . The cleavage solution was

separated from the resin by filtration. After most of the cleavage cocktail was evaporated *in vacuo*, the crude peptide was triturated using anhydrous ethyl ether. The crude peptide was then dissolved in H₂O/CH₃CN mixture (1:1, 2 mL), purified via preparative HPLC and then lyophilized to give a brownish powder obtained as a TFA salt.

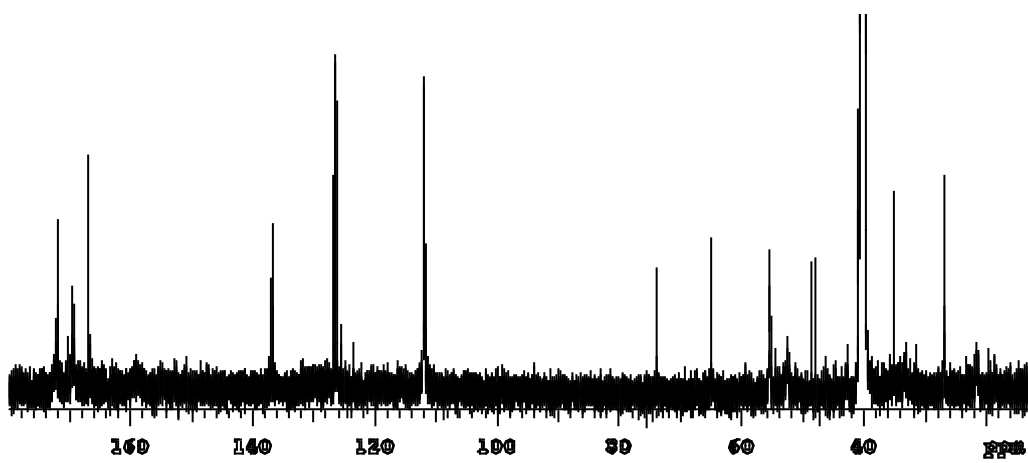
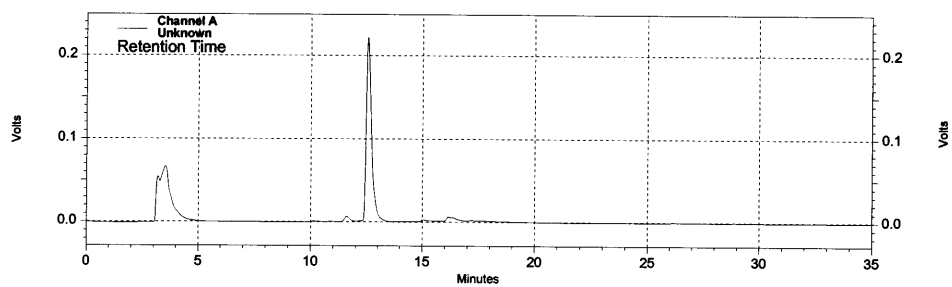
**1SG**

^1H NMR (500 MHz, DMSO-d_6) δ 8.59 (d, $J = 8.0$ Hz, 1H), 8.18 (t, $J = 8.5$ Hz, 1H), 7.67 (d, $J = 7.4$ Hz, 1H) 7.38 (dd, $J = 7.5, 3.0$ Hz, 1H), 7.25 (d, $J = 7.5$ Hz, 1H), 7.06 (dd, $J = 3.0, 7.4$ Hz, 1H), 6.57 (s, 2H), 4.39-4.33 (m, 1H), 4.00 (s, 2H), 3.84 (d, $J = 8.5$ Hz, 2H), 3.62 (s, 2H), 3.19 (t, $J = 6.0$ Hz 2H), 2.99 (t, $J = 6.0$ Hz, 2H), 2.76 (d, $J = 7.0$ Hz, 2H); ^{13}C NMR (125 MHz, DMSO-d_6) δ 172.7, 170.0, 169.9, 167.1, 137.0, 136.8, 127.0, 126.8, 126.7, 112.0, 74.0, 64.8, 55.8, 48.6, 48.0, 34.9, 27.2; LRMS (MALDI) calc'd $(\text{M}+\text{H})^+$ 395, found 395; analytical HPLC: purity = 93 %, retention time = 12.7 min (5-90% B in 25 min).

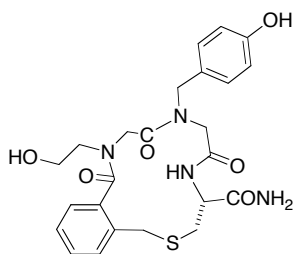
 ^1H NMR



COSY

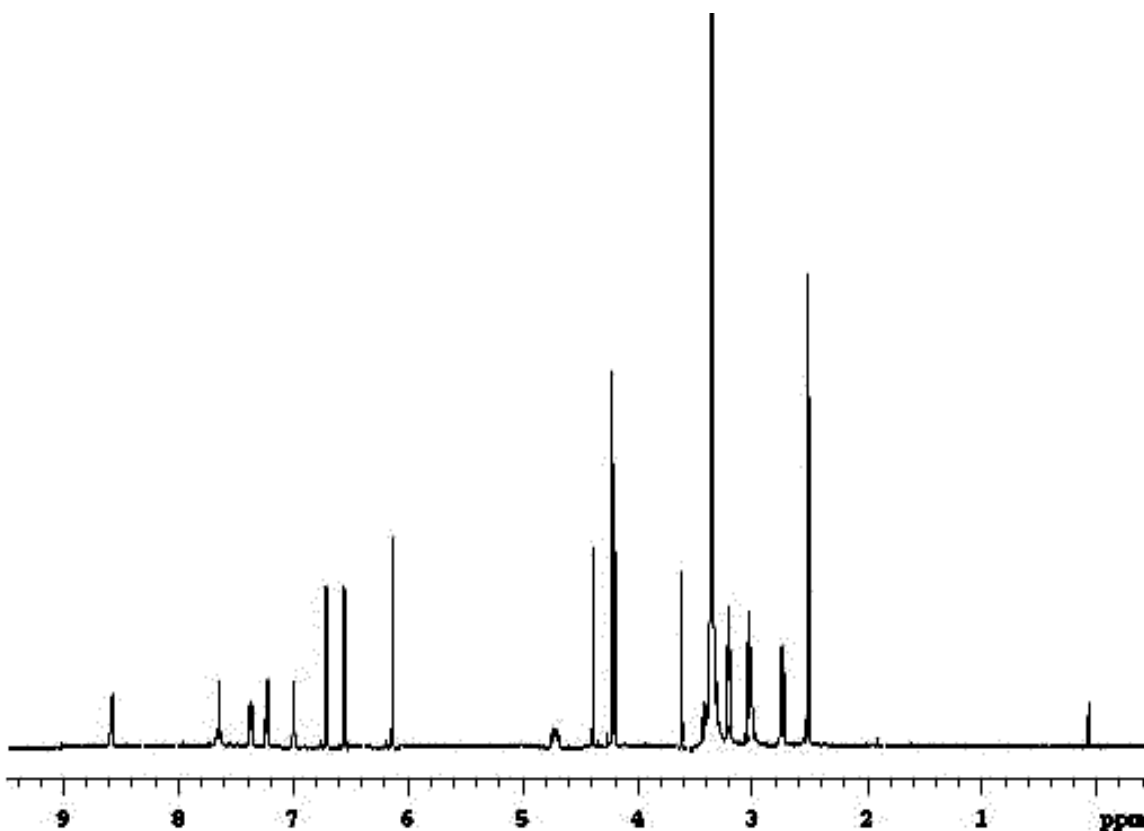
¹³C NMR

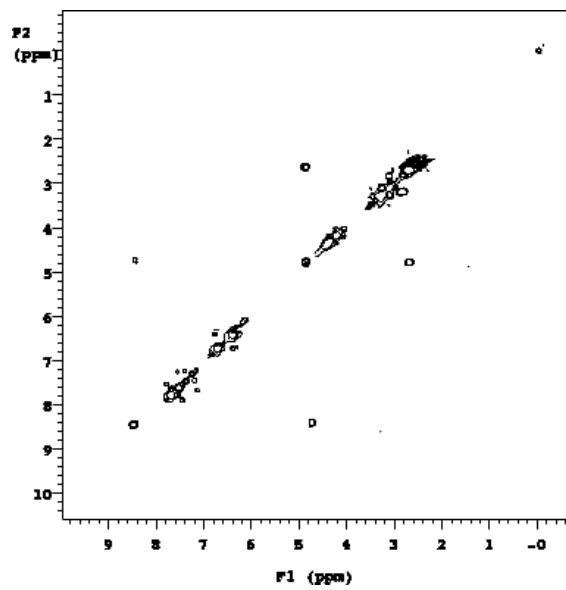
HPLC



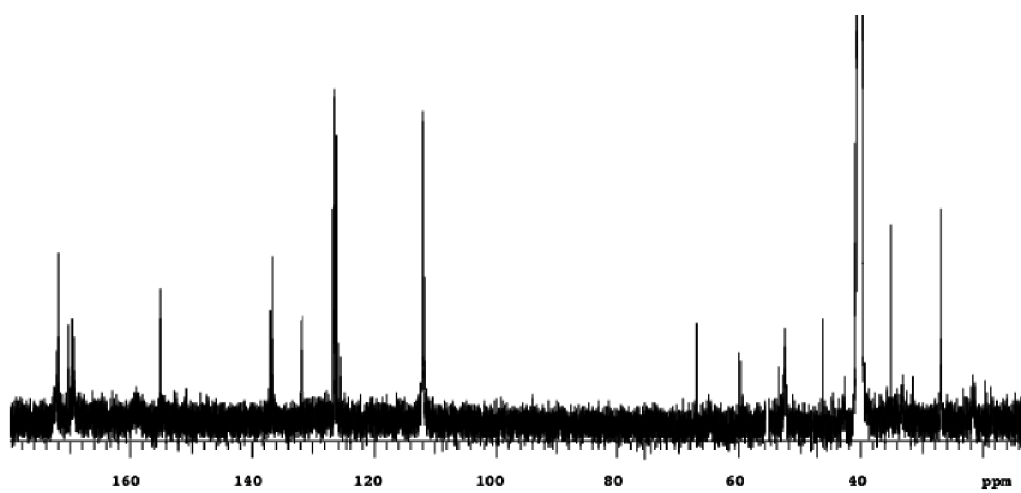
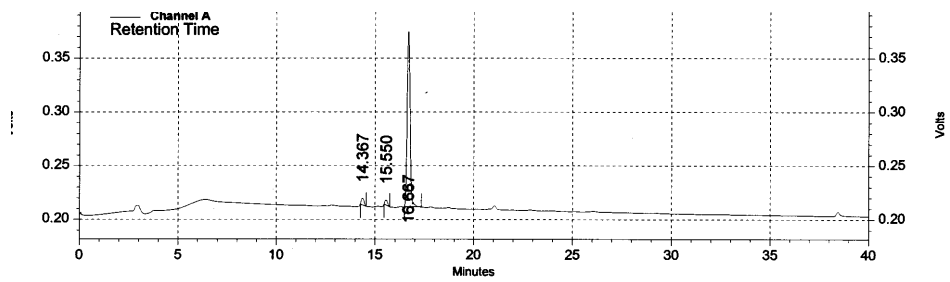
1SY

^1H NMR (500 MHz, DMSO-d_6) δ 8.60 (d, $J = 7.8$ Hz, 1H), 7.64 (d, $J = 8.5$ Hz, 1H), 7.39 (dd, $J = 8.5, 3.5$ Hz, 1H), 7.22 (dd, $J = 3.5, 8.0$ Hz, 1H), 7.00 (d, $J = 8.0$ Hz, 1H), 6.77 (d, $J = 7.0$ Hz, 2H), 6.56 (d, $J = 7.0$ Hz, 2H), 6.15 (s, 2H), 4.78-4.71 (m, 1H), 4.39 (s, 2H), 4.23-4.19 (m, 4H), 3.62 (s, 2H), 3.19 (t, $J = 7.5$ Hz, 2H), 3.00 (t, $J = 7.5$ Hz, 2H), 2.77 (d, $J = 8.5$ Hz, 2H); ^{13}C NMR (125 MHz, DMSO-d_6) δ 172.8, 170.5, 170.0, 169.9, 155.5, 137.4, 137.3, 132.0, 132.1, 126.8, 126.7, 126.6, 112.0, 111.9, 67.4, 60.0, 59.9, 53.8, 53.1, 46.3, 35.6, 27.7; MALDI MS calc'd for $(\text{M}+\text{H}^+)$ 501, found 501; analytical HPLC: purity = 89 %, retention time = 16.7 min (5-95% B in 30 min).

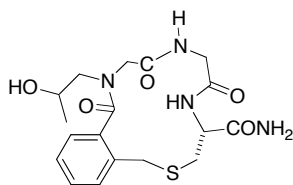
 ^1H NMR



COSY

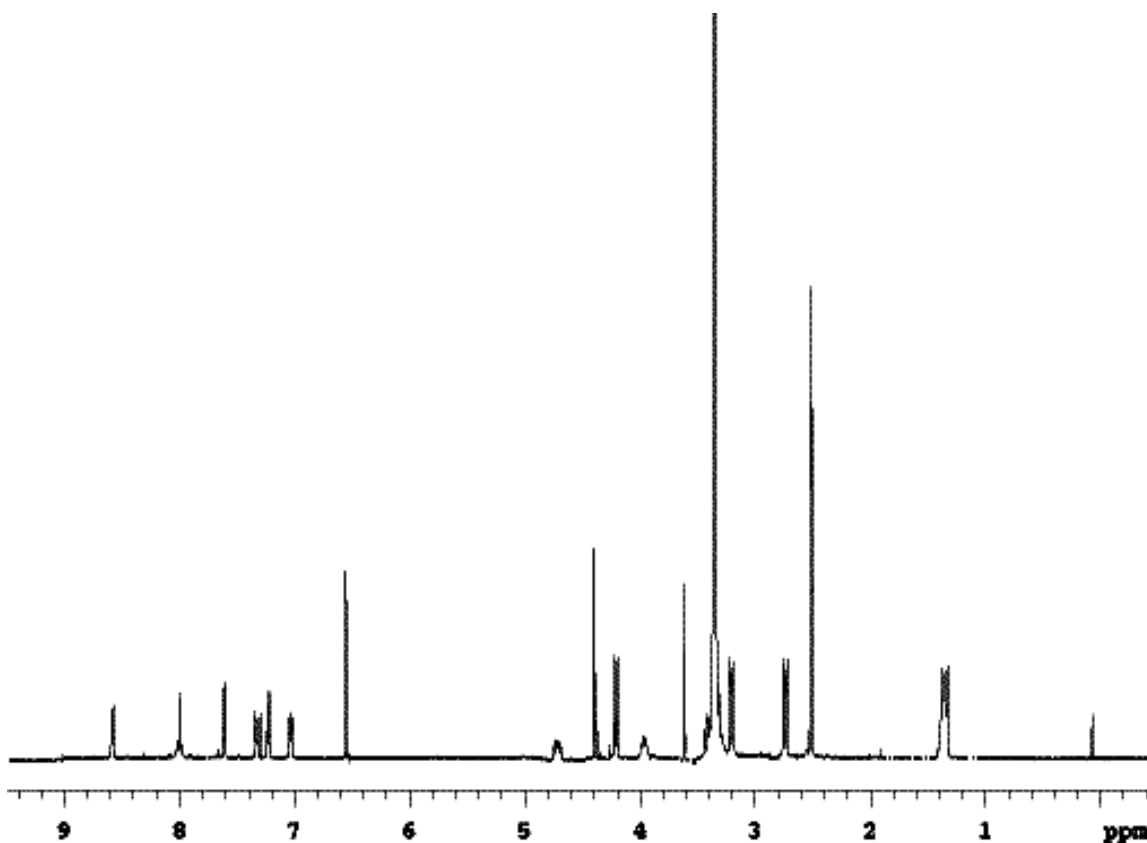
¹³C NMR

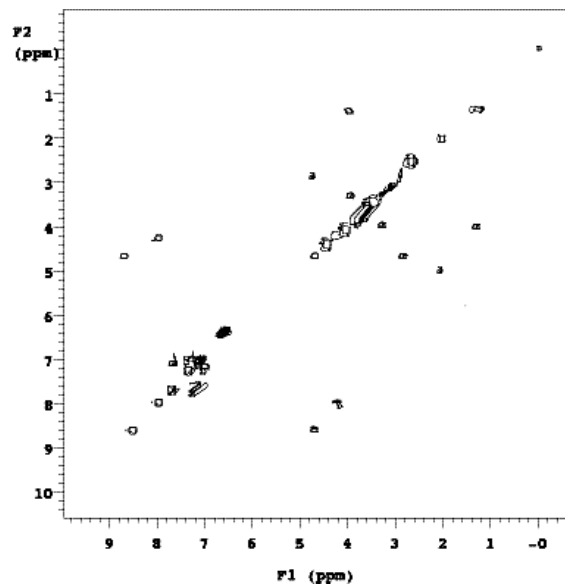
HPLC



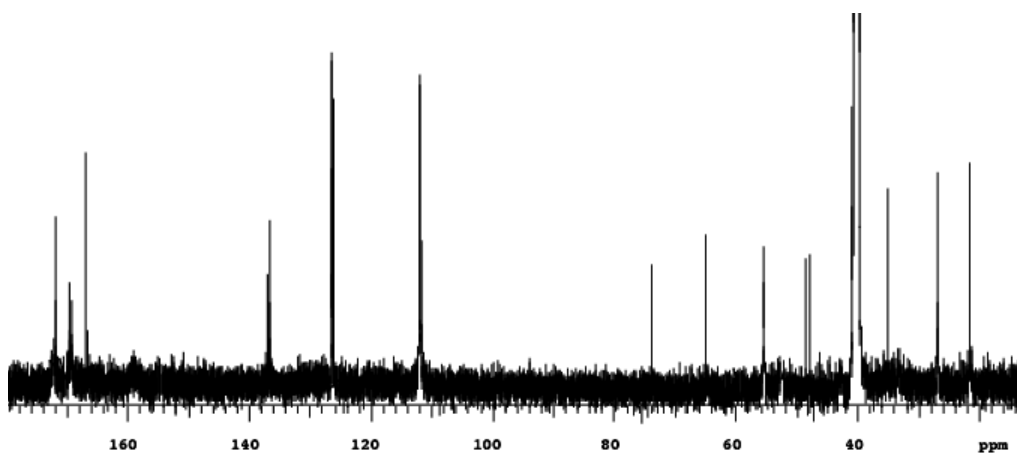
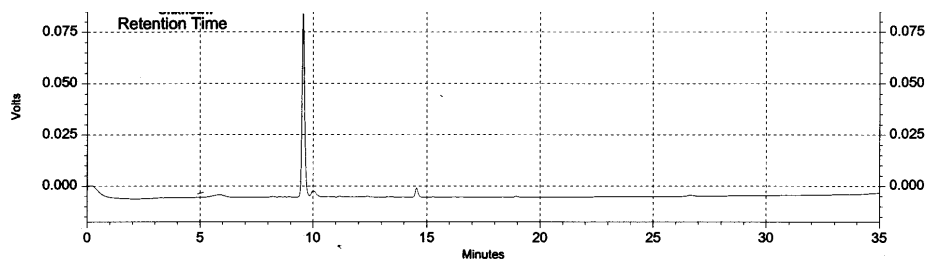
1TG

^1H NMR (500 MHz, DMSO-d_6) δ 8.59 (d, $J = 7.0$ Hz, 1H), 8.02 (t, $J = 7.8$ Hz, 1H), 7.67 (d, $J = 7.5$ Hz, 1H), 7.37 (dd, $J = 3.7, 8.0$ Hz, 1H), 7.22 (d, $J = 8.0$ Hz, 1H), 7.04 (dd, $J = 3.7, 7.5$ Hz, 1H), 6.57 (s, 2H), 4.78-4.69 (m, 1H), 4.40 (s, 2H), 4.23 (d, $J = 7.8$ Hz, 2H), 3.99-3.94 (m, 1H), 3.62 (s, 2H), 3.20 (d, $J = 9.5$ Hz, 2H), 2.78 (d, $J = 8.5$ Hz, 3H), 1.39 (bd, $J = 8.5$ Hz, 3H); ^{13}C NMR (125 MHz, DMSO-d_6) δ 172.7, 170.0, 169.9, 166.8, 137.1, 136.8, 126.7, 126.3, 112.0, 111.9, 74.0, 64.8, 55.5, 48.6, 48.0, 35.0, 27.0, 21.6; LRMS (MALDI) calc'd ($\text{M}+\text{Na}^+$) 431, found 431; analytical HPLC: purity = 93 %, retention time = 9.8 min (8-70% B in 30 min).

 ^1H NMR



COSY

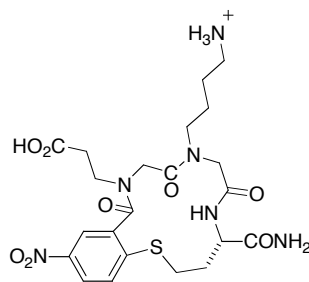
¹³C NMR

HPLC

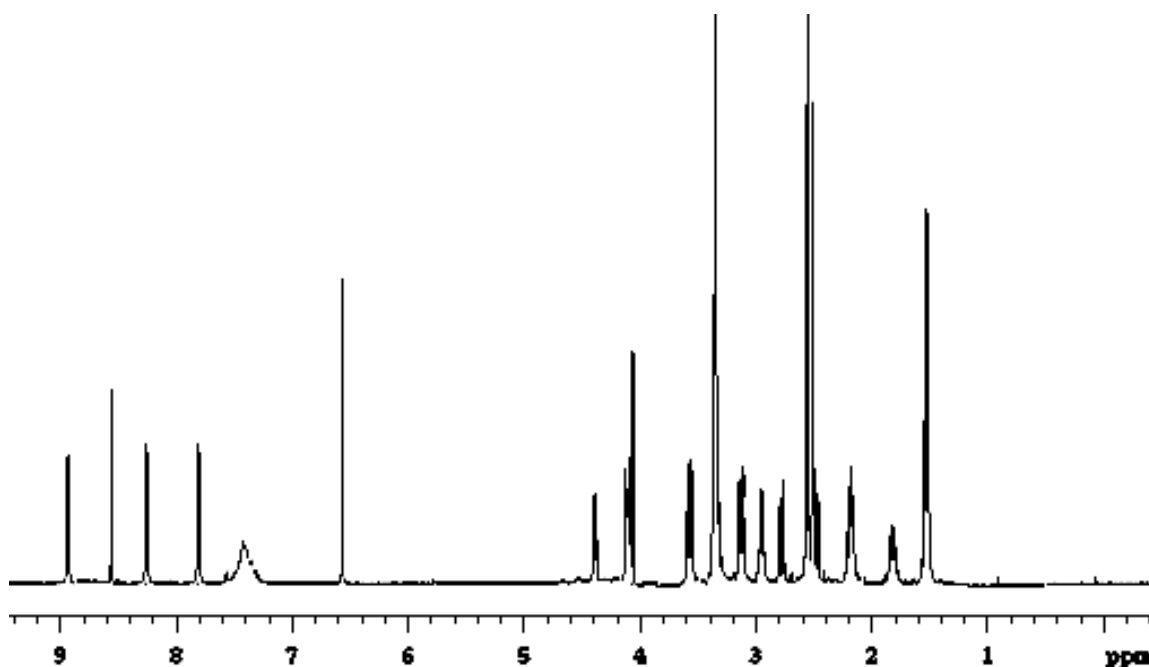
Synthetic Procedures and Spectral Data for Compounds 2

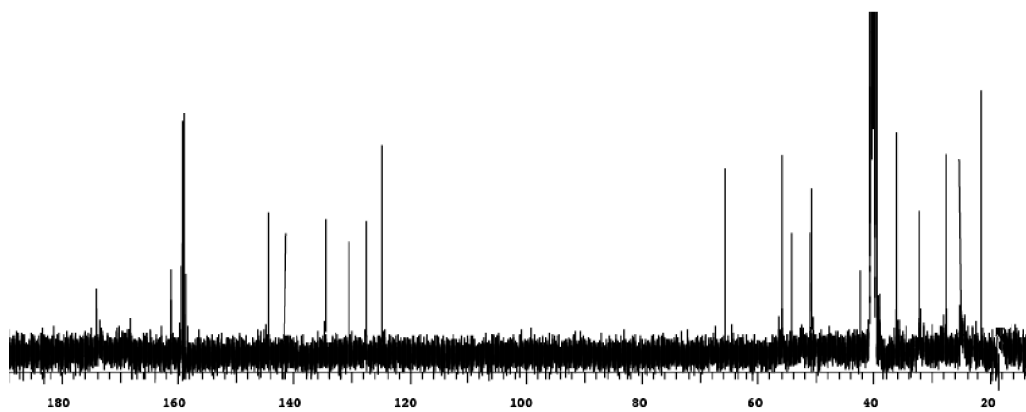
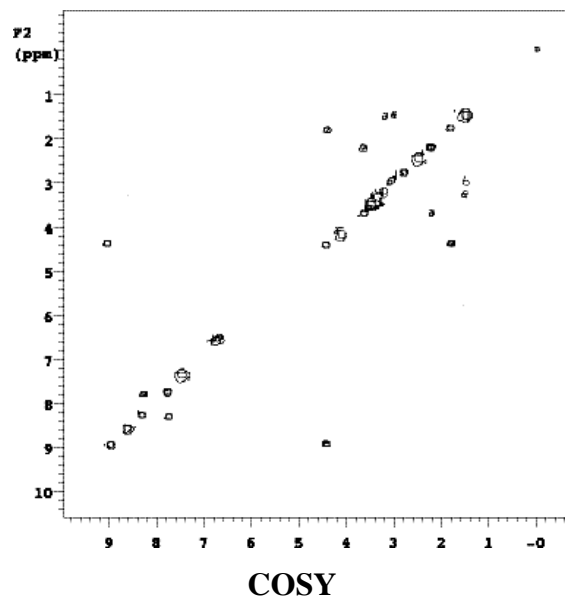
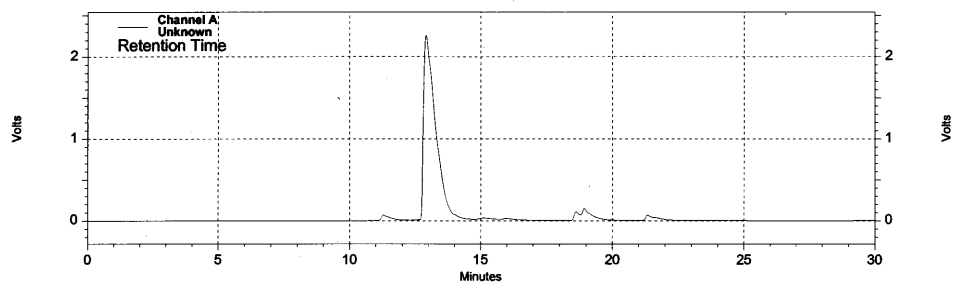
Rink amide MBHA resin (0.100 g, 0.72 mmol/g loading) was swelled with CH_2Cl_2 (10 mL/g) in a 3 mL fritted syringe for 30 min. The Fmoc protecting group on the Rink handle was removed by treating the resin with 20 % piperidine in DMF (2 x 1.5 mL, 10 min and then 15 min). The resin was then washed with DMF (3x), MeOH (3x), DMF (1x), MeOH (1x), CH_2Cl_2 (2x), MeOH (2x), and CH_2Cl_2 (3x), after which, Fmoc-Cys(Mmt)-OH (3 equiv.), DIC (3 equiv.), HOBT (3 equiv.), and DIEA (5 equiv.) in DMF (1.5 mL) were added. After gentle shaking for 2 h, the reaction mixture was then drained and the resin was subjected to the washing cycle and Fmoc deprotection as previously described. The resin was washed again, transferred to the microwave reaction vessel, then treated with bromoacetic acid (2M.), DIC (2M.), in DMF (1.5 mL) and irradiated with microwave at 50 °C, 1 atm (open vessel), for 1 min. After washing with DMF (9x), the resin was then treated with primary amine (2 M.), in DMF or DMSO (1.5 mL), and microwaved at 50 °C, 1 atm (open vessel), for 1 min. The washing cycle with DMF was repeated. Then the two microwave reactions and washing cycles were repeated. The resin was transferred back to the syringe and 2-fluoro-5-nitrobenzoic acid moiety was introduced by treating the resin with 2-fluoro-5-nitrobenzoyl chloride (3 equiv.) and DIEA (3 equiv.) in CH_2Cl_2 (ca 1.5 mL) for 40 min. The Mmt protecting group of the homocysteine was removed by treatment with 1% TFA and 5% TIS in CH_2Cl_2 (2 mL, 7x 2 min each, or until yellow color disappeared). After the resin was washed, macrocyclization was affected by adding K_2CO_3 (10 equiv.) in DMF and microwaved at 50 °C, 1 atm (open vessel), for 15 min. The reaction mixture was then drained and the resin was washed with H_2O (5x), DMF (3x), MeOH (3x), DMF (1x), MeOH (1x), CH_2Cl_2 (2x), MeOH (2x), and CH_2Cl_2 (3x) and then dried under vacuum for 4 h. The peptide was cleaved from the resin by treatment with a mixture of 90 % TFA, 5 % TIS, and 5 % H_2O . The cleavage solution was separated from the resin by filtration. After most of the cleavage cocktail was evaporated *in vacuo*, the crude peptide was triturated using anhydrous ethyl ether. The crude peptide was then dissolved in $\text{H}_2\text{O}/\text{CH}_3\text{CN}$ mixture

(1:1, 2 mL), purified via preparative HPLC and then lyophilized to give a powder obtained as a TFA salt.

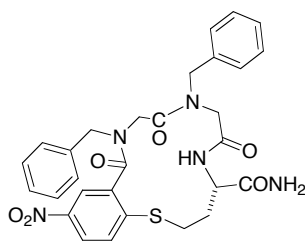
**2EK**

^1H NMR (500 MHz, DMSO- d_6) δ 8.98 (d, $J = 7.6$ Hz, 1H), 8.71 (s, 1H), 8.16 (d, $J = 7.5$ Hz, 1H), 7.80 (d, $J = 7.5$ Hz, 1H), 7.45 (bs, 3H), 6.58 (s, 2H), 4.39-4.36 (m, 1H), 4.18-4.07 (m, 4H), 3.60 (t, $J = 6.0$ Hz, 2H), 3.18 (t, $J = 7.0$ Hz, 2H), 2.98 (t, $J = 5.3$ Hz, 2H), 2.81 (t, $J = 6.0$ Hz, 2H), 2.22 (t, $J = 8.0$ Hz, 2H), 1.87-1.79 (m, 2H), 1.58-1.47 (m, 4H);
 ^{13}C NMR (125 MHz, DMSO- d_6) δ 174.0, 161.7, 159.5, 159.2, 158.9, 144.7, 142.2, 135.0, 130.6, 128.1, 125.4, 65.8, 56.0, 54.5, 51.4, 51.2, 42.5, 36.5, 32.4, 27.9, 25.2, 21.6;
 MALDI MS calc'd for $\text{C}_{22}\text{H}_{30}\text{N}_6\text{O}_8\text{S}$ ($\text{M}+\text{H}^+$) 539, found 539; analytical HPLC purity = 95%, retention time = 13.0 min (5-95% B in 30 min).

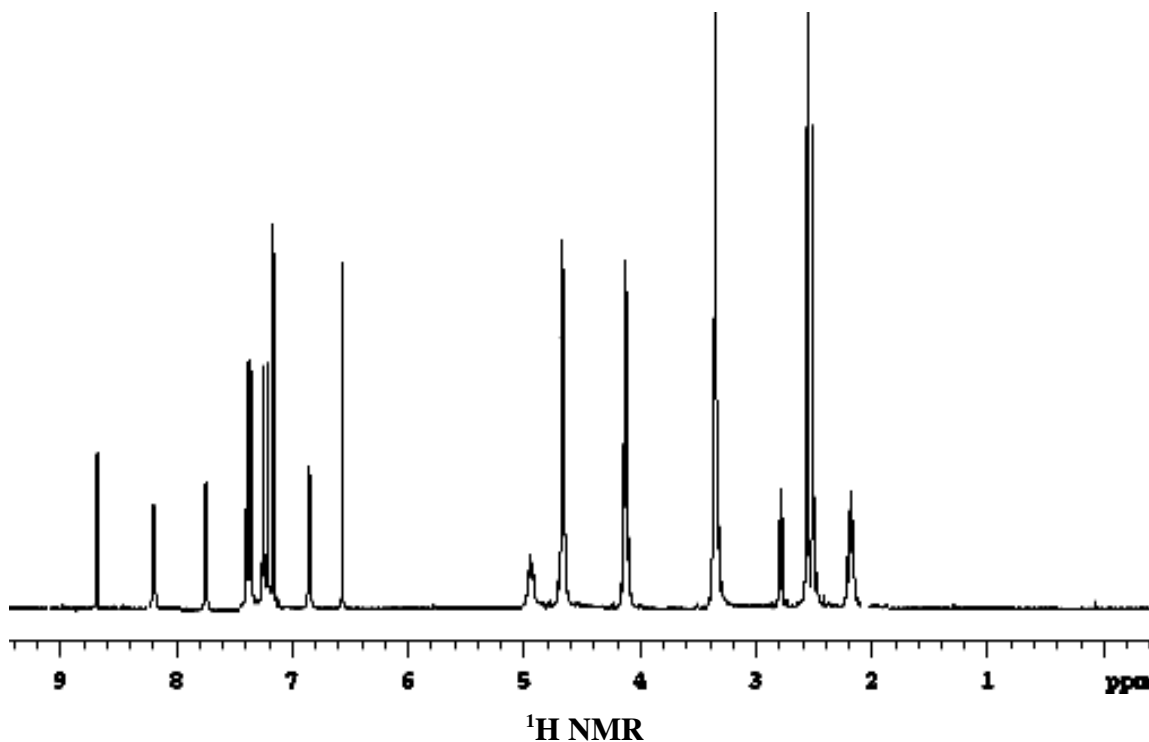
 ^1H NMR

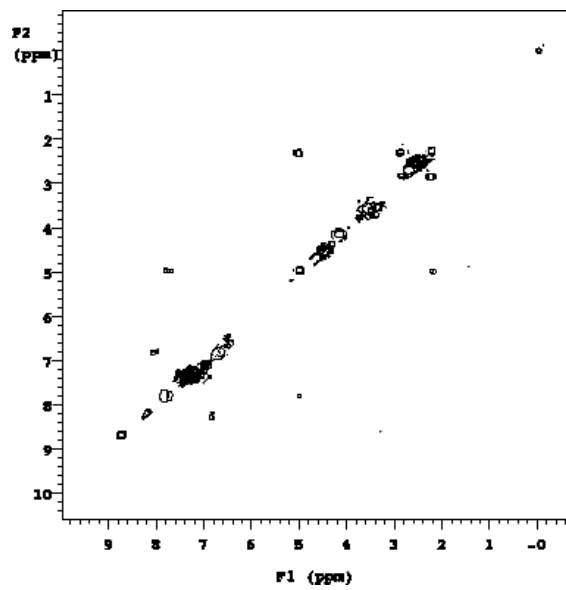
¹³C NMR

HPLC

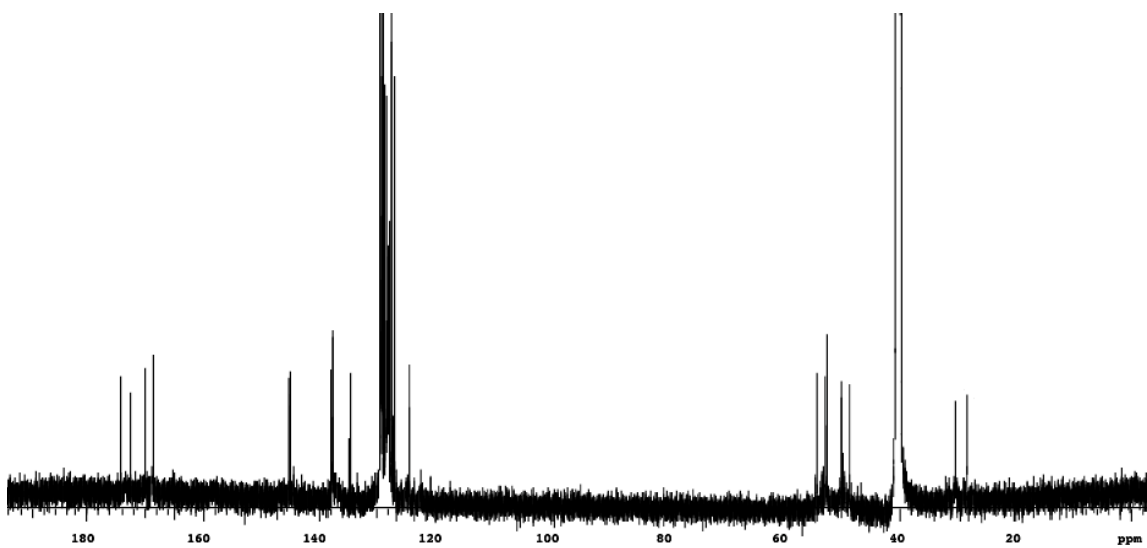
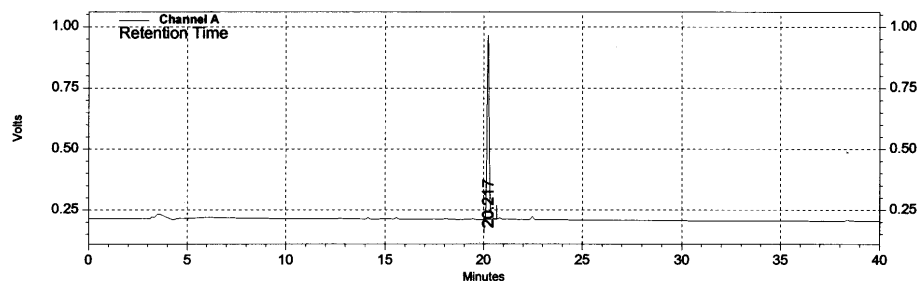
**2FF**

^1H NMR (500 MHz, DMSO- d_6) δ 8.70 (s, 1H), 8.22 (d, $J = 7.0$ Hz, 1H), 7.77 (d, $J = 8.5$ Hz, 1H), 7.40-7.35 (m, 4H), 7.28-7.19 (m, 6H), 6.86 (d, $J = 7.0$ Hz, 1H), 6.58 (s, 2H), 4.98-4.92 (m, 1H), 4.76-4.65 (s, 4H), 4.11-4.18 (s, 4H), 2.76 (t, $J = 6.5$ Hz, 2H), 2.18-2.22 (m, 2H); ^{13}C NMR (125 MHz, DMSO- d_6) δ 174.5, 172.7, 170.2, 168.8, 145.6, 137.9, 137.7, 134.7, 129.4, 129.3, 129.1, 129.0, 128.7, 128.2, 128.1, 127.9, 127.4, 124.9, 54.3, 52.8, 52.7, 49.9, 48.5, 30.4, 28.9; MALDI MS calc'd for $\text{C}_{29}\text{H}_{29}\text{N}_5\text{O}_6\text{S}$ ($\text{M}+\text{H}^+$) 576, found 576; analytical HPLC: purity = 99 %, retention time = 20.2 min (8-70% B in 30 min).

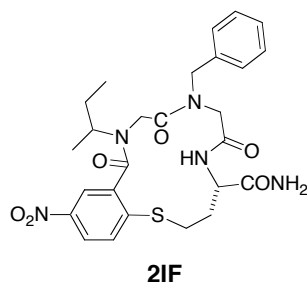




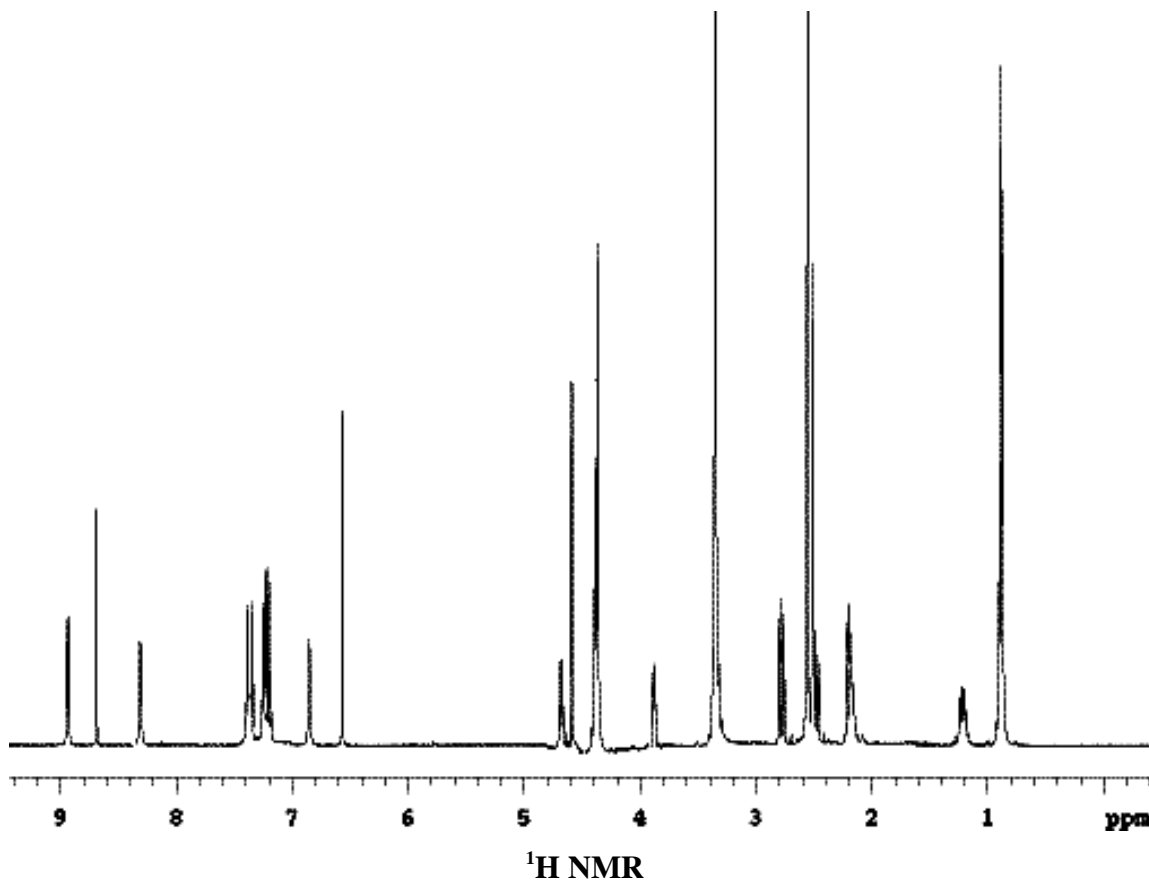
COSY

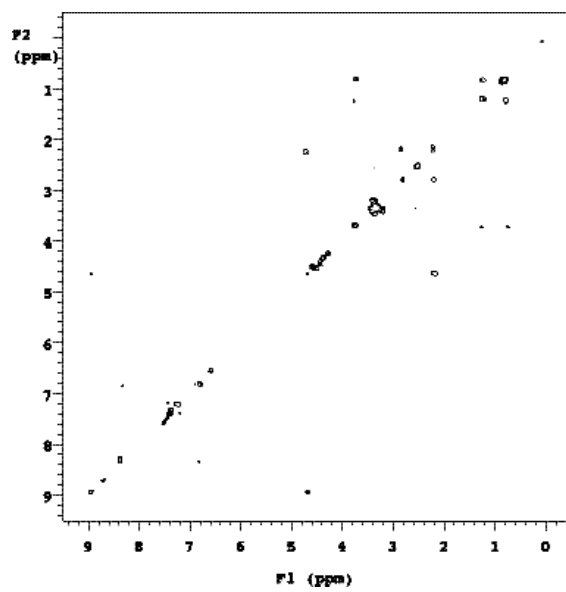
¹³C NMR

HPLC

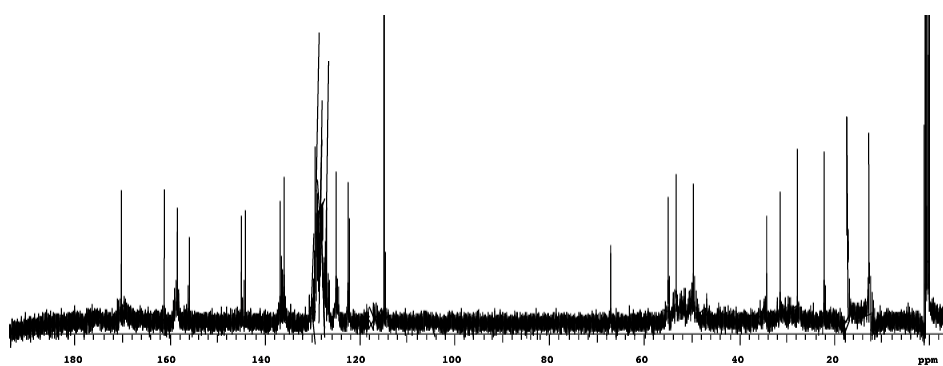
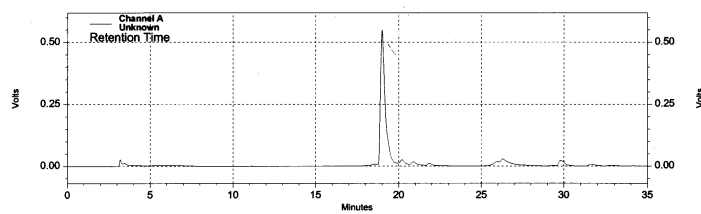


^1H NMR (500 MHz, DMSO-d_6) δ 8.92 (d, $J = 7.4$ Hz, 1H), 8.71 (s, 1H), 8.39 (d, $J = 7.2$ Hz, 1H), 7.38 (d, $J = 10.0$ Hz, 2H), 7.24 – 7.17 (m, 3H), 6.83 (d, $J = 7.2$ Hz, 1H), 6.58 (s, 2H), 4.72-4.68 (m, 1H), 4.62 (s, 2H), 4.39-4.35 (m, 4H), 3.90-3.87 (m, 1H), 2.79 (t, $J = 6.9$ Hz, 2H), 2.21-2.17 (m, 2H), 1.23-1.17 (m, 2H), 0.95-0.84 (m, 6H); ^{13}C NMR (125 MHz, MeCN-d_3) δ 170.4, 161.5, 158.8, 156.2, 144.6, 144.1, 137.1, 136.6, 129.3, 128.7, 128.5, 127.2, 125.0, 122.4, 67.5, 55.4, 53.7, 49.8, 34.9, 31.6, 27.9, 22.1, 17.4, 13.1; MALDI MS calc'd for $\text{C}_{26}\text{H}_{31}\text{N}_5\text{O}_6\text{S}$ ($\text{M}+\text{H}^+$) 542, found 542; analytical HPLC: purity = 93 %, retention time = 19.3 min (8-70% B in 30 min).

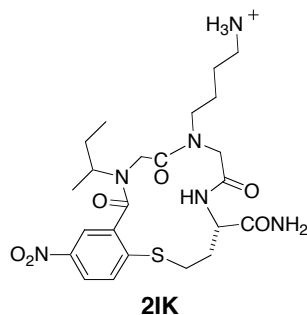




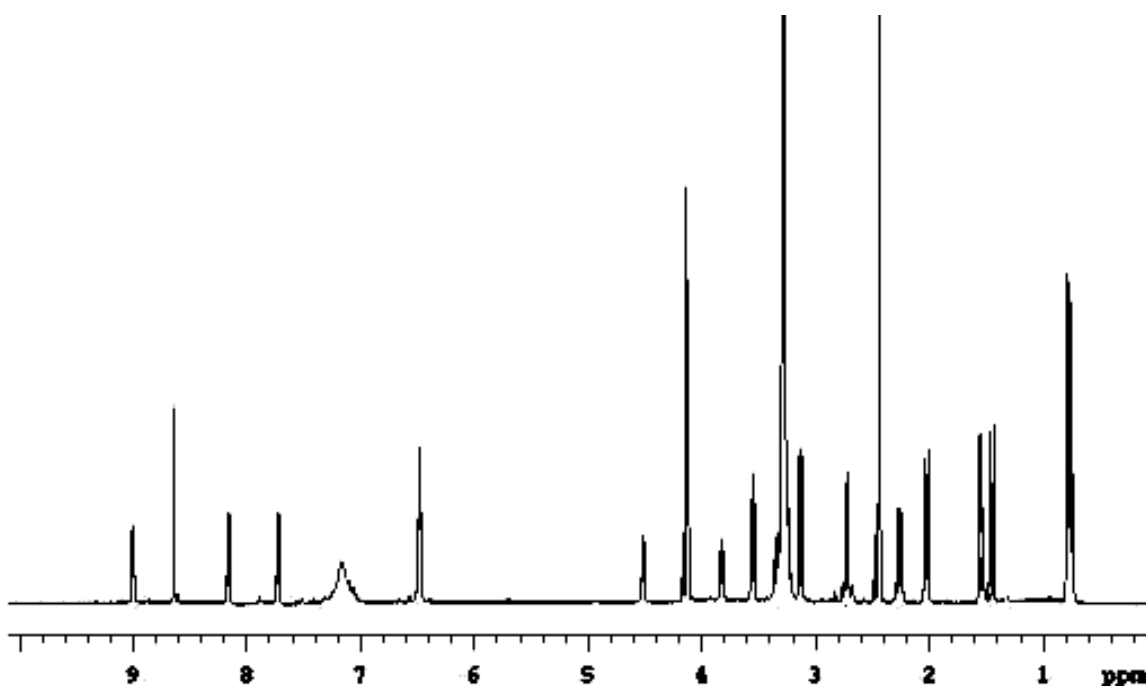
COSY

¹³C NMR

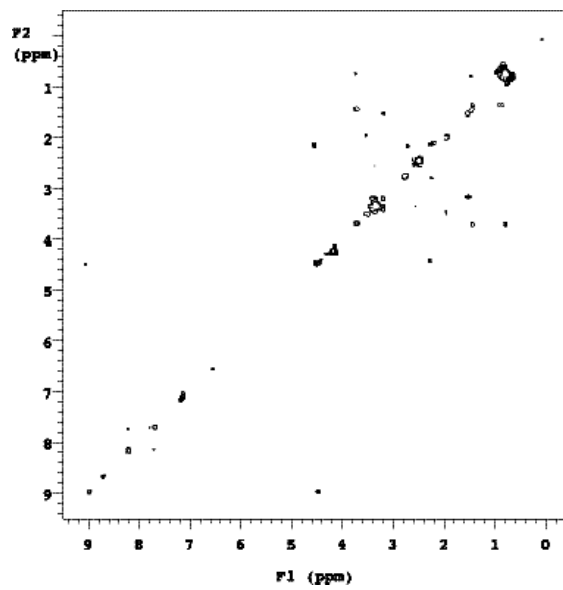
HPLC



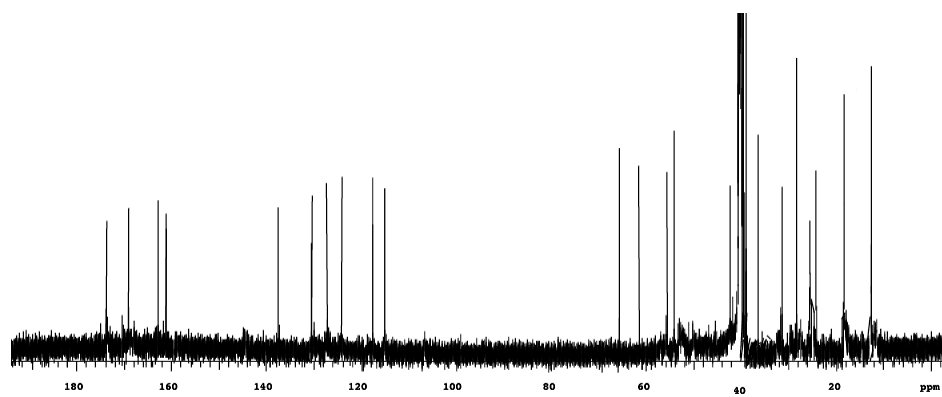
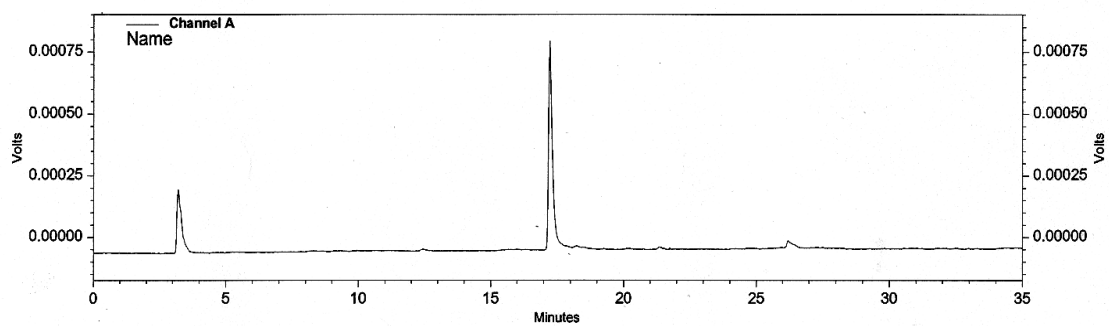
^1H NMR (500 MHz, DMSO- d_6) δ 9.00 (d, $J = 7.0$ Hz, 1H), 8.66(s, 1H), 8.18 (d, $J = 8.0$ Hz, 1H), 7.75 (d, $J = 8.0$ Hz, 1H), 7.21 (bs, 3H), 6.51 (s, 2H), 4.57-4.73 (m, 1H), 4.18-4.13 (m, 4H), 3.82-3.78 (m, 1H), 3.57 (t, $J = 6.5$ Hz, 2H), 3.18-3.15 (m, 2H), 2.77 (t, $J = 5.5$ Hz, 2H), 2.11-2.08 (m, 2H), 2.02-1.99(m, 2H), 1.57-1.54 (m, 2H), 1.47-1.42 (m, 2H), 0.79-0.71 (m, 6H); ^{13}C NMR (125 MHz, DMSO- d_6) δ 174.1, 169.0 163.0, 161.2, 137.6, 130.4, 126.9, 124.3, 117.6, 115.2, 65.1, 61.4, 55.7, 54.2, 42.5, 42.0, 36.4, 31.8, 28.2, 25.3, 24.8, 18.3, 12.7; MALDI MS calc'd for $\text{C}_{23}\text{H}_{34}\text{N}_6\text{O}_6\text{S}$ ($\text{M}+\text{H}^+$) 523, found 523; analytical HPLC purity = 95 %, retention time = 17.4 min (5-95% B in 30 min).



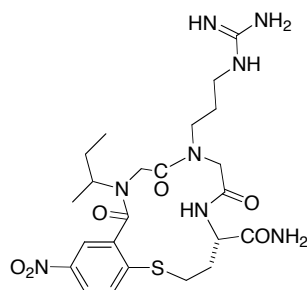
^1H NMR



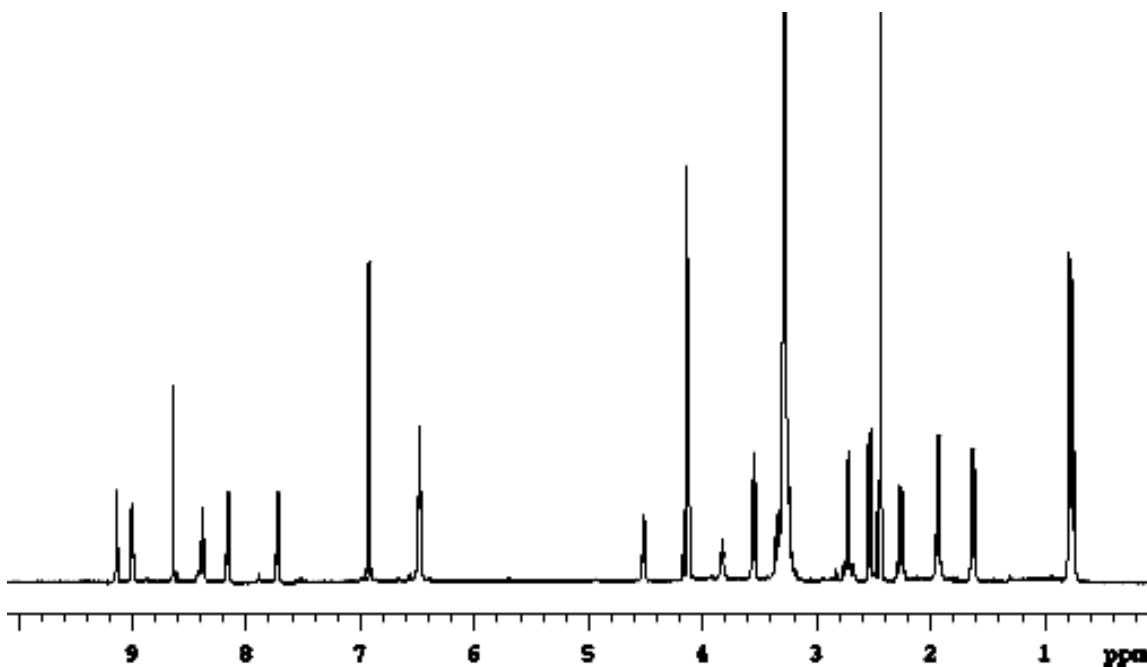
COSY

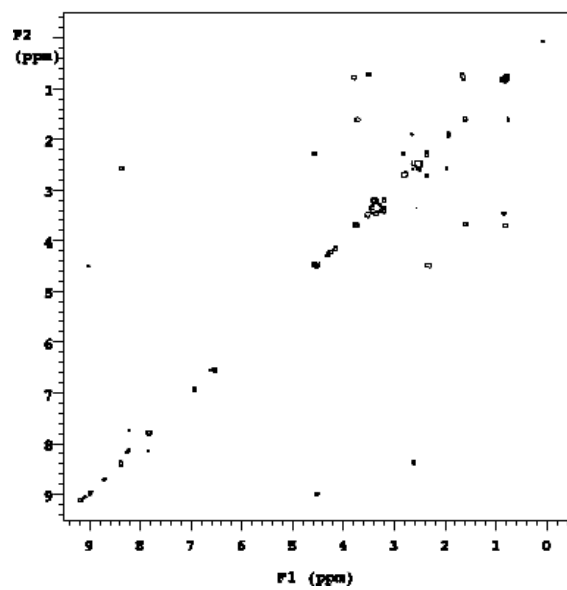
¹³C NMR

HPLC

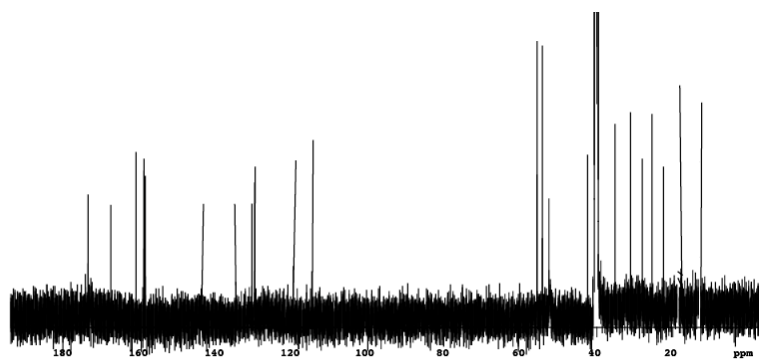
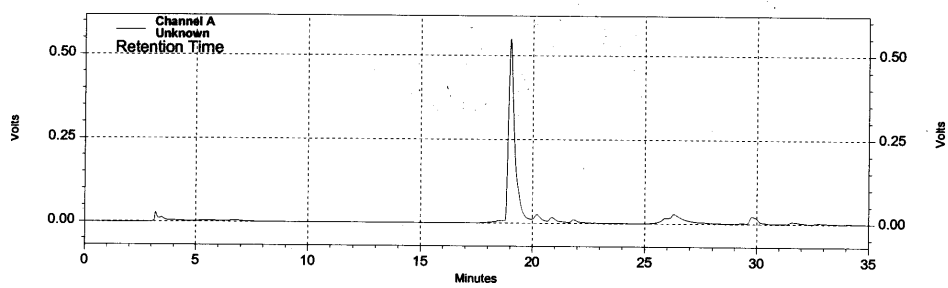
**2IR**

^1H NMR (500 MHz, DMSO-d_6) δ 9.17 (s, 1H), 8.99 (d, $J = 8.5$ Hz, 1H), 8.63 (s, 1H), 8.38 (t, $J = 7.5$ Hz, 1H), 8.17 (d, $J = 6.8$ Hz, 1H), 7.76 (d, $J = 6.8$ Hz, 1H), 7.97 (s, 2H), 7.51 (s, 2H), 4.57-4.53 (m, 1H), 4.18-4.06 (m, 4H), 3.83-3.78 (m, 1H), 3.57 (t, $J = 7.0$ Hz, 2H), 2.77 (t, $J = 7.4$ Hz, 2H), 2.58-2.54 (m, 2H), 2.29-2.22 (m, 2H), 1.98-1.94 (m, 2H), 1.64-1.59 (m, 2H), 0.82-0.76 (m, 6H); ^{13}C NMR (125 MHz, DMSO-d_6) δ 174.0, 167.8, 161.2, 159.8, 159.7, 144.6, 135.0, 131.6, 130.7, 120.1, 115.1, 55.8, 54.2, 52.5, 42.5, 38.7, 34.7, 30.6, 28.0, 25.9, 22.8, 17.7, 12.6; MALDI MS calc'd for $\text{C}_{23}\text{H}_{34}\text{N}_8\text{O}_6\text{S}$ ($\text{M}+\text{H}^+$) 551, found 551; analytical HPLC purity = 90 %, retention time = 19.1 min (8-70% B in 30 min).

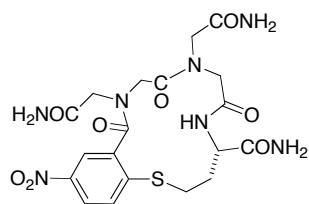
 ^1H NMR



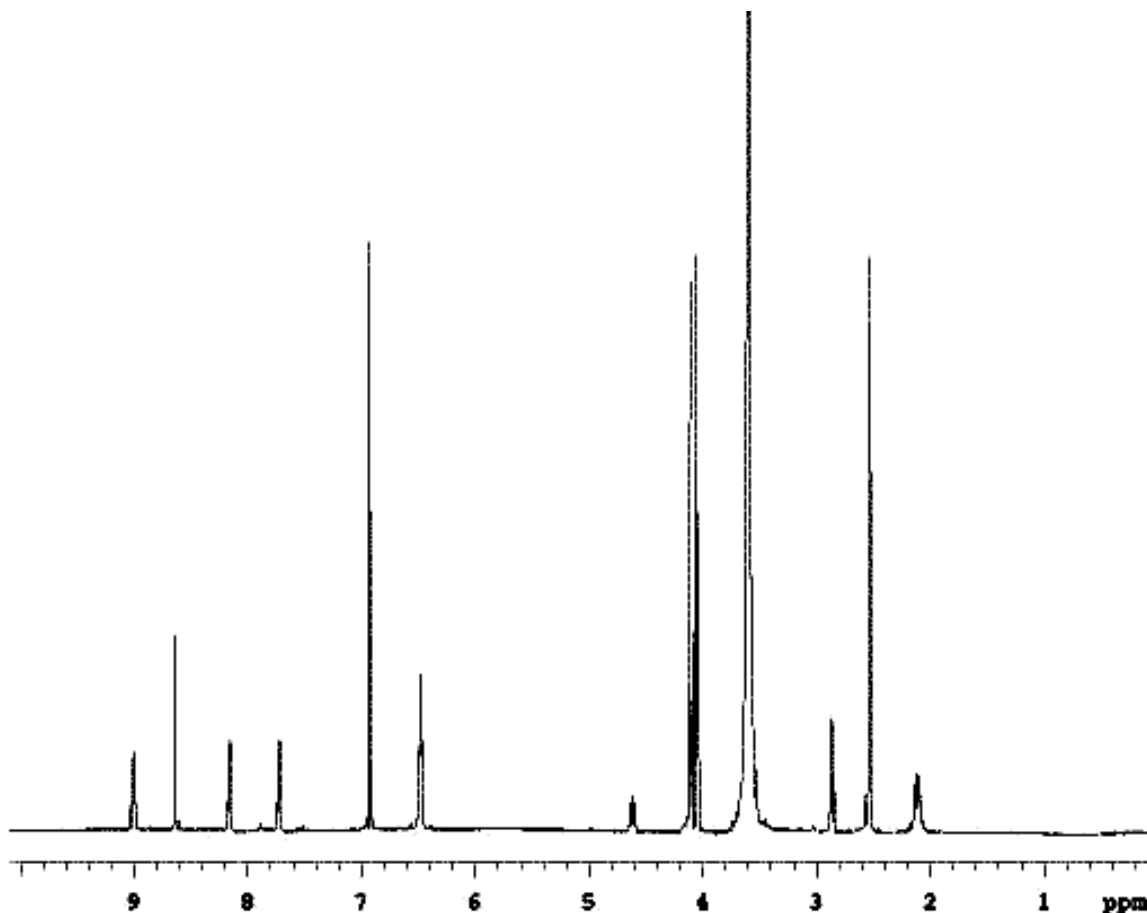
COSY

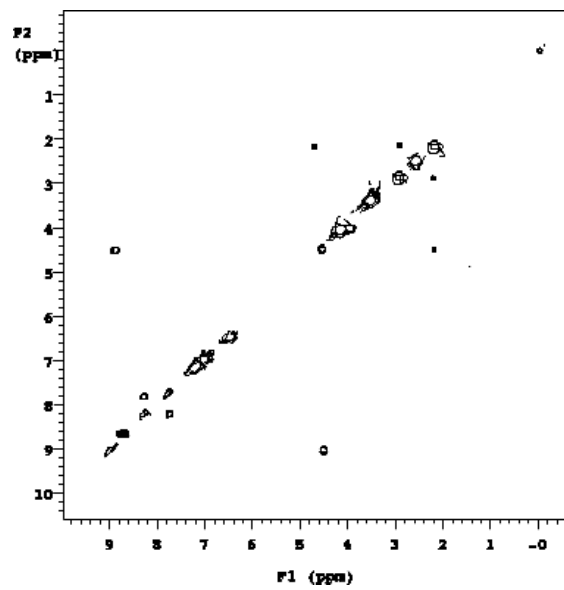
¹³C NMR

HPLC

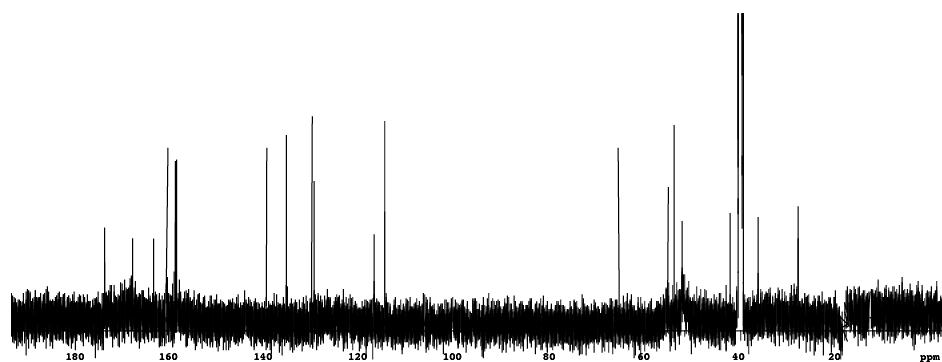
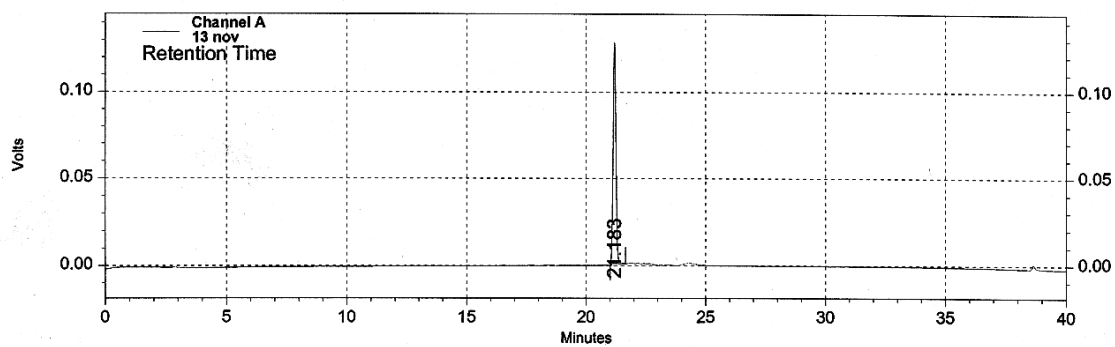
**2NN**

^1H NMR (500 MHz, DMSO- d_6) δ 9.00 (d, $J = 8.5$ Hz, 1H), 8.64 (s, 1H), 8.817 (d, $J = 7.02$ Hz, 1H), 7.77 (d, $J = 7.02$ Hz, 1H), 6.96 (s, 4H), 6.52 (s, 2H), 4.63-4.59 (m, 1H), 4.17-4.04 (s, 8H), 2.86 (t, $J = 7.5$ Hz, 2H), 2.18-2.05 (m, 2H); ^{13}C NMR (125 MHz, DMSO- d_6) δ 174.6, 168.7, 164.3, 161.2, 159.5, 159.4, 139.8, 135.4, 130.6, 130.4, 117.4, 114.7, 64.6, 55.3, 54.8, 52.5, 42.5, 36.4, 28.0; MALDI MS calc'd for $\text{C}_{19}\text{H}_{23}\text{N}_7\text{O}_8\text{S}$ ($\text{M}+\text{H}^+$) 510, found 510; analytical HPLC: homogeneous single peak, retention time = 21.2 min (8-70% B in 30 min).

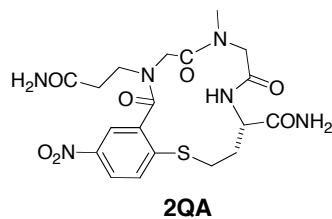
 ^1H NMR



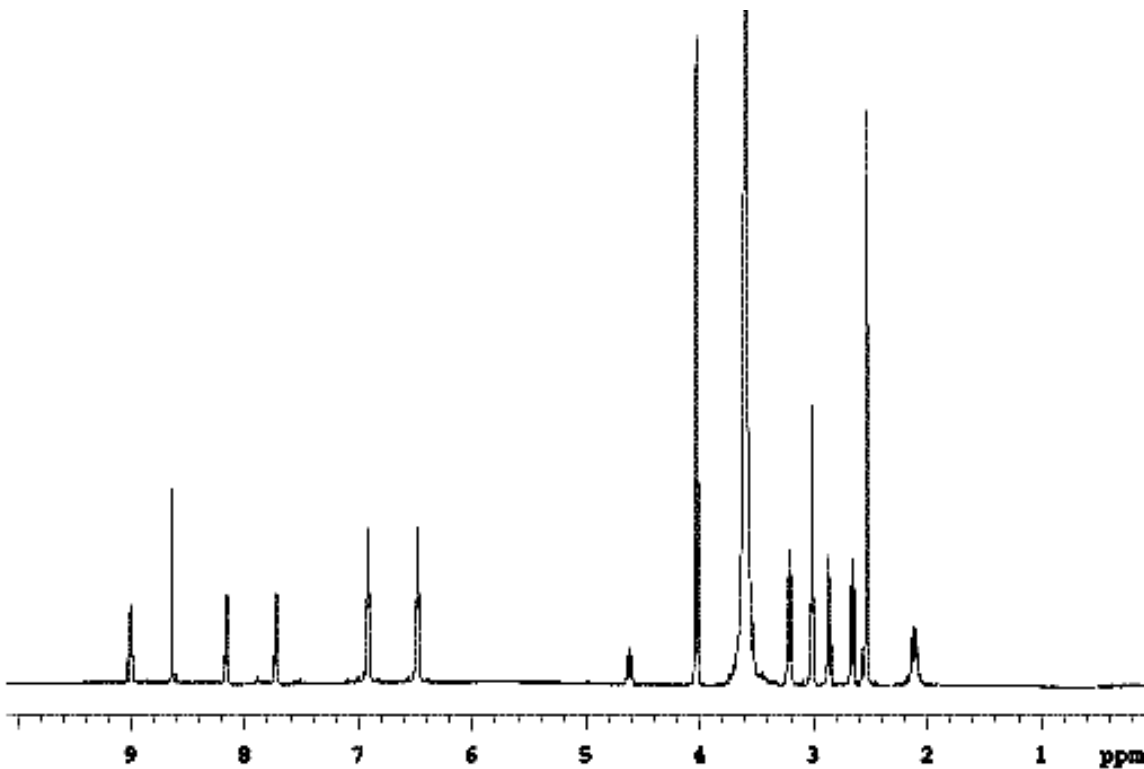
COSY

¹³C NMR

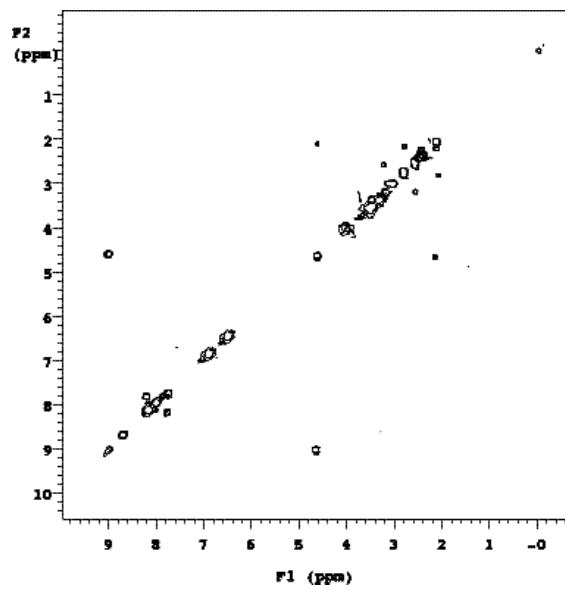
HPLC



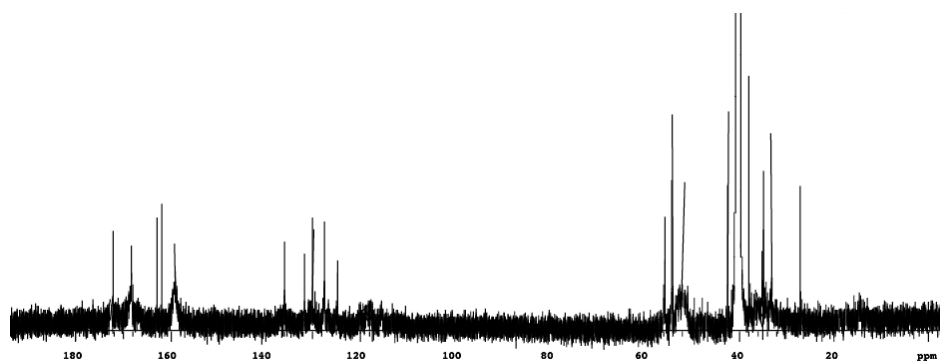
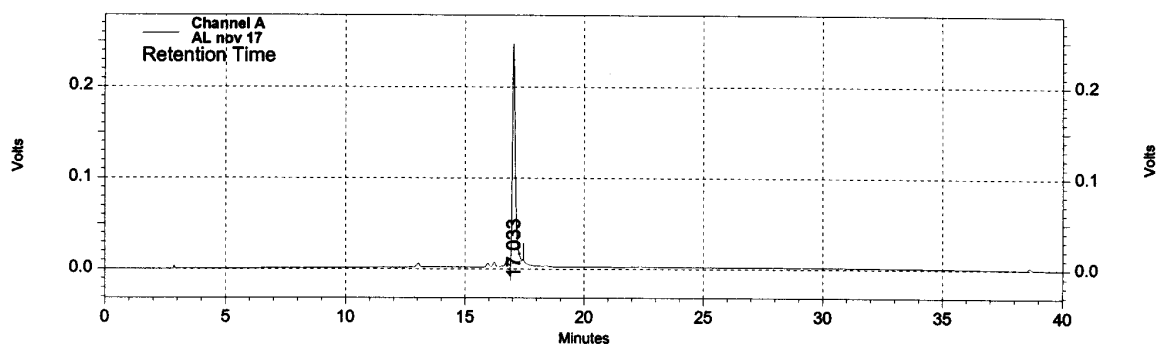
^1H NMR (500 MHz, DMSO-d_6) δ 9.00 (d, $J = 6.5$ Hz, 1H), 8.64 (s, 1H), 8.18 (d, $J = 7.8$ Hz, 1H), 7.77 (d, $J = 7.8$ Hz, 1H), 6.96 (s, 2H), 6.52 (s, 2H), 4.63-4.57 (m, 1H), 4.08-4.00 (m, 4H), 3.21 (t, $J = 6.5$ Hz, 2H), 3.00 (s, m), 2.88 (t, $J = 5.5$ Hz, 2H), 2.67 (t, $J = 6.5$ Hz, 2H), 2.17-2.09 (m, 2H); ^{13}C NMR (125 MHz, DMSO-d_6) δ 172.6, 168.8, 163.0, 162.2, 159.2, 135.5, 131.7, 130.6, 130.1, 127.8, 125.2, 55.7, 54.2, 52.0, 42.8, 37.8, 35.1, 33.8, 26.8; MALDI MS calc'd for $\text{C}_{19}\text{H}_{24}\text{N}_6\text{O}_7\text{S}$ ($\text{M}+\text{Li}^+$) 487, found 487; analytical HPLC purity = 99 %, retention time = 17.0 min (8-70% B in 30 min).



^1H NMR



COSY

¹³C NMR

HPLC

Conformational Analyses

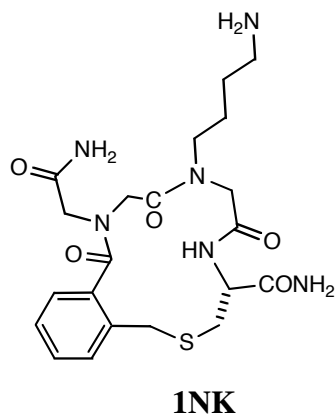
CD. CD measurements were obtained on an Aviv (model 202 DS) spectrometer. For these experiments the cyclic peptidomimetics were dissolved in H₂O with ~1 % NaHCO₃: MeOH (65:35 v/v) (c = 0.1 mg/ml, 0.1 cm path length). The CD spectra were recorded at 25 °C.

Molecular Simulations. CHARMM (Molecular Simulations Inc.) was used for the molecular simulations performed in this work. Explicit atom representations were used throughout the study. The residue topology files (RTF) for all the peptidomimetics were built using QUANTA2000 (Molecular Simulations Inc.).

Molecular Simulation Experiments for 1nk and 2ff. Quenched molecular dynamics simulations were performed using the CHARMM standard parameters. All molecules were modeled as neutral compounds in a dielectric continuum of 45 (simulating DMSO). Thus, the starting conformers were minimized using 1000 steps of steepest descent (SD) and 3000 steps of the adopted basis Newton-Raphson method (ABNR) respectively. The minimized structures were then subjected to heating, equilibration, and dynamics simulation. Throughout, the equations of motions were integrated using the Verlet algorithm with a time step 1 fs, and SHAKE was used to constrain all bond lengths containing polar hydrogens. Each peptidomimetic was heated to 1000 K over 10 ps and equilibrated for another 10 ps at 1000 K, then molecular dynamics runs were performed for a total time of 600 ps with trajectories saved every 1 ps. The resulting 600 structures were thoroughly minimized using 1000 steps of SD followed by ABNR until an RMS energy derivative of $\leq 0.001 \text{ kcal mol}^{-1} \text{ \AA}^{-1}$ was obtained. Structures with energies less than $3.50 \text{ kcal mol}^{-1}$ relative to the global minimum were selected for further analysis. The QUANTA2000 package was again used to display and to classify the selected structures into conformational groups. The best clustering was obtained using a grouping method based on calculation of RMS deviation of atom subsets; in this study these were the ring backbone atoms. Thus, threshold cutoff values 0.72 \AA were selected to obtain families with reasonable homogeneity. The lowest energy from each family was

considered as a typical representative of the family as a whole. Defined distances were measured and compared to distances of various β -turn types.

Table A2. QMD Data for Compound **1NK**.



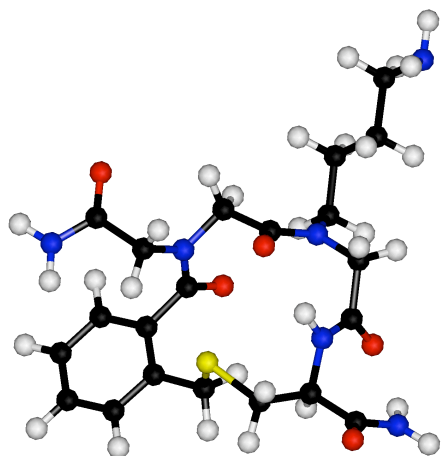
Residue	family 1	family 2	family 3	family 4
	lowest energy conformer	lowest energy conformer	lowest energy conformer	lowest energy conformer
number in family	183	108	48	22
lowest energy conformer (kcal/mol)	0.00	0.05	2.31	3.73
distance (\AA) $i+1-i+2^*$	5.34	5.35	5.38	5.27
distance (\AA) O_i-NH_{i+3}	4.78	4.79	4.34	3.50

* $i+1-i+2$ is measured from β -carbons of the side chains.

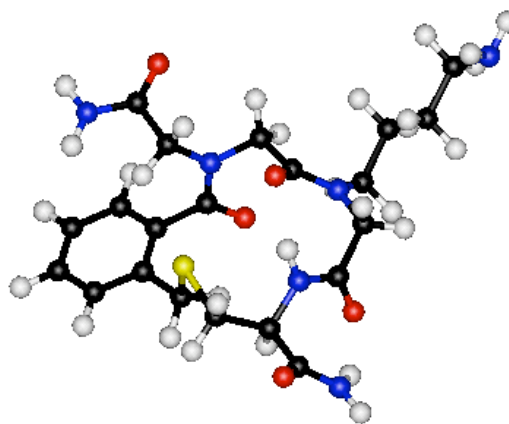
Figure A1. Backbone Conformation of the Lowest Energy Structures for Compound 1NK

● C ● S ● O ● N ○ H

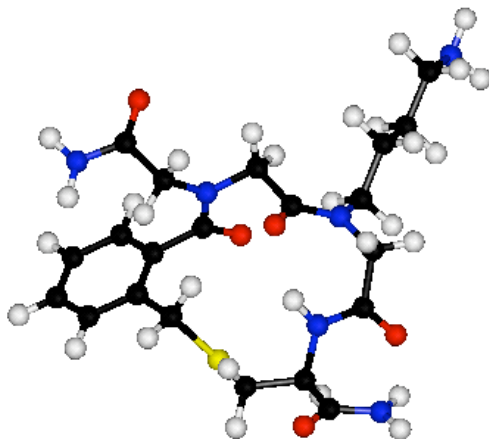
family 1



family 2



family 3



family 4

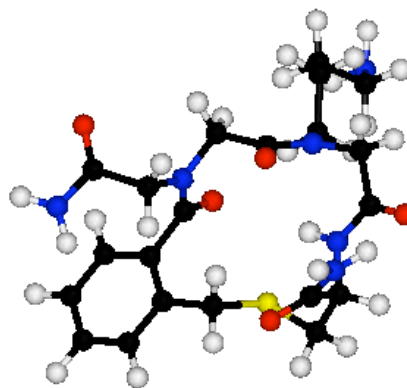
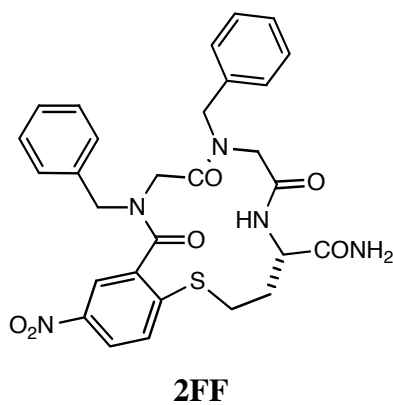


Table A2. QMD Data for Compound **2FF**

Residue	family 1	family 2	family 3
	lowest energy conformer	lowest energy conformer	lowest energy conformer
number in family	120	63	37
lowest energy conformer (kcal/mol)	0.00	1.25	4.79
distance (Å) $i+1 - i+2^*$	5.36	4.79	4.85
distance (Å) $O_i - NH_{i+3}$	2.05	4.22	5.98

* $i+1 - i+2$ is measured from β -carbons of the side chains.

Figure A2. Backbone Conformation of the Lowest Energy Structure for Compound **2FF**

● C

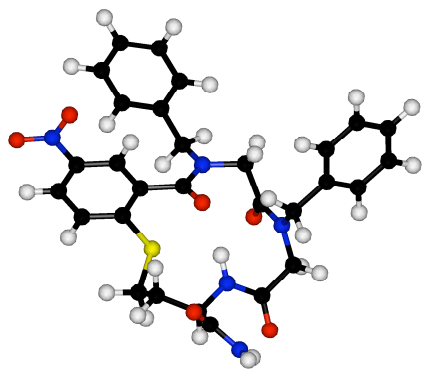
● S

● O

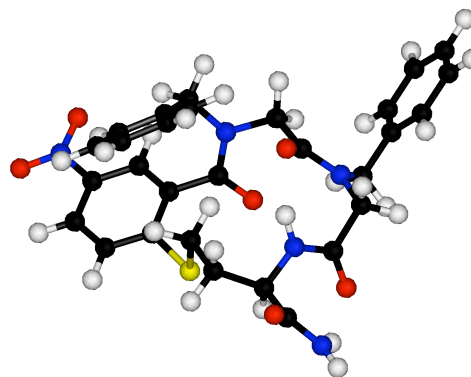
● N

○ H

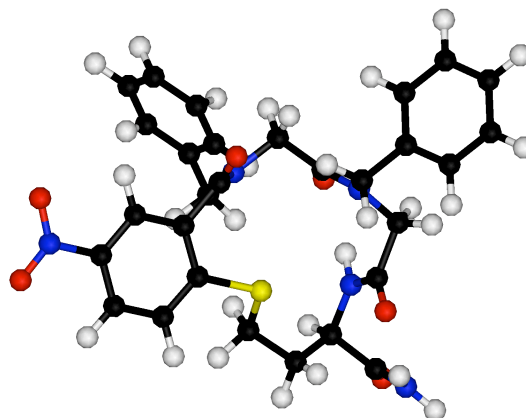
family 1



family 2



family 3



Temperature Coefficient ^1H NMR Experiment (500 MHz, DMSO-d_6):

Temperature coefficients of amide protons were measured via several 1D experiments in the range of 25-55 °C adjusted in 5 °C increments with an equilibration time of approximately 30 min after successive temperature steps.

Figure A3. Temperature Coefficient for **1NK**.

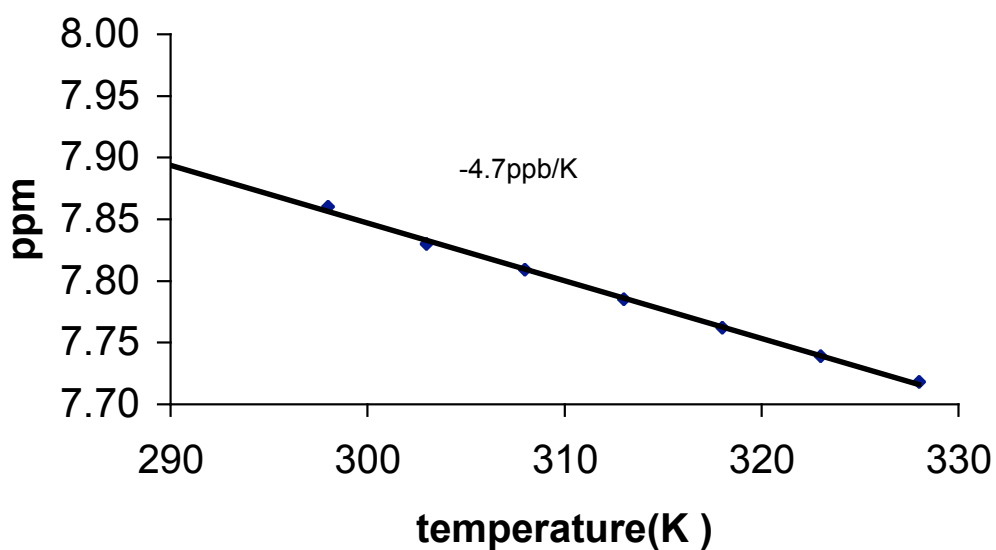
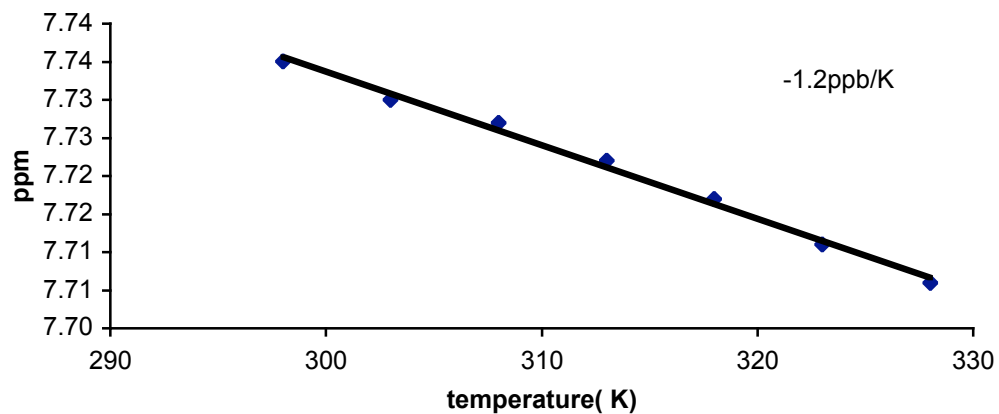


Figure A4. Temperature Coefficient for **2FF**.



VITA

Name: Ernest Nnanabu

Permanent Address: Dept of Chemistry
% Dr Kevin Burgess
Texas A&M University M.S. 3255
College Station, TX 77843

Education: M.S., Chemistry, Texas A&M University, 2006
College Station, TX
B.S., Chemistry, Linfield College, 2002
McMinnville, OR